

# MODEL VALIDATION FOR UNCERTAIN SYSTEMS

Thesis by  
Roy S. R. Smith

In Partial Fulfillment of the Requirements  
for the Degree of  
Doctor of Philosophy

California Institute of Technology  
Pasadena, California

1990

(Submitted September 19, 1989)



To Maggie

## Acknowledgements

Many people have contributed to the enjoyment and productivity of my stay at Caltech. Firstly, I would like to thank my advisor, John Doyle, for his guidance in this research. He can see the long term directions of control theory, and provides his students with a guiding framework in which to work. He has given me the support and the freedom to pursue my own ideas. Thanks John.

The financial support of several organizations is also acknowledged: Caltech, via the Program in Advanced Technology, the National Science Foundation, the Jet Propulsion Laboratories, and the National Aeronautics and Space Administration.

To those that have read, and commented on, this thesis I also offer thanks. Among these are the members of my committee, Manfred Morari, Thanasis Sideris, Joel Burdick, and P.P. Vaidyanathan, as well as the various visitors and graduate students, Andy Packard, Harold Stalford, Matt Newlin, Bobby Bodenheimer, Kemin Zhou, and Peter Young. Gary Balas, Lane Dailey and Ricardo Sánchez-Peña have also provided friendship and support. To the many people who have spent long hours in the lab and made my time there much more enjoyable, thanks.

There are also those who have unwittingly influenced me in the nature and style of my research. Although they may be horrified to learn of the extent of their influence, I would like to thank the following: Richard Bates, for providing a role model and encouraging me to think. Bruce Francis, for asking, tongue in cheek, what information could an experiment possibly offer a control theorist. Keith Glover, for teaching me, among other things, to punt.

Mostly, however, I would like to thank Margaret Rankin, my spouse. Our lives, over the last four years, could certainly have been spent doing far better things. Without her support and encouragement this thesis could not have been written. This is indeed our thesis.

## Abstract

Modern robust control synthesis techniques aim at providing robustness with respect to uncertainty in the form of both additive noise and plant perturbations. On the other hand, most popular system identification methods assume that all uncertainty is in the form of additive noise. This has hampered the application of robust control methods to practical problems. This thesis begins to address this disparity by considering the connection between uncertain models and data. The model validation problem addressed here is this: given experimental data and a model with both additive noise and norm-bounded perturbations, is it possible that the model could produce the observed input-output data? This question is reformulated as an optimization problem: what is the minimum norm noise required to account for the data and meet the constraint imposed by the perturbation uncertainty? The assumptions typically used for robust control analysis are introduced and shown to lead to a constant matrix problem. This problem is studied in detail, and bounds on the size of the required noise are developed. The dimensionality issues that arise in the consideration of the structured singular value ( $\mu$ ) also arise here.

A geometric framework is used to introduce a variation on  $\mu$ . This is extended to allow the consideration of robust control analysis problems that include input and output data. The more general problem is then used to illustrate the connection between  $\mu$  and the model validation theory.

The application of the theory is illustrated by a study of a laboratory process control experiment. Typical steps in the identification of a robust control model for a physical system are discussed. It is shown, by example, how the model validation theory can be used to provide insight into the limitations of uncertain models in describing physical systems.

# Contents

Acknowledgements . . . . .	iv
Abstract . . . . .	v
List of Figures . . . . .	x
<b>1 Introduction</b>	<b>1</b>
1.1 The Organization of the Thesis . . . . .	3
<b>2 Models and Robust Control</b>	<b>5</b>
2.1 Generic Models for Robust Control . . . . .	5
2.1.1 Notation . . . . .	5
2.1.2 The Generic Model . . . . .	7
2.1.3 Assumptions on $P$ and $\Delta$ . . . . .	10
2.2 Analysis . . . . .	13
2.2.1 Measures of Performance . . . . .	13
2.2.2 Robust Stability and $\mu$ . . . . .	14
2.2.3 Robust Performance . . . . .	15
2.2.4 Properties of $\mu$ . . . . .	16
2.3 Synthesis . . . . .	17
2.4 Identification and the Role of Model Validation . . . . .	18
<b>3 The Model Validation Problem</b>	<b>24</b>
3.1 Properties of the Model Validation Problem . . . . .	24
3.2 Formulation of Optimization Problems . . . . .	27
3.2.1 Removal of the Equality Constraint . . . . .	28
3.3 Assumptions on $P$ , $w$ and $\Delta$ . . . . .	30

3.3.1	Rationale of the Constant Matrix Formulation . . . . .	31
3.3.2	Model Requirements . . . . .	34
3.3.3	Formulation with the Euclidean Spatial Norm . . . . .	35
3.4	Solving the Model Validation Problem: A Summary of the Results . . . .	37
<b>4</b>	<b>Lagrange Multipliers and Duality</b>	<b>39</b>
4.1	Preliminaries . . . . .	39
4.2	Optimization Problems . . . . .	41
4.3	Lagrange Multipliers . . . . .	42
<b>5</b>	<b>Application of Lagrange Techniques to the Model Validation Problem</b>	<b>46</b>
5.1	Formulation of the Lagrangians . . . . .	47
5.1.1	Properties of the Lagrangian: $L(x, \lambda)$ , The Unconstrained Case . .	49
5.1.2	Properties of the Lagrangian: $L_e(x_e, \lambda)$ , The Constrained Case . .	52
5.1.3	Properties of the Sets $\Lambda$ and $\Lambda_e$ . . . . .	53
5.1.4	The Boundary of $\Lambda_e$ . . . . .	54
5.1.5	Properties of the Dual Function: $h_e(\lambda)$ . . . . .	56
5.2	Solving the Model Validation Problem . . . . .	56
5.2.1	Solution via the Dual Problem . . . . .	56
5.2.2	Bounds on a Solution to the Model Validation Problem . . . . .	58
5.3	The Dual Function at the Boundary: $\partial\Lambda_e$ . . . . .	59
5.3.1	When is $h_e(\lambda)$ finite on $\partial\Lambda_e$ ? . . . . .	60
5.3.2	Finding a Kuhn-Tucker Saddlepoint on the Boundary . . . . .	61
5.3.3	The Single Perturbation Block Case . . . . .	62
<b>6</b>	<b>Skewed <math>\mu</math></b>	<b>65</b>
6.1	Motivation for a Generalization of $\mu$ . . . . .	65
6.2	Skewed $\mu$ : $\mu_s$ . . . . .	67
6.3	A Geometric Interpretation . . . . .	74
6.4	An Algorithm for $\mu_s(M)$ . . . . .	78
6.4.1	Outline of the $\mu_s(M)$ Algorithm . . . . .	78
6.4.2	On the Calculation of $c(\alpha)$ . . . . .	79

6.4.3	An Imperfect Algorithm . . . . .	80
6.5	Numerical Examples . . . . .	81
6.5.1	A Geometric Example of $\mu(M)$ and $\mu_s(M)$ . . . . .	81
6.5.2	The Pathological Example Revisited . . . . .	82
6.5.3	Algorithm to Plot the Boundaries of $W(\alpha)$ . . . . .	83
<b>7</b>	<b>A General Interconnection Structure</b>	<b>85</b>
7.1	Formulation of the General Problem . . . . .	86
7.1.1	Interconnection Structure . . . . .	86
7.1.2	Applicable problems . . . . .	89
7.2	Reformulation of the General Problem . . . . .	91
7.3	Application to the Model Validation Problem . . . . .	96
7.4	A Geometric Interpretation . . . . .	103
7.4.1	A Numerical Range Function . . . . .	103
7.4.2	Properties of $W'(\alpha)$ . . . . .	104
7.5	Relationship to the Lagrangian Formulation . . . . .	106
7.5.1	The Existence of a Kuhn-Tucker Saddlepoint . . . . .	106
7.6	A Summary of the Application of $\psi_s(M, \mathcal{X})$ to the Model Validation Problem . . . . .	112
<b>8</b>	<b>A Study of Several Numerical Examples</b>	<b>114</b>
8.1	Case 1 . . . . .	114
8.2	Case 2 . . . . .	119
8.3	Case 3 . . . . .	122
8.3.1	A Single Block Boundary Problem . . . . .	124
8.3.2	An Application to $\mu$ - the 4 Block Counterexample . . . . .	128
<b>9</b>	<b>An Experimental Example</b>	<b>132</b>
9.1	The Two Tank Experiment . . . . .	133
9.1.1	A Physical Description . . . . .	133
9.1.2	The Scope of the Model Validation Problem . . . . .	134
9.2	Modeling the System . . . . .	135



9.2.1	<i>Development of a Nominal Model</i> . . . . .	135
9.2.2	<i>Development of a Description of the Uncertainty</i> . . . . .	138
9.3	<i>A Numerical Model of the System</i> . . . . .	143
9.3.1	<i>A Full Range Nonlinear Model with Uncertainty</i> . . . . .	143
9.3.2	<i>A Linear Model</i> . . . . .	145
9.3.3	<i>The Discrete Version of the Interconnection Structure</i> . . . . .	149
9.4	<i>A Model Validation Problem</i> . . . . .	150
9.4.1	<i>The Experimental Datum</i> . . . . .	150
9.4.2	<i>Solving the Constant Matrix Problems</i> . . . . .	152
9.4.3	<i>A Discussion of the Results</i> . . . . .	155
9.5	<i>Analysis of a More Sophisticated Model</i> . . . . .	157
9.5.1	<i>A Nominal Linear Model</i> . . . . .	158
9.5.2	<i>The Model Validation Analysis</i> . . . . .	159
9.6	<i>A Discussion of the Example</i> . . . . .	159
<b>10</b>	<b>Conclusions and Future Directions</b>	<b>162</b>
	Appendices . . . . .	165
	A <i>State Space Realizations for the Experimental Example</i> . . . . .	165
	Bibliography . . . . .	169

## List of Figures

2.1	Example Block Diagram . . . . .	7
2.2	Generic Model Structure Including Uncertainty . . . . .	8
2.3	Nyquist Diagram of an Example Uncertain SISO System . . . . .	11
2.4	The Generic Structure for Synthesis . . . . .	18
2.5	The Generic Structure for Identification and Model Validation Problems . . . . .	19
2.6	An Example Identification Problem . . . . .	20
5.1	Example $\lambda$ Space Illustrating $\Lambda_e$ , $\partial\Lambda_e$ , and $\partial_0\Lambda_e$ . . . . .	55
6.1	System to be Considered for $\mu$ Problems . . . . .	66
6.2	Generic Model Structure Including Uncertainty . . . . .	67
6.3	Boundaries of $W(\alpha)$ for $\alpha = 0, 1, 5.6, 15,$ and $20$ . $I_s = \emptyset$ . ( $\mu(M)$ ) . . . . .	82
6.4	Boundaries of $W(\alpha)$ for $\alpha = 0, 1, 5.6, 15,$ and $20$ . $I_s = \{1\}$ . . . . .	83
6.5	Boundaries of $W(\alpha)$ for $\alpha = 0, 1,$ and $5$ . $I_s = \{1\}$ . ( $a = 2$ ) . . . . .	84
7.1	The General Interconnection Structure . . . . .	87
7.2	The Generic System with a Reparametrization to give Scalar Constraints . . . . .	92
8.1	Case 1: Dual Function: $h(\lambda)$ (solid line) and the minimum eigenvalue of the quadratic term: $V^*(B + \lambda A)V$ (dashed line) . . . . .	117
8.2	Case 1: $W'(\alpha)$ for $\alpha = 0.165$ and the supporting hyperplane defined by $\langle \xi, \nu \rangle \geq 0$ , $\xi = [0.1256, 1]^T$ . . . . .	118
8.3	Case 2: Dual Function: $h(\lambda)$ (solid line) and the minimum eigenvalue of the quadratic term: $V^*(B + \lambda A)V$ (dashed line) . . . . .	121
8.4	Case 2: $W'(\alpha)$ for $\alpha = 5.5$ & $8.51$ and the supporting hyperplane defined by $\langle \xi, \nu \rangle \geq 0$ , $\xi = [0, 1]^T$ . . . . .	122

8.5	Case 3 with Block Structure (3): Dual Function: $h(\lambda)$ (solid line) and the minimum eigenvalue of the quadratic term: $V^*(B + \lambda A)V$ (dashed line)	125
8.6	Case 3 for Block Structure (3): $W'(\alpha)$ for $\alpha = 1$ and the supporting hyperplane defined by $\langle \xi, \nu \rangle \geq 0$ , $\xi = [1, 1]^T$	128
9.1	Schematic Diagram of the Two Tank System	133
9.2	Transfer Function Between $f_{hc} + f_{cc}$ and $h_1$ . Experimental data and theoretical model (solid line)	140
9.3	Transfer Function Between $f_{hc} - f_{cc}$ and $t_1$ . Experimental data and models (solid lines). $h_1 = 0.15$ and $h_1 = 0.75$	141
9.4	A Numerical Nonlinear Model of Tank 1	144
9.5	Nyquist Plot of the Transfer Function: $f_h + f_c$ to $h_1$ . Circles indicate the equivalent additive uncertainty bound	147
9.6	Nyquist Plot of the Transfer Function: $f_h$ to $t_1$ . Circles indicate the equivalent additive uncertainty bound	148
9.7	The Equivalent Digital System: $P(z)$	149
9.8	Model Validation Experiment: Input/Output Datum	151
9.9	Magnitude of the Discrete Fourier Transform of $y(n)$ (upper plot) and $u(n)$ (lower plot)	153
9.10	Magnitude of $W(k)$	155
9.11	Time Domain Results: $x(n)$	156
9.12	Model Validation Results: $W(k)$ and $x(n)$	160

# Chapter 1

## Introduction

This decade has witnessed the attention of control theorists return to more physically motivated paradigms for the solution of control problems. Principle among these is the robust control paradigm in which the system model includes uncertainty in the form of perturbations as well as noise.

Robustness has become a desirable feature of the solutions to control problems. In this context robustness means the preserving of system characteristics, stability or performance, for example, in the presence of unknown perturbations and noise.

In order to pose a meaningful problem, the perturbations and the noise are assumed to be norm-bounded leading to a set description as a system model. The choice of norm is a compromise between those that best describe the system and those that lead to mathematically tractable problems. Assuming a power or energy bound on the unknown signals leads to induced norm problems which can be solved using the recent results in  $H_\infty$  theory. If the perturbations are assumed to be bounded by the same induced norm, a unifying framework can be used for the consideration of these problems.

Robust control theory now gives the engineer the power to describe physical systems with a model which includes two types of uncertainty: additive noise and block structured, norm-bounded uncertainty entering the model in a linear fractional manner. Linear models in which the only uncertainty is in the form of additive noise cannot account for a loss of stability not predicted by the nominal model. Robust control models can capture this feature, essentially being able to include unmodeled but bounded

dynamics.

Before the robust control methods can be applied, a bound on the uncertainty must be quantified. Current identification methods are well developed in the case where all of the residuals, or uncertainty, are attributed to additive noise. For models with both additive noise and norm-bounded perturbations, no such identification methods exist. This has hindered the application of robust control theory to practical problems.

Once a system is modeled, perhaps by *ad hoc* methods, and the engineer is confident of the applicability of the model, the robust control theory gives techniques for designing systems which are theoretically robust. This theory, or any other for that matter, makes no statements about the performance or the stability of the actual physical system. Such a statement requires assumptions on the behavior of the system and the applicability of the model. This presents a problem; the engineer must be confident that the model will describe all input-output behaviors of the system. This condition can never be guaranteed, but it is possible to test a necessary condition: the model must be able to describe all observed input-output behaviors of the system. This is simply the model validation question to be considered here.

Assuming the perturbations and noise to be norm-bounded gives a set description for the model. The model validation question: *Can the model account for the observed data?* is answered by attempting to find a member of the model set which maps the observed inputs onto the observed outputs.

The problem of finding such a member of the model set is formulated as an optimization problem. A series of problems can be considered; the one analyzed in detail here arises from imposing the constraints that the inputs are mapped to the outputs and the perturbations meet the assumed norm bound. The objective then becomes finding the minimum norm noise signal meeting these constraints. If the norm of the required noise is less than the bound assumed by the model, then the model accounts for the data. If the required noise has norm greater than the assumed bound, then the model cannot account for the data. Comparing the norm of the required noise to the assumed bound also gives an idea of how much a model must be changed in order to account for the data.

The properties of this optimization problem are studied in detail. It is possible to

formulate a convex optimization problem to find a bound on the solution. A test is available to determine whether or not the bound is actually a solution to the desired problem. In certain cases, when there is only one unknown perturbation, for example, the bound is guaranteed to be exact.

This thesis examines the connection between robust control models and reality, and it is befitting that a real system is used as an example of the theory. Models of a laboratory chemical process have been studied with this theory. Experimental input-output data is presented and analyzed using the model validation techniques. It is shown, by example, how the theory presented here can be used in identifying the system.

## 1.1 The Organization of the Thesis

Chapter 2 introduces and discusses the robust control theory with particular emphasis on the models and assumptions used by the theory. In this context the structured singular value, more commonly known as  $\mu$ , is presented. In subsequent chapters it will be shown that the model validation problem has certain properties in common with  $\mu$ ; in particular, those involving the number of perturbation blocks.

Identification of systems with respect to robust control models is considered and used to motivate the model validation problem. Chapter 2 concludes with a formal statement of the general model validation problem.

The general problem is reformulated as an optimization problem in Chapter 3. The assumptions commonly used for the robust control analysis of systems are introduced and used to refine the optimization problem. In particular, the fact that the input-output data will be in a discrete form is used to motivate a constant matrix formulation of the optimization. This formulation will be considered throughout the remainder of the thesis. At this point a summary of the results is presented.

Lagrange multiplier techniques will be used to study the properties of the optimization problem. Chapter 4 reviews the required theory on Lagrange multipliers and duality.

Chapter 5 considers the Lagrange multiplier approach to this problem in detail. There is a strong relationship between the Lagrange multipliers used here and the scalings used in the calculation of an upper bound to  $\mu$ . This is used to illustrate a connection between

stable models and certain convexity properties of the domain of the dual function. A more detailed study of the dual function indicates when Lagrange techniques can be expected to yield a solution to the required optimization problem. It is shown that for models with only a single perturbation uncertainty such a solution always exists.

Chapter 6 introduces a variation on the  $\mu$  problem, named *skewed  $\mu$* . While there is a good engineering motivation for the consideration of this problem, it is not fundamentally different from  $\mu$  and can be calculated via an iteration on  $\mu$ . It is used to introduce a geometric framework for a class of optimization problems. Both  $\mu$  and the model validation problem can be considered in this manner.

A general framework for  $\mu$  problems with input-output data is introduced in Chapter 7. The properties of these problems can be studied with the geometric framework of the previous chapter. This is done for the model validation problem leading to a means of calculating a bound on the solution to the model validation problem. The geometric framework also leads to necessary and sufficient conditions for the existence of Lagrange multipliers at the solution of the model validation problem. The dimensionality (with respect to the number of perturbation blocks) properties that  $\mu$  exhibits can be seen easily in the geometric framework. The dimensionality properties of the model validation problem are similarly obtained.

Chapter 8 presents three numerical examples. The Lagrange multiplier techniques and the geometric framework are tied together by studying each example from both points of view. Also included is a four perturbation block example illustrating the limitations of the Lagrange multiplier approach.

The experimental example is studied in a tutorial manner in Chapter 9. Typical steps in the identification of the system are presented to illustrate how the model validation techniques can be used to gain an understanding of the physical system.

## Chapter 2

# Models and Robust Control

This chapter introduces and discusses the models used in the robust control paradigm. Other methodologies attribute the differences between experimental observation and model predictions to additive noise. Robust control models consider uncertainty to arise from both perturbations and additive noise. The simple example in the next section will make this point clear. A generic robust control model structure is introduced and discussed in detail. The analysis and synthesis theories are also outlined as it will be shown that there exists a strong connection between these theories and the model validation problem.

## 2.1 Generic Models for Robust Control

Both perturbations and noise can be represented in the models used for robust control. Uncertainty in the model is represented by set descriptions of the unknown perturbations and noise. Several assumptions on the nature of the uncertainty are possible. This chapter will discuss the issues that arise as a result of the more commonly used assumptions. A thorough understanding of the form of the model is a prerequisite to considering the model validation problem.

### 2.1.1 Notation

The following notation will be used throughout this thesis. Other symbols and terms will be defined as needed.



$\mathbf{R}$	field of real numbers
$\mathbf{C}$	field of complex numbers
$\gamma_{\max}(A)$	maximum eigenvalue of a matrix $A$
$\gamma_{\min}(A)$	minimum eigenvalue of a matrix $A$
$\sigma_{\max}(A)$	maximum singular value of a matrix $A$
$\sigma_{\min}(A)$	minimum singular value of a matrix $A$
$\rho(A)$	spectral radius of $A$
$A^T$	transpose of a matrix (or vector) $A$
$A^*$	complex-conjugate transpose of a matrix (or vector) $A$
$\dim(A)$	dimension of $A$
$\text{Ker}(A)$	kernel of $A$
$\text{co}[S]$	convex hull of a set $S$
$L_{\infty}(0, \infty)$	time domain Lebesgue space
$\langle x, y \rangle$	inner product of vectors $x$ and $y$ ( $= x^*y$ )
$\oplus$	direct sum
$:=$	“is defined by”
$\blacktriangleright$	Q.E.D

Block diagram descriptions will frequently be used to describe matrix and system operations. For example the block diagram illustrated in Figure 2.1 represents the equations

$$x = P_{11}u + P_{12}v \quad (2.1)$$

$$y = P_{21}u + P_{22}v \quad (2.2)$$

where  $P_{11}u$ , for example, can represent one of several operations. If  $u, v \in \mathbf{R}$  or  $\mathbf{C}$ ,  $P_{ij} \in \mathbf{R}$  or  $\mathbf{C}$ , then the above represents matrix multiplication. Alternatively the  $P_{ij}$  could be considered as more general operators. For example,  $u, v \in L_{\infty}(0, \infty)$ , and the  $P_{ij}$  are convolution operators.

In the above  $u, v, x$ , and  $y$  could be vectors, and Figure 2.1 and Equations 2.1 and 2.2 would represent matrix operations.

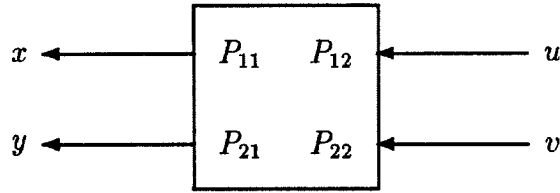


Figure 2.1: Example Block Diagram

### 2.1.2 The Generic Model

A model is considered to be an interconnection of lumped components and perturbation blocks. The inputs to the model, denoted by  $w$ , can represent control inputs, disturbances, and noise. The outputs, denoted by  $e$ , can represent system outputs and other variables of interest. The use of the notation  $e$  is motivated by the robust analysis and synthesis approach discussed in Sections 2.2 and 2.3.

In order to treat large systems of interconnected components, it is necessary to use a model formulation that is general enough to handle interconnections of systems. To illustrate this point consider an affine model description:

$$e = (G + \Delta G_0)w, \quad \|\Delta\| \leq 1,$$

where  $w$  is the input and  $e$  is the output.  $\Delta$  is an unknown but bounded operator, referred to as a perturbation. While such a description could be applied to a large class of linear systems, it is not general enough to describe the interconnection of models. More specifically, an interconnection of affine models is not necessarily affine. As an example, consider unity gain positive feedback around the above system. The new input-output description is

$$e = (G + \Delta G_0)[I - (G + \Delta G_0)]^{-1} w.$$

It is not possible to represent the new system with an affine model. Note that stability questions arise from the consideration of the invertibility of  $[I - (G + \Delta G_0)]$ .

The model structure to be used, referred to as a linear fractional transformation, is given by

$$e = [P_{21}\Delta(I - P_{11}\Delta)^{-1}P_{12} + P_{22}]w, \quad (2.3)$$

where the  $\Delta$  is norm-bounded. Figure 2.2 shows a block diagram equivalent to the system described by Equation 2.3. In general, the elements  $P_{ij}$  are matrix operators and  $\Delta$  is a block diagonal matrix operator.

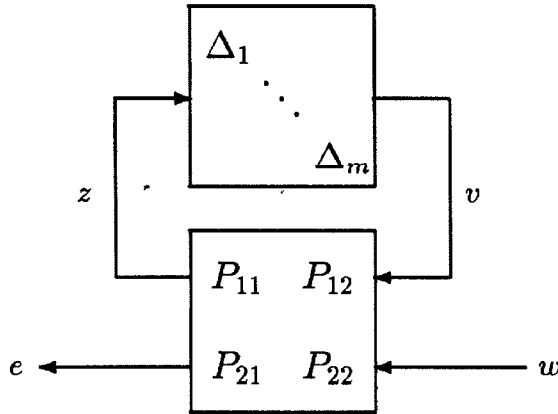


Figure 2.2: Generic Model Structure Including Uncertainty

Linear fractional transformations have the required property that they are preserved under interconnection: any interconnection of linear fractional transformations is still a linear fractional transformation. Consider the previous example. The original system can be modeled in this form by

$$P_{11} = 0, \quad P_{12} = G_0, \quad P_{21} = I, \quad \text{and} \quad P_{22} = G.$$

The system with unity gain feedback is then

$$P_{11} = G_0(I - G)^{-1}, \quad P_{12} = I, \quad P_{21} = G_0(I - G)^{-1}, \quad \text{and} \quad P_{22} = G(I - G)^{-1}.$$

The distinction between perturbations and noise in the model can be seen from both Equation 2.3 and Figure 2.2. Additive noise will enter the model as a component of  $w$ . The  $\Delta$  block represents the unknown but bounded perturbations. It is possible that for some  $\Delta$ ,  $(I - P_{11}\Delta)$  is not invertible. This type of model can describe nominally stable systems which can be destabilized by perturbations. Attributing unmodeled effects purely to additive noise will not have this characteristic.

An interconnection of models of this form will lead to a model with multiple perturbation elements. This is illustrated in Figure 2.2 where the  $\Delta$  in Equation 2.3 is of block diagonal form. Choosing  $\Delta$  to be block diagonal is without loss of generality as the inputs and outputs can always be rearranged in order that this is so. It will be assumed that a model contains  $m$  such blocks:  $\Delta_i$ , and that each block is square. The restriction to square blocks is also without loss of generality as the input and/or outputs of  $P$  can be augmented with zero inputs or outputs.

The block structure is a  $m$ -tuple of integers,  $(k_1, \dots, k_m)$ , giving the dimensions of each  $\Delta_i$  block. It is convenient to define a set  $\Delta$  with the appropriate block structure representing all possible  $\Delta$  blocks, consistent with that described above. By this it is meant that each member of the set of  $\Delta$  be of the appropriate type (complex matrices, real matrices, or operators, for example) and have the appropriate dimensions. In Figure 2.2 the elements  $P_{11}$  and  $P_{12}$  are not shown partitioned with respect to the  $\Delta_i$ . For consistency the sum of the column dimensions of the  $\Delta_i$  must equal the row dimension of  $P_{11}$ . Now define  $\Delta$  as

$$\Delta := \left\{ \text{diag} (\Delta_1 \dots \Delta_m) \mid \dim(\Delta_i) = k_i \right\}.$$

It is assumed that each  $\Delta_i$  is norm-bounded. Scaling  $P$  allows the assumption that the norm bound is one. If the input to  $\Delta_i$  is  $z_i$  and the output is  $v_i$ , then

$$\|v_i\| = \|\Delta_i z_i\| \leq \|z_i\|.$$

It will be convenient to denote the unit ball of  $\Delta$ , the subset of  $\Delta$  norm-bounded by one, by  $\mathbf{B}\Delta$ . More formally

$$\mathbf{B}\Delta := \left\{ \Delta \in \Delta \mid \|\Delta\| \leq 1 \right\}.$$

Linear fractional equations of the form given in Equation 2.3 will be abbreviated to

$$e = F_u(P, \Delta)w$$

where the  $F_u(\cdot, \cdot)$  indicates that the loop is closed around the upper block.  $F_l(\cdot, \cdot)$  will denote the loop closed around a lower block. The uncertain model is now specified by

$$e = F_u(P, \Delta)w, \quad \Delta \in \mathbf{B}\Delta \tag{2.4}$$

References to a robust control model will imply a set description of the form given in Equation 2.4.

### 2.1.3 Assumptions on $P$ and $\Delta$

It will be assumed that the elements of  $P$  are either real-rational transfer function matrices or complex valued matrices. The second case arises in the frequency by frequency analysis of systems.

In modeling a system,  $P_{22}$  defines the nominal model. Input/output effects not described by the nominal model can be attributed to either  $w$  or the perturbation  $\Delta$ . Unmodeled effects which can destabilize a system should be accounted for in  $\Delta$ . Examples would include unmodeled nonminimum phase behavior and nonlinear dynamics. The  $\Delta$  can loosely be considered as accounting for the following. This list is by no means definitive and is only included to illustrate some of the physical effects better suited to description with  $\Delta$ .

- Unmodeled dynamics. Certain dynamics may be difficult to identify, and there comes a point when further identification does not yield significant design performance improvement.
- Known dynamics which have been bounded and included in  $\Delta$  to simplify the model. As controller complexity depends on the order of the model, a designer may not wish to explicitly include all of the known dynamics.
- Parameter variations in a differential equation model. For example, linearization constants which can vary over operating ranges.
- Nonlinear or inconsistent effects. At some point a linear model will no longer account for the residual error in identification experiments.

Several assumptions on  $\Delta$  are possible. In the most general case  $\Delta$  is a bounded operator. Alternatively,  $\Delta$  can be considered as a linear time varying multiplier. This assumption can be used to capture nonlinear effects which shift energy between frequencies. Analysis and synthesis are possible with this assumption; Doyle and Packard [1] discuss the implications of this assumption on robust control theory.

This thesis will focus on the assumption that  $\Delta$  is an unknown complex constant at each frequency. This assumption is implicit in the usual treatment of robust control

analysis and synthesis. The engineering significance of this can be seen by considering the following single-input, single-output example.

A system with additive uncertainty is modeled as

$$y = (G + W\Delta)u \quad (2.5)$$

where  $G$  is the nominal transfer function and  $W$  is a frequency weighting on the uncertainty. The interconnection structure for this example is

$$P = \begin{bmatrix} 0 & W \\ 1 & G \end{bmatrix}. \quad (2.6)$$

A typical Nyquist diagram for such a system is given in Figure 2.3.

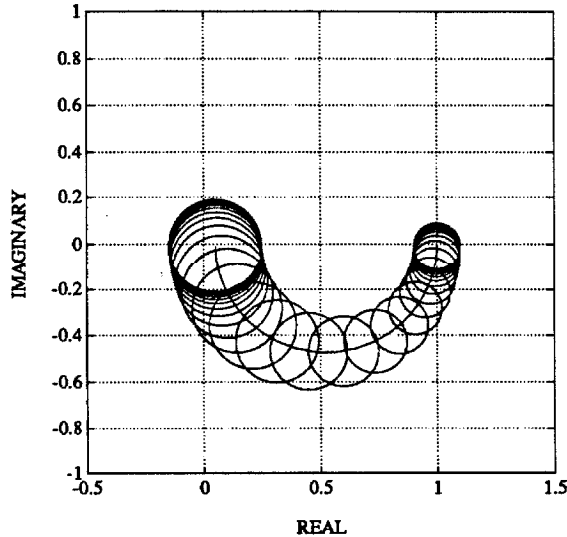


Figure 2.3: Nyquist Diagram of an Example Uncertain SISO System

At each frequency  $\omega$  the transfer function  $F_u(P, \Delta)$  for a particular perturbation  $\Delta$ , lies in a circle, centered at  $G(j\omega)$ , of radius  $|W(j\omega)|$ . Note that the inclusion of a perturbation  $\Delta$  allows elements of the model  $F_u(P, \Delta)$  to be nonminimum phase even though the nominal transfer function is not.

It is possible to further restrict  $\Delta$  to be in  $\mathbf{R}^{n \times n}$ . While this could be a good model for real parameter variations, it is mathematically difficult to handle. In some physical problems the effects of several real parameter variations can usually be modeled well as a single complex variation. For examples the reader is referred to Laughlin [2] and Smith *et al.* [3].

The designer must select the assumptions on  $P$  and  $\Delta$ . An inevitable tradeoff arises between the ideal assumptions given the physical considerations of the system and those for which good synthesis techniques exist. The synthesis questions will be addressed in more detail in Section 2.3.

Systems often do not fall neatly into one of the usual choices of  $\Delta$  discussed above. Consider a nonlinear system linearized about an operating point. If a range of operation is desired, then the linearization constants can be considered to lie within an interval. The model will have a  $\Delta$  block representing the variation in the linearization constants. If this is considered to be a fixed function of frequency, then the model can be considered to be applicable for small changes about any operating point in the range. The precise meaning of small will depend on the effect of the other  $\Delta$  blocks in the problem.

If the  $\Delta$  block is assumed to be time varying, then arbitrary variation is allowed in the operating point. However, this variation is now arbitrarily fast, and the model set now contains elements which will not realistically correspond to any observed behavior in the physical system.

The robust control synthesis theory gives controllers designed to minimize the maximum error over all possible elements in the model set. Including nonphysically motivated signals or conditions can lead to a conservative design as it may be these signals or conditions that determine the worst case error and consequently the controller. Therefore, the designer wants a model which describes all physical behaviors of the system but does not include any extraneous elements.

The most commonly used assumption, which will be treated in this thesis, is that  $\Delta$  is an unknown complex constant at each frequency. The Euclidean norm is assumed spatially giving the maximum singular value as the induced norm. The generic model is therefore

$$e = F_u(P, \Delta)w, \quad \Delta \in \Delta, \quad \sigma_{\max}(\Delta) \leq 1. \quad (2.7)$$

## 2.2 Analysis

### 2.2.1 Measures of Performance

The previous section illustrated that the model has a set representation. In developing the notion of performance the inputs and outputs of a system will also be specified in terms of sets. The generic notation introduced in Section 2.1.2 and Figure 2.2 will be used here. As in the case of the generic model,  $w$  could represent command inputs, noise, and disturbances. For a meaningful definition of performance,  $e$  represents signals which must be kept small, in a sense to be defined below. Such signals could be tracking error or actuator effort, for example. The elements of  $P$  will now be considered to be real-rational transfer functions.

The inputs  $w$  are described only as members of a set. The performance question is then: *For all  $w$  in this set, are all possible outputs  $e$  also in some set?* The following set descriptions are considered, where  $\mathbf{B}$  again denotes the unit ball.

$$\text{Power : } \quad \mathbf{BP} := \left\{ w \mid \lim_{T \rightarrow \infty} \frac{1}{2T} \int_{-T}^T |w(t)|^2 dt \leq 1 \right\} \quad (2.8)$$

$$\text{Energy : } \quad \mathbf{BL}_2 := \left\{ w \mid \|w\|_2^2 = \int_{-\infty}^{\infty} |w(t)|^2 dt \leq 1 \right\} \quad (2.9)$$

$$\text{Magnitude : } \quad \mathbf{BL}_\infty := \left\{ w \mid \|w\|_\infty = \text{ess sup}_t |w(t)| \leq 1 \right\} \quad (2.10)$$

These norms are defined for scalar signals for clarity. The choice of  $w$  and  $e$  as the above sets defines the performance criteria. Consider only the nominal model ( $\Delta = 0$ ,  $e = P_{22}w$ ). The performance can be considered as a test on the induced norm of the system. More formally,

**Lemma 2.1 (Nominal Performance)**

*For all  $w$  in the input set,  $e$  is in the output set*

*iff*  $\|P_{22}\| < 1$ .

Only certain combinations of input and output sets lead to meaningful induced norms. The current work in robust control theory focuses on the cases  $w, e \in \mathbf{BP}$  and  $w, e \in \mathbf{BL}_2$ . Both of these cases lead to the following induced norm.



$$\|P\|_\infty = \sup_\omega \sigma_{\max} [P(j\omega)]. \quad (2.11)$$

The choice of other input and output sets can lead to meaningful norms with engineering significance. For example  $w, e \in \mathbf{BL}_\infty$  is arguably a more suitable choice for some problems and leads to  $\|p\|_1$  as a performance measure where

$$\|p\|_1 = \int_0^\infty |p(t)| dt. \quad (2.12)$$

and  $p(t)$  is the convolution kernel of  $P$ . For a discussion on the other possible selections of input and output sets, and the mathematical advantages of the induced norms, the reader is referred to Doyle [4]. The major advantage of choosing  $\mathbf{BP}$  or  $\mathbf{BL}_2$  is that the test for robust stability ( $F_u(P, \Delta)$  stable for all  $\Delta \in \mathbf{B}\Delta$ ) can also be formulated in terms of the same norm. It will be seen that this allows the performance test to be treated as an additional  $\Delta$  block.

### 2.2.2 Robust Stability and $\mu$

It will be assumed that the interconnection structure  $P$  consists of stable transfer function matrices, where stability is taken to mean that the system has no poles in the closed right half plane. In practice this amounts to assuming that  $P_{22}$  (the nominal model) is stable as the other elements,  $P_{11}$ ,  $P_{12}$ , and  $P_{21}$ , are weighting functions and can be chosen to be stable.

Consider the case where the model has only one  $\Delta$  block ( $m = 1$ ). This is often referred to as unstructured, and the well known result (refer to Zames [5] and Doyle and Stein [6]) is given in the following lemma.

#### Lemma 2.2 (Robust Stability, Unstructured)

$F_u(P, \Delta)$  is stable for all  $\Delta$ ,  $\sigma_{\max}(\Delta) \leq 1$ ,

iff  $\|P_{11}\|_\infty < 1$ .

A generalization of the above is required in order to handle  $F_u(P, \Delta)$  models with more than one  $\Delta$  block ( $m > 1$ ). The positive real valued function  $\mu$  can be defined on a matrix  $M$  by

$$\det(I - M\Delta) \neq 0 \quad \text{for all } \Delta \in \Delta, \quad \sigma_{\max}(\Delta) \leq \gamma,$$

iff  $\gamma\mu(M) < 1$ .

The use of  $\gamma$  is simply to illustrate that  $\mu$  scales, i.e.,

for all  $\alpha \in \mathbf{R}$ ,  $\mu(\alpha M) = |\alpha|\mu(M)$ .

In practice the test is normalized to one with the scaling being absorbed into the interconnection structure. An alternative definition of  $\mu$  is the following. Define a ball of elements of  $\Delta$  of size  $\delta$  by

$$\mathbf{B}_\delta \Delta := \left\{ \Delta \mid \Delta \in \Delta, \sigma_{\max}(\Delta_i) \leq \delta \right\}.$$

Then

$$\mu(M) := \begin{cases} 0 & \text{if no } \Delta \in \Delta \text{ solves } \det(I + M\Delta) = 0 \\ \text{otherwise} & \\ \left[ \min_{\Delta \in \Delta} \left\{ \delta \mid \exists \Delta \in \mathbf{B}_\delta \Delta \text{ such that } \det(I + M\Delta) = 0 \right\} \right]^{-1} & \end{cases}$$

Note that  $\mu$  is essentially defined as the answer to the following robust stability problem.

**Lemma 2.3 (Robust Stability, Structured)**

$F_u(P, \Delta)$  stable for all  $\Delta \in \mathbf{B}\Delta$

iff  $\|\mu(P_{11})\|_\infty < 1$ .

where

$$\|\mu(P_{11})\|_\infty := \sup_\omega \mu[P_{11}(j\omega)].$$

The use of this notation masks the fact that  $\mu$  is also a function of the structure of  $\Delta$ . In applying the matrix definition of  $\mu$  to a real-rational  $P_{11}$ , it has been assumed that  $\Delta$  is a complex constant at each frequency.

### 2.2.3 Robust Performance

The obvious extension to the above is to consider performance in the presence of perturbations  $\Delta$ . For  $e, w \in \mathbf{BP}$  or  $\mathbf{BL}_2$  robust performance is a simple extension of robust stability.

**Lemma 2.4 (Robust Performance)**

$F_u(P, \Delta)$  is stable and  $\|F_u(P, \Delta)\|_\infty \leq 1$  for all  $\Delta \in \mathbf{B}\Delta$

iff  $\|\mu(P)\|_\infty < 1$ ,

where  $\mu$  is taken with respect to an augmented structure  $\widehat{\Delta}$ ,

$$\widehat{\Delta} := \left\{ \text{diag}(\Delta, \Delta_{m+1}) \mid \Delta \in \Delta, \dim(\Delta_{m+1}) = \dim(w) \times \dim(c) \right\}.$$

$\Delta_{m+1}$  can loosely be thought of as a performance block appended to the  $\Delta$  blocks:  $\Delta_1 \dots \Delta_m$ . This result is the major benefit of the choice of input and output signal norms; the norm test for performance is the same as that for stability.

### 2.2.4 Properties of $\mu$

The results presented here are due to Doyle [7]. Fan and Tits [8, 9] have done extensive work on algorithms for tightening the bounds on the calculation of  $\mu$ . Packard [10] has also worked on improvement of the bounds and the extension of these results to the repeated block cases. The upper bound results are particularly important as they will be used to classify models in the development of the model validation problem.

Using  $\Delta = \{\lambda I \mid \lambda \in \mathbf{C}\}$  reduces the definition of  $\mu$  to that of the spectral radius.

$$\Delta = \{\lambda I \mid \lambda \in \mathbf{C}\} \Rightarrow \mu(M) = \rho(M).$$

For the other extreme consider  $\Delta = \{\Delta \mid \Delta \in \mathbf{C}^{n \times n}\}$ ; the definition of  $\mu$  now reduces to that for the maximum singular value,

$$\Delta = \{\Delta \mid \Delta \in \mathbf{C}^{n \times n}\} \Rightarrow \mu(M) = \sigma_{\max}(M).$$

Observe that every possible  $\Delta$  contains  $\{\lambda I \mid \lambda \in \mathbf{C}\}$  and every possible  $\Delta$  is contained in  $\mathbf{C}^{n \times n}$ . These then act as bounds on  $\mu$  for any set  $\Delta$  giving

$$\rho(M) \leq \mu(M) \leq \sigma_{\max}(M).$$

The above bounds are conservative but can be improved by using the following transformations. Define the set

$$\mathcal{D} := \left\{ \text{diag}(d_1 I_1, \dots, d_m I_m) \mid \dim(I_i) = k_i, d_i \in \mathbf{R}, d_i > 0 \right\}, \quad (2.13)$$

where  $m$  is now the total number of  $\Delta$  blocks. Packard [10] shows that the restriction that  $d_i$  be positive real is without loss of generality. For the purposes of bounding  $\mu$  it can be assumed that  $d_m = 1$ . The definition given here, with  $d_m$  not necessarily equal to one, will be used for the model validation problems presented in subsequent chapters. Now define  $\mathcal{Q}$  as the set of unitary operators contained in  $\Delta$ :

$$\mathcal{Q} := \{Q \in \Delta \mid Q^*Q = I\}. \quad (2.14)$$

It is easy to show (refer to Doyle [7]) that  $\mu(M)$  is invariant with respect to certain operations on these sets. The bounds on  $\mu(M)$  can be tightened to

$$\max_{Q \in \mathcal{Q}} \rho(QM) \leq \mu(M) \leq \inf_{D \in \mathcal{D}} \sigma_{\max}(DM D^{-1}). \quad (2.15)$$

It has been shown by Doyle [7] that the lower bound is always equal to  $\mu$  but the implied optimization has local maxima which are not global. For the upper bound Safonov and Doyle [11], have shown that finding the infimum is a convex problem but the upper bound is equal to  $\mu$  only in certain special cases. One such case of relevance here is when  $m \leq 3$ . Computational experience has yet to produce an example where these bounds differ by more than 15 percent. In practically motivated problems the gap is usually much less.

### 2.3 Synthesis

The problem of synthesizing a controller for systems of the type described above can be posed in terms of the preceding analysis. Referring to Figure 2.4, the problem is to find  $K$  such that  $K$  stabilizes  $P$  and

$$\text{For all } \Delta \in \mathbf{B}\Delta, \quad \|\mu(F_l(P, K))\|_{\infty} \leq 1.$$

This is equivalent to guaranteeing that the performance specification is achieved for all members of the  $F_u(P, \Delta)$  model.

This problem has not yet been solved.  $H_{\infty}$  synthesis solves a closely related problem; find  $K$  such that  $K$  stabilizes  $P$  and

$$\|F_l(P, K)\|_{\infty} \leq 1.$$

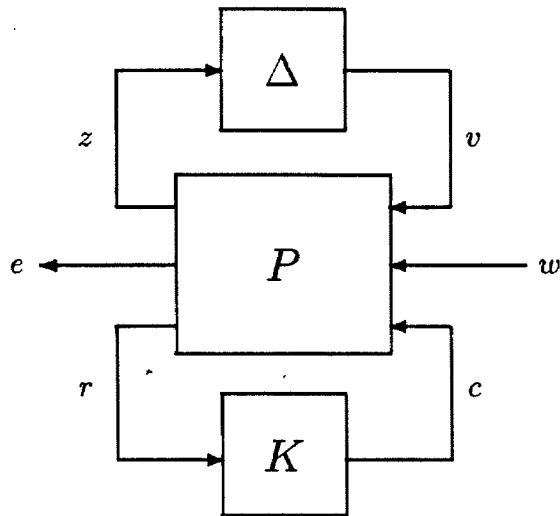


Figure 2.4: The Generic Structure for Synthesis

For more detail on the  $H_\infty$  problem refer to Francis [12] or Doyle *et al.* [13]. Current approaches to the synthesis problem involve iterative application of the above and the procedure for finding an upper bound for  $\mu$ . This involves finding a solution to

$$\inf_{\substack{D \in \mathcal{D} \\ K \text{ stabilizing}}} \|DF_l(P, K)D^{-1}\|_\infty.$$

The reader is referred to Doyle [14] for details of this problem. If this is considered as an optimization of two variables,  $D$  and  $K$ , the problem is convex in each of the variables separately, but not jointly convex. Doyle [4] gives an example where this method reaches a local nonglobal minimum.

## 2.4 Identification and the Role of Model Validation

The preceding sections have introduced a generic model and illustrated the techniques available for the analysis of a system and the synthesis of robust controllers. An engineer having a physical system and wishing to apply the above theory is immediately faced with a problem: how to select good nominal models, bounds on the perturbations and weights on the input and output sets.

An identification methodology is required such that given input-output experiments, and some assumptions on the system, the methodology gives a weighted  $F_u(P, \Delta)$  model which will lead to a satisfactory control design. In the case where uncertainty is attributed to additive noise the procedures for generating models are relatively well developed. Whether or not these models lead to good controller designs is another question. For a terse treatment of the subject the reader is referred to Doyle [15]. Ljung [16] provides a comprehensive treatment of the methods available for identifying systems where the noise is assumed to be stochastic. Such methods are of value here for identifying nominal models.

For the purposes of identification and model validation, the generic  $(P, \Delta)$  structure is modified. Figure 2.5 shows the structure that will be used throughout as the generic identification and model validation structure. In identification experiments certain inputs to the system are known. The input is now partitioned into  $u$  and  $w$  with  $u$  representing the system inputs that are known. As in the previous sections,  $w$  represents the unknown inputs from a specified set: **BP** or **BL<sub>2</sub>**. The output  $y$  represents the measured outputs and is assumed to be known.

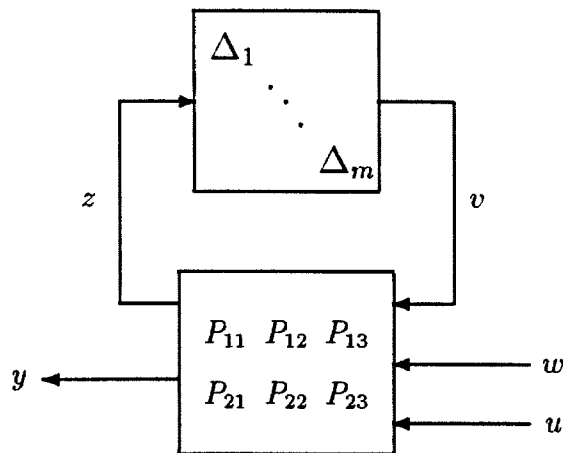


Figure 2.5: The Generic Structure for Identification and Model Validation Problems

It must be stressed that although the same notation is used for interconnection structures for identification, synthesis, and analysis, the elements of the interconnection

structure will change depending upon the use of the structure. For identification,  $P$  will most closely resemble the usual notion of a model of a system. To pose the synthesis problem, the system outputs would be compared to some ideal response or a setpoint input. Additional outputs, actuator action or other internal variables of interest, would be added to make the synthesis problem meaningful. Weights, reflecting the desired performance, would be factored into the inputs and outputs. For the analysis problem, a controller would also be factored into the interconnection structure to form the closed loop system. An example of an interconnection structure for a physically motivated problem is given in Smith *et al.* [3]. The  $F_u(P, \Delta)$  style of notation is used in order that each of these problems be considered in its most general form.

The “black box” identification problem, given  $u$  and  $y$  find the “best” model, is improperly posed. A large set of models will be able to produce the observed data and the measure of suitability of these will depend strongly on the design performance objectives. For example, consider the system illustrated in Figure 2.6.

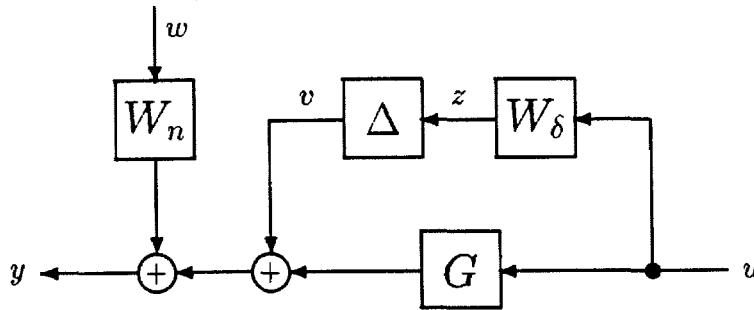


Figure 2.6: An Example Identification Problem

Given any input-output datum  $y$  and  $u$ , it is possible to attribute the discrepancies between the nominal behavior ( $y = Gu$ ) and the observed behavior entirely to  $W_n w$ . Similarly, these residuals can also be attributed entirely to  $\Delta W_\delta$ . In this context the term ambiguity will be introduced; ambiguity is uncertainty about uncertainty. Such a system would present little problem in practice as an experiment with  $u = 0$  could be used to estimate  $W_n w$ , and an additional experiment such that  $Gu \gg W_n w$  could give

a good estimate of  $\Delta W_\delta$ . The goal of good experimental design is to reduce ambiguity in the modeling process.

The above trivially illustrates the value of information about the structure of the model in the identification procedure. First principles modeling will often provide such information and an initial nominal model. Engineering judgement will always be required in the generation of  $F_u(P, \Delta)$  models.

Even if a good model, based on past data, were available, the designer must assume that this model will accurately predict all possible future behaviors of the system. Again judgement is required on the quality and sufficiency of the past data.

A necessary condition for the suitability of a given model is that it can account for all past data. In the robust control framework this means that for each observed input-output datum there exists a model in the model set able to generate that datum. The model validation theory presented here is a test of this condition for  $F_u(P, \Delta)$  models. Consider the data to be a series of experiments. For each experiment the model validation problem is as follows.

**Problem 2.5 (Model Validation)** *Given a model  $F_u(P, \Delta)$  and an input-output datum  $(u, y)$ , does there exist  $(w, \Delta)$ ,  $\|w\| \leq 1$ ,  $\Delta \in \mathbf{B}\Delta$ , such that*

$$y = F_u(P, \Delta) \begin{bmatrix} w \\ u \end{bmatrix}.$$

This simply requires that there is an element of the model set and an element of the unknown input signal set such that the observed datum is produced exactly.

This thesis will present and discuss a method for finding  $(w, \Delta)$  meeting the constraints of the model:  $\|w\| \leq 1$  and  $\Delta \in \mathbf{B}\Delta$ . A  $(w, \Delta)$  pair meeting these constraints will be referred to as admissible. Note that no statement is made relating the particular element of the model set or the particular element of the input signal set to any physical system or signal. Such a relationship does not exist; the only physical meaning that can be drawn from the model is whether or not the model describes the system behavior. Strictly speaking, the only indicator of system behavior is the observed input-output behavior. If, however, for any experimental datum  $(u, y)$  no admissible  $(w, \Delta)$  exists, then the model cannot account for all of the observed behavior and can be considered as



inadequate in its ability to describe the physical system. Such a tool is of use in culling inappropriate models from a group of candidate models.

The model validation test is therefore a necessary condition for any model to describe a physical system. Model validation is a misleading term; strictly speaking, it is never possible to validate a model, only to invalidate it. The fact that every experiment can be accounted for in this manner provides little information about the model and the system. There may be experiments, as yet unperformed, which will invalidate the model. The particular  $w$  and  $\Delta$  do not necessarily bear any relationship to physical signals, but if a consistent property is observed in the  $w$  or  $\Delta$ , then it may be possible to reformulate the model with greater fidelity. There is no guarantee of this, but any such model could of course be tested against the experimental data with the model validation procedure.

In a stochastic additive noise model framework, where all of the observed behaviors are attributed to a nominal model plus noise, identification methods are such that the resulting model is consistent with the past data. In the case of robust control models, no such identification methods exist and *ad hoc* models will require a model validation technique.

The model validation theory has two additional uses. Large systems of many interconnected components can lead to models with a large number of  $\Delta$  blocks. The control design problem is simplified, both conceptually and numerically, if a suitable model with fewer  $\Delta$  blocks can be found. Model validation gives a means of testing such reduced models against the experimental data.

Of significant interest to operating engineers is the problem of fault detection. Given a design model and a controller in operation, the model validation theory gives a means of continuously assessing whether or not the physical system is still described by the design model. It will be seen that the techniques presented here produce the  $v$  and  $w$  (from which the  $\Delta$  can be calculated) that come closest to satisfying the conditions of the model. Gradual deterioration in a system may manifest itself as increasing  $\|\Delta\|$  and  $\|w\|$  required for accountability of the data. A sudden failure may be identified by a sudden jump in the size of the required  $\Delta$  and  $w$ .

Although the model validation question previously posed has a yes/no answer, the theory presented here will, in general, produce  $\Delta$  and  $w$  which can account for the input-output observations. This information is of engineering significance.

## Chapter 3

# The Model Validation Problem

The previous chapter introduced the model validation problem. This is now considered in greater detail. The assumptions on  $F_u(P, \Delta)$  that lead to a meaningful model validation question are considered. The model validation problem is stated in very general terms and then reformulated as a series of computable tests on a candidate signal. This in turn is considered as an optimization problem to find the best, in a sense to be defined later, candidate signal.

Several assumptions are introduced in order to formulate a finite dimensional optimization problem. These assumptions are consistent with those commonly used in robust control analysis and synthesis. An engineering discussion on their significance is also given.

The optimization problems that are studied in the remainder of this thesis are presented. In certain cases it is not always possible to obtain a solution to the desired problem. Consideration of a simpler problem leads to a bound on the solution. This situation is analogous to the gap between  $\mu(M)$  and its upper bound (Equation 2.15) for  $m > 3$ . The relationship between the gap in the  $\mu$  analysis case and the model validation case will be studied in more detail in subsequent chapters.

### 3.1 Properties of the Model Validation Problem

Section 2.4 introduced the statement of the problem. For completeness it is repeated here. Consider the model  $F_u(P, \Delta)$ ,  $\Delta \in \mathbf{B}\Delta$  given as a model for a physical system.

Input output data is taken in a series of experiments. For each datum, or experiment, the model validation question posed below can be asked. Although necessary and sufficient conditions will be derived with respect to a single datum, the model validation theory provides only a necessary condition for the model to describe the system. For each datum the model validation problem is as follows.

**Problem 3.1 (Model Validation)** *Given a model  $F_u(P, \Delta)$  and an input-output datum,  $(u, y)$ , does there exist  $(w, \Delta)$ ,  $\|w\| \leq 1$ ,  $\Delta \in \mathbf{B}\Delta$ , such that*

$$y = F_u(P, \Delta) \begin{bmatrix} w \\ u \end{bmatrix}.$$

Any  $(w, \Delta)$  pair meeting the conditions of Problem 3.1 will be referred to as admissible. The properties of an admissible  $(w, \Delta)$  are

$$\|\Delta\| \leq 1, \quad \Delta \in \mathbf{B}\Delta, \quad (3.1)$$

$$\|w\| \leq 1,$$

and, using the notation introduced for generic identification models in Figure 2.5,

$$y = F_u(P, \Delta) \begin{bmatrix} w \\ u \end{bmatrix} = P_{21}v + P_{22}w + P_{23}u.$$

These conditions are satisfied for every member of the model set accounting for the datum. The conditions on  $\Delta$  can be expressed as a condition on the signals  $v$  and  $z$ . If  $v$  and  $z$  are partitioned conformally with the  $\Delta$  blocks, Equation 3.1 is equivalent to

$$\|v_i\| \leq \|z_i\|, \quad i = 1, \dots, m$$

or

$$\|v_i\| \leq \|(P_{11}v + P_{12}w + P_{13}u)_i\|, \quad i = 1, \dots, m.$$

For convenience define  $x$  as the vector

$$x = \begin{bmatrix} v \\ w \end{bmatrix} \quad (3.2)$$

and define  $R_i$  as a projection of  $v$  onto  $v_i$ .

$$R_i = \text{block row}(0_1, \dots, 0_{i-1}, I_i, 0_{i+1}, \dots, 0_m), \quad (3.3)$$

$$\text{where } \dim(0_j) = k_j \times k_j, \dim(I_i) = k_i \times k_i.$$

A two element row vector notation will be used to consider the partition of  $x$  into  $v$  and  $w$  and  $P[x^T \ u^T]^T$  into  $z$  and  $y$ :

$$[R_i \ 0]x = v_i, \quad [0 \ I]x = w, \quad [R_i \ 0]P \begin{bmatrix} x \\ u \end{bmatrix} = z_i, \quad \text{and} \quad [0 \ I]P \begin{bmatrix} x \\ u \end{bmatrix} = y.$$

The existence of an admissible  $(w, \Delta)$  can now be reduced to  $m + 1$  norm conditions and an equality condition. Using the above definitions and the square of the norms for the test, Theorem 3.2 immediately follows.

**Theorem 3.2 (Model Validation)**

*There exists an admissible  $(w, \Delta)$  for the model validation problem:*

$$y = F_u(P, \Delta) \begin{bmatrix} w \\ u \end{bmatrix}, \quad \|w\| \leq 1, \quad \Delta \in \mathbf{B}\Delta,$$

*iff there exists  $x$  such that the following conditions are satisfied.*

$$i) \quad \|[R_i \ 0]x\|^2 \leq \left\| [R_i \ 0]P \begin{bmatrix} x \\ u \end{bmatrix} \right\|^2, \quad i = 1, \dots, m \quad (3.4)$$

$$ii) \quad \|[0 \ I]x\|^2 \leq 1 \quad (3.5)$$

$$iii) \quad y = [0 \ I]P \begin{bmatrix} x \\ u \end{bmatrix} \quad (3.6)$$

It will be assumed throughout that the model is robustly stable. This assumption is discussed in more detail in Section 3.3.2. Robust stability is equivalent to

$$\mu(P_{11}) < 1.$$

For each admissible  $(w, \Delta)$  the signal  $v$  can be calculated from

$$v = \Delta(I - P_{11}\Delta)^{-1}(P_{12}w + P_{13}u).$$

Note that  $\Delta$  being admissible implies that  $(I - P_{11}\Delta)$  is invertible. For every admissible  $(w, \Delta)$  there exists an  $x$ , where  $x$  is defined by Equation 3.2. This  $x$  will also be referred to as admissible.

It should also be noted that given an admissible  $x$  it is possible to calculate a  $\Delta$  such that

$$v = \Delta z$$

and  $\|\Delta\| = \|v\|/\|z\|$ . Taking each  $\Delta_i$  as

$$\Delta_i = \frac{1}{\|z_i\|^2} v_i z_i^*$$

gives such a  $\Delta$ . With the exception of the scalar case, and the trivial case where  $v = 0$ , the choice of  $\Delta$  is not unique.

### 3.2 Formulation of Optimization Problems

Several optimization problems will be posed to find an admissible  $x$ . The generic structure of the optimization problems will be

$$\min_x f(x) \quad \text{subject to } g_i(x) \leq 0, \quad i = 1, \dots, m.$$

Theorem 3.2 gives  $m + 2$  computable conditions on a candidate vector  $x$  such that  $x$  meets the conditions if and only if there exists  $w$  and  $\Delta$  accounting for the observed datum. The above can be posed as an optimization problem in a number of ways. If any one of the  $m + 1$  inequality relationships is selected as an objective function, the remaining  $m$  inequality relationships and the equality relationship form constraints.

A physically motivated choice for an objective function is

$$\|w\|^2 = \|[0 \ I] x\|^2,$$

giving the following as the constrained optimization problem.

#### Problem 3.3 (Minimum $\|w\|$ Optimization)

$$\begin{aligned} \min_x f(x) \quad \text{subject to} \quad & g_i(x) \leq 0, \quad i = 1, \dots, m \\ & \text{and} \quad g_e(x) = 0, \end{aligned} \tag{3.7}$$

where

$$\begin{aligned} f(x) &= \|[0 \ I] x\|^2, \\ g_i(x) &= \|[R_i \ 0]x\|^2 - \left\| [R_i \ 0]P \begin{bmatrix} x \\ u \end{bmatrix} \right\|^2, \end{aligned}$$

and

$$g_e(x) = y - [0 \ I]P \begin{bmatrix} x \\ u \end{bmatrix}. \tag{3.8}$$

In the single  $\Delta$  block case ( $m = 1$ )  $R_i = I$ . An alternative optimization problem arises by considering  $g_i(x)$  ( $i = 1$ ) as the objective function and  $f(x) - 1$  and  $g_e(x)$  as the constraints. This optimization finds  $w$  and  $v$ , meeting the problem constraints, such that  $\|z\| - \|v\|$  is maximized. In any practically motivated problem, all components of  $v$  will be reflected in the output  $y$  effectively penalizing the size of  $v$ . This optimization

problem can then be thought of as finding the minimum  $\|\Delta\|$  that accounts for the datum. Such a problem could be of engineering significance in attempting to reduce the bound on the size of the perturbations included in a model. Section 3.3.1 will give an engineering motivation for minimum  $\|w\|$  problem. It is this problem that will be considered in the remainder of this thesis.

If  $\hat{x}$  solves Problem 3.3, in other words  $\hat{x}$  achieves the minimum of  $f(x)$  subject to the constraints, then it only remains to test the condition:

$$\| [0 \ I] \hat{x} \| \leq 1. \quad (3.9)$$

If Equation 3.9 is satisfied then  $\hat{x}$  is admissible and the model can account for the datum. If  $\hat{x}$  solves Problem 3.3 and Equation 3.9 is not satisfied, the model cannot account for the datum.

### 3.2.1 Removal of the Equality Constraint

This section will introduce a reparametrization of  $x$  which removes the equality condition of Equation 3.8 and reduces the dimension of the search over  $x$ . This is achieved by parametrizing all solutions of Equation 3.8 and substituting this parametrization back into the optimization problem.

Consider the solutions to

$$y - P_{23}u = [P_{21} \ P_{22}] x \quad (3.10)$$

as

$$x = x_0 \oplus x_1 \quad (3.11)$$

with  $x_0$  being a solution to

$$y - P_{23}u = [P_{21} \ P_{22}] x_0$$

and

$$x_1 \in \text{Ker}[P_{21} \ P_{22}].$$

There is a unique  $x_0$  orthogonal to the kernel of  $[P_{21} \ P_{22}]$ . A means of obtaining  $x_0$  from any solution to Equation 3.10 will subsequently be given.

In attempting to perform this parametrization of  $x$ , several possibilities can arise. Certain of these immediately lead to a solution to the model validation problem.

- i)  $y - P_{23}u \notin \text{Range}[P_{21} P_{22}]$ . In this case there is no admissible  $x$  and consequently no  $w$  or  $\Delta$  that can account for the datum.
- ii)  $y - P_{23}u \in \text{Range}[P_{21} P_{22}]$  but  $\text{Ker}[P_{21} P_{22}]$  is trivial. There is a unique  $x$  specified by the input  $u$  and output  $y$ . It only remains to calculate the norms of  $w$  and  $\Delta$  to determine if this  $x$  is admissible.
- iii)  $y - P_{23}u \in \text{Range}[P_{21} P_{22}]$  and  $\dim(\text{Ker}[P_{21} P_{22}]) > 0$ . This is the generic case where the reparametrization of  $x$  has removed the equality constraint and reduced the dimension of the search for  $x$  by restricting it to the kernel of  $[P_{21} P_{22}]$ .

The first two possibilities give an immediate answer to the model validation question. In the first case the answer is no: the model cannot account for the datum. In the second case either answer is possible depending upon the outcome of the calculation of the norms of  $w$  and  $\Delta$ . The case of interest is the third. Throughout the remainder of this thesis it is assumed that  $y - P_{23}u \in \text{Range}[P_{21} P_{22}]$  and  $\dim(\text{Ker}[P_{21} P_{22}]) > 0$ .

A singular value decomposition will allow the restriction of the search to the kernel of  $[P_{21} P_{22}]$ . A detailed description of the singular value decomposition and algorithms for its calculation are discussed in Golub and Van Loan [17]. The discussion presented here will assume that  $P$  is a matrix and  $x$  is a vector. These assumptions will be considered in more detail in the next section.

There exists  $U_p$  and  $V_p$ ,  $U_p^*U_p = I$ ,  $V_p^*V_p = I$  such that

$$[P_{21} P_{22}] = U_p \Sigma V_p^*$$

where  $\Sigma$  is the matrix of singular values. Note that in the case where the row and column dimensions of  $[P_{21} P_{22}]$  are not equal,  $\Sigma$  will not be diagonal. However, all of the nonzero elements are on the main diagonal, and the partitioning described below is still applicable. If the kernel of  $[P_{21} P_{22}]$  is nonzero then  $\Sigma$  has one or more zeros on the main diagonal. Partition  $U_p$  and  $V_p$  accordingly with  $\Sigma_+$  being the diagonal matrix of nonzero singular values. Then



$$\begin{bmatrix} P_{21} & P_{22} \end{bmatrix} x = \begin{bmatrix} U_+ & U \end{bmatrix} \begin{bmatrix} \Sigma_+ & 0 \\ 0 & 0 \end{bmatrix} \begin{bmatrix} V_+^* \\ V^* \end{bmatrix} x.$$

For  $x$  defined by  $x = Vx_e$ , i.e., the span of the right singular vectors corresponding to the zero singular value,

$$\begin{aligned} \begin{bmatrix} P_{21} & P_{22} \end{bmatrix} x &= \begin{bmatrix} U_+ & U \end{bmatrix} \begin{bmatrix} \Sigma_+ & 0 \\ 0 & 0 \end{bmatrix} \begin{bmatrix} V_+^* \\ V^* \end{bmatrix} Vx_e \\ &= \begin{bmatrix} U_+ & U \end{bmatrix} \begin{bmatrix} \Sigma_+ & 0 \\ 0 & 0 \end{bmatrix} \begin{bmatrix} 0 \\ x_e \end{bmatrix} \\ &= 0. \end{aligned}$$

Note that the columns of  $V$  are orthogonal to each other and of unit norm. The assumption that  $x_0$  be orthogonal to all columns of  $V$  is simple to enforce. Given any solution  $\hat{x}_0$ ,

$$y - P_{23}u = \begin{bmatrix} P_{21} & P_{22} \end{bmatrix} \hat{x}_0,$$

$x_0$  can be calculated by

$$x_0 = (I - VV^*)\hat{x}_0.$$

This then gives a suitable parametrization of  $x$  in terms of  $x_e$ . It is convenient to define the set  $\mathcal{X}_e$  as the set of all  $x$  meeting the equality constraint (Equation 3.8). More formally,

$$\mathcal{X}_e = \left\{ x \mid x = x_0 + Vx_e \right\}. \quad (3.12)$$

### 3.3 Assumptions on $P$ , $w$ and $\Delta$

The previous sections have posed the model validation problem and an associated optimization problem. The formulation is very general; the operators  $P_{ij}$  may have infinite dimensional kernels and the resulting optimization will then be infinite dimensional. This section will introduce assumptions which will lead to the consideration of a simpler problem, the constant matrix problem. Although simpler, this problem is not without engineering significance.

### 3.3.1 Rationale of the Constant Matrix Formulation

This section will introduce the assumptions typically used with  $\mu$  analysis:  $\Delta$  is a complex constant at each frequency, and the interconnection structure  $P$  consists of matrices of real-rational transfer functions. Only an outline will be given here. For a more concrete example, Chapter 9 will study an experimental problem in detail using the method discussed below.

As an example, the bounded power framework will be discussed here. To be amenable to numerical optimization, this problem must be formulated in a digital framework. Two properties must be preserved in the digital format: the norm of the signals and the mapping of the input onto the output. It should be noted that the actual data will almost certainly be digital. In the case that it is not, an analog recording for example, it will have to be digitized in order to perform numerical computations. The digital domain is the most appropriate for the practical consideration of real data.

To see how this might be done, consider an experimental datum  $(y(n), u(n))$ ,  $n = 0, \dots, L - 1$  consisting of  $L$  samples with a sample period of  $T$  seconds. It is assumed that the datum arises from the sampling of underlying continuous time signals  $y(t)$  and  $u(t)$ . The quantity of interest is the power of the signals, defined for a signal  $w(t)$  by

$$\|w(t)\|_P = \left\{ \lim_{\tau \rightarrow \infty} \frac{1}{2\tau} \int_{-\tau}^{\tau} |w(t)|^2 dt \right\}^{1/2} \quad (3.13)$$

The notation is somewhat misleading as  $\|\bullet\|_P$  is only a seminorm. In order to apply a Discrete Fourier Transform (DFT) analysis, it will be assumed that  $y(t)$  and  $u(t)$  are periodic. This will have the effect of requiring  $v(t)$  and  $w(t)$  to also be periodic. Note however that this assumption removes the limit from the calculation of the power seminorm. By appropriate selection of  $T$  and  $L$ , the integral in Equation 3.13 can be replaced by a summation leading to the following approximation.

$$\|w(t)\|_P \approx \left\{ \frac{1}{TL} \sum_{n=0}^{L-1} T |w(n)|^2 \right\}^{1/2}$$

Now consider a DFT pair,

$$W(k) = \sum_{n=0}^{L-1} w(n) e^{-j \frac{2\pi}{L} kn}$$

$$w(n) = \frac{1}{L} \sum_{k=0}^{L-1} W(k) e^{j \frac{2\pi}{L} kn}.$$

Parseval's relation for this pair is

$$\sum_{n=0}^{L-1} |w(n)|^2 = \frac{1}{L} \sum_{k=0}^{L-1} |W(k)|^2.$$

The reader is referred to Oppenheim and Schaffer [18] for a thorough discussion on the properties of this transform.

This now gives

$$\|w(t)\|_P \approx \frac{1}{L} \left\{ \sum_{k=0}^{L-1} |W(k)|^2 \right\}^{1/2}. \quad (3.14)$$

The signals under consideration are now in the discrete frequency domain. The  $W(k)$  can be considered as samples of the  $z$ -transform of  $w(n)$  on the unit circle at the points

$$z = e^{j \frac{2\pi}{L} k}, \quad k = 0, \dots, L-1.$$

The interconnection structure  $P$  must also be transformed into the digital domain.  $P$  is generally specified as a function of a continuous frequency variable  $s$ . The transformation of  $P(s)$  to an equivalent digital system  $P(z)$  must preserve the convolution properties. In the digital case convolution refers to periodic rather than linear convolution. The input and output signals will be equal to sampled versions of continuous time signals only if the continuous time signals are periodic.

To determine an equivalent digital system  $P(z)$ , consider  $P(s)$  to be preceded by a zero order hold and followed by a sampler of period  $T$ . For simplicity it will be assumed that the hold and the sampler operate at the same time points. This assumption is not necessary but simplifies the calculation of the equivalent digital system. Kwakernaak and Sivan [19] study this problem for more general systems than those presented here. Chapter 9 will provide, by example, more detail on this procedure.

Now consider  $P(z)$  evaluated at the same  $L$  discrete frequency points,

$$z = e^{j \frac{2\pi}{L} k}, \quad k = 0, \dots, L-1.$$

The notation  $P(k)$  will be used to denote

$$P(k) = P(z) \Big|_{z=e^{j \frac{2\pi}{L} k}}.$$

The requirement that the inputs  $v$ ,  $w$ , and  $u$  are mapped onto the outputs  $y$  and  $z$  is now simply

$$\begin{bmatrix} Z(k) \\ Y(k) \end{bmatrix} = P(k) \begin{bmatrix} V(k) \\ W(k) \\ U(k) \end{bmatrix}, \quad k = 0, \dots, L-1.$$

Assuming  $\Delta$  to be independent between frequencies allows the problem to be considered as  $L$  constant matrix problems. Furthermore, as  $y(n)$  and  $u(n)$  are real, it suffices to consider only the points  $k = 0, \dots, L/2$ .

The minimum of Equation 3.14 is achieved by minimizing  $|W(k)|^2$  at each  $k$ . This then gives  $L/2 + 1$  constant matrix problems with the final test being the following condition.

$$\|w(t)\|_P \approx \frac{1}{L} \left\{ |W(0)|^2 + 2 \sum_{k=1}^{L/2-1} |W(k)|^2 + |W(L/2)|^2 \right\}^{1/2} \leq 1.$$

Note that the assumptions on  $\Delta$  have allowed the corresponding norm constraints to be applied independently at each frequency. The equality constraint can also be applied at each frequency. In contrast to this, note that if the norm relationship for one of the  $\Delta_i$  blocks was chosen as an objective, the constraint  $\|w\| \leq 1$  would not decompose into frequency by frequency bounds. This is another reason for the choice of  $\|w\|$  as the optimization objective function.

Formulating a meaningful experiment and equivalent digital problem requires considerable engineering judgement. The reader is referred to Chapter 9 for a discussion of some of the engineering issues.

The above discussion provides an engineering motivation for considering a frequency by frequency approach to the problem. A discrete frequency domain representation will be obtained for  $W(k)$  and simple calculation will provide one for  $\Delta(k)$ . An inverse DFT could provide a time domain version of  $w(n)$  and  $\Delta(n)$ . Care must be taken in interpreting these as causality has not been assumed in the derivation of the  $W(k)$  and  $V(k)$ . This situation is analogous to that for  $\mu$  analysis.

Solving the model validation optimization problems can produce sampled versions of  $w(t)$  and  $v(t)$  consistent with the input-output data and the assumed norm bound on the uncertainty. This does not mean that these signals exist in the physical system.

### 3.3.2 Model Requirements

The analysis treatment given by Doyle [7, 4] includes the possibility of repeated  $\Delta$  blocks. The model validation theory presented here currently handles only the nonrepeated case. This represents some loss of generality, and future work should include this case. The discussion to be presented here assumes that the spatial norm is the Euclidean norm. This assumption is discussed in the next section.

Models including unstable transfer functions pose a problem for model validation. It is not possible to set up an experiment which would allow the testing of the system with the assumptions on the input and output signals:  $y$  and  $u$  both in  $\mathbf{BP}$  or in  $\mathbf{BL}_2$ . In practice an unstable physical system would be stabilized by a feedback controller before experiments are performed. This can easily be handled in the model validation framework as the interconnection structure  $P$  will now include the stabilized system. The interconnection structures to be considered here are therefore restricted to be stable for all  $\Delta \in \mathbf{B}\Delta$ . This is only a constraint on the nominal model.

Robust stability is equivalent to the condition that

$$\|\mu(P_{11})\|_\infty < 1,$$

where it is understood that  $P_{11}$  is a function of frequency. For the case of a single  $\Delta$  block this is simply

$$\sup_\omega \sigma_{\max}(P_{11}) < 1. \quad (3.15)$$

Consider the subset of stable models, denoted  $\sigma$ -stable, defined by

$$\inf_{D \in \mathcal{D}} \sigma_{\max}(DP_{11}D^{-1}) < 1 \text{ for all } \omega,$$

where  $\mathcal{D}$  is defined by Equation 2.13. There exist stable models which are not  $\sigma$ -stable as

$$F_u(P, \Delta) \text{ is stable iff } \|\mu(P_{11})\|_\infty < 1$$

and

$$\|\mu(P_{11})\|_\infty \leq \inf_{D \in \mathcal{D}} \sigma_{\max}(DP_{11}D^{-1}).$$

The upper bound is only guaranteed to be equal to  $\mu$  for three or fewer blocks. In this case all stable models are  $\sigma$ -stable.

### 3.3.3 Formulation with the Euclidean Spatial Norm

Doyle [4] argues that the difference between spatial norms in control design problems is less significant than between temporal norms. The Euclidean norm provides a more convenient mathematical formulation and will be used here.

Define the matrices,  $T_i$ ,  $i = 1, \dots, m$  by

$$\begin{aligned} T_i &= R_i^T R_i \\ &= \text{diag}(0_1, \dots, 0_{i-1}, I_i, 0_{i+1}, \dots, 0_m). \end{aligned}$$

The model validation theorem is now as follows.

#### Theorem 3.4 (Model Validation, Constant Matrix)

*There exists an admissible  $(w, \Delta)$  for the model validation problem:*

$$y = F_u(P, \Delta) \begin{bmatrix} w \\ u \end{bmatrix}, \quad \|w\| \leq 1, \quad \Delta \in \mathbf{B}\Delta,$$

*iff there exists  $x$  such that:*

- i)  $x^* \begin{bmatrix} T_i & 0 \\ 0 & 0 \end{bmatrix} x \leq [x^* \ u^*] P^* \begin{bmatrix} T_i & 0 \\ 0 & 0 \end{bmatrix} P \begin{bmatrix} x \\ u \end{bmatrix}, \quad i = 1, \dots, m.$
- ii)  $x^* \begin{bmatrix} 0 & 0 \\ 0 & I \end{bmatrix} x \leq 1.$
- iii)  $y = [0 \ I] P \begin{bmatrix} x \\ u \end{bmatrix}.$

The minimum  $\|w\|$  optimization problem for this formulation of the model validation problem is given below. Note that the equality constraint (condition *iii* above) is reflected as a restriction on the search to  $x \in \mathcal{X}_e$ .

#### Problem 3.5 (Minimum $\|w\|$ , Constant Matrix)

$$\min_{x \in \mathcal{X}_e} f(x) \quad \text{subject to } g_i(x) \leq 0, \quad i = 1, \dots, m,$$

where

$$f(x) = x^* \begin{bmatrix} 0 & 0 \\ 0 & I \end{bmatrix} x \tag{3.16}$$

and

$$g_i(x) = x^* \begin{bmatrix} T_i & 0 \\ 0 & 0 \end{bmatrix} x - \begin{bmatrix} x^* & u^* \end{bmatrix} P^* \begin{bmatrix} T_i & 0 \\ 0 & 0 \end{bmatrix} P \begin{bmatrix} x \\ u \end{bmatrix}. \quad (3.17)$$

The reparametrization of Section 3.2.1 can be used to cast the problem into one in terms of  $x_e$  rather than  $x$ . This results in different objective and constraint functions. The notation  $f_e(x_e)$  and  $g_{ei}(x_e)$  will be used to distinguish these from those of Equations 3.16 and 3.17 above.

### Problem 3.6

$$\min_{x_e} f_e(x_e) \quad \text{subject to } g_{ei}(x_e) \leq 0, \quad i = 1, \dots, m,$$

where

$$f_e(x_e) = (x_0^* + x_e^* V^*) \begin{bmatrix} 0 & 0 \\ 0 & I \end{bmatrix} (x_0 + V x_e) \quad (3.18)$$

and

$$g_{ei}(x_e) = (x_0^* + x_e^* V^*) \begin{bmatrix} T_i & 0 \\ 0 & 0 \end{bmatrix} (x_0 + V x_e) - \begin{bmatrix} x_0^* + x_e^* V^* & u^* \end{bmatrix} P^* \begin{bmatrix} T_i & 0 \\ 0 & 0 \end{bmatrix} P \begin{bmatrix} x_0 + V x_e \\ u \end{bmatrix}. \quad (3.19)$$

Consider the constraint equations in more detail.

$$g_{ei}(x_e) = (x_e^* V^* + x_0^*) \begin{bmatrix} T_i - P_{11}^* T_i P_{11} & -P_{11}^* T_i P_{12} \\ -P_{12}^* T_i P_{11} & -P_{12}^* T_i P_{12} \end{bmatrix} (x_0 + V x_e) - 2 \operatorname{Re} \left\{ (x_0^* + x_e^* V^*) \begin{bmatrix} P_{11}^* \\ P_{12}^* \end{bmatrix} T_i P_{13} u \right\} - u^* P_{13}^* T_i P_{13} u$$

This formulation is somewhat cumbersome but clearly shows the structure of the quadratic term. The constraints are indefinite quadratic inequalities. In contrast, the objective function is a positive semidefinite quadratic.

### 3.4 Solving the Model Validation Problem: A Summary of the Results

The previous sections have formulated the model validation problem and, in the constant matrix case, set up an optimization problem to solve it. Having now introduced this problem, and sufficient notation, it is appropriate to outline the results that will be developed in subsequent chapters.

The approach taken is to consider the application of Lagrange multipliers to Problem 3.5. It is well known, and detailed in Chapter 4, that finding a saddlepoint of the Lagrangian is a sufficient condition for solving the optimization problem.

There is a strong relationship between the model validation problem and  $\mu$ . There is also a strong relationship between the Lagrange multipliers and the  $D$  scalings of the upper bound calculation (Equation 2.15). As is the case with  $\mu$  and its upper bound, the Lagrange multiplier approach does not always yield the solution. The block structure dimensionality issues that arise in the consideration of the upper bound for  $\mu$  also arise in the model validation problem.

In considering any equivalence between the number of blocks in the model validation and  $\mu$  problems, one must count the equality constraint as a block. The following situations arise:

- $m = 1$  The single perturbation block problem can always be solved by finding a saddlepoint of the Lagrangian. This is shown in Section 5.3.3.
- $m = 2$  If  $\dim(V) > 1$  then a saddlepoint of the Lagrangian still exists. The dimensionality of  $V$  enters here, and not in the similar three block  $\mu$  problem, because of the difference between the equality constraint and the usual  $\Delta$  block constraint. Section 7.5 provides these results.
- $m \geq 3$  A saddlepoint of the Lagrangian does not always exist. Section 8.3.2 presents a counterexample. In the four block  $\mu$  case it is known that the upper bound is not necessarily equal to  $\mu$ .

In the cases where a solution to Problem 3.5 can be found, the model validation question, *Does the model account for the datum?*, can be answered exactly. As in the  $\mu$



case, it is possible to bound the solution to Problem 3.5. This is based on always being able to answer the  $m = 1$  problem and is considered in more detail in Section 5.2.2.

A geometric framework, which allows the inclusion of known inputs and outputs in robust analysis problems, is introduced in Chapters 6 and 7. The model validation problem and  $\mu$  are then considered as subproblems of the general problem. The dimensionality issues are inherited from the underlying general problem. The existence of Lagrange multipliers (or  $D$  scalings for  $\mu$ ) is then the result of a simple geometric condition involving a separating hyperplane.

## Chapter 4

# Lagrange Multipliers and Duality

This chapter reviews some well known optimization results about Lagrange multipliers and duality. These will be used in subsequent chapters to study the model validation optimization problem. Lagrange multipliers may not be the most effective way to solve this optimization, but their use in this case leads to an interesting analogy with the current calculation techniques for  $\mu$ . The reader is referred to Wismer and Chattergy [20] for an introduction to the subject and Mangasarian [21] for more comprehensive details. Rockafellar [22] is a complete reference on convexity.

Chapters 6 and 7 will introduce and use an geometric interpretation of Lagrange multipliers. Luenberger [23] is a good background reference for this approach.

### 4.1 Preliminaries

The following presents the notion of convexity and develops tests for the convexity of quadratic forms. These definitions and results are commonly known but are included here for completeness.

$\Gamma \in \mathbf{C}^n$  is a *convex set* if for all  $x_1, x_2 \in \Gamma$ , and for all  $\alpha \in \mathbf{R}, \alpha \in [0, 1]$ ,

$$(1 - \alpha)x_1 + \alpha x_2 \in \Gamma.$$

A functional  $f(x)$  defined on a convex set  $\Gamma \subset \mathbf{C}^n$  (for all  $x \in \Gamma, f(x) \in \mathbf{R}$ ), is called a *convex functional* if for all  $x_1, x_2 \in \Gamma$  and  $\alpha \in \mathbf{R}, \alpha \in [0, 1]$ ,

$$(1 - \alpha)f(x_1) + \alpha f(x_2) \geq f((1 - \alpha)x_1 + \alpha x_2).$$

The above functional  $f(x)$  is *strictly convex* if for all  $x_1, x_2 \in \Gamma$  and  $\alpha \in \mathbf{R}$ ,  $\alpha \in (0, 1)$ ,

$$(1 - \alpha)f(x_1) + \alpha f(x_2) > f((1 - \alpha)x_1 + \alpha x_2).$$

A functional  $f(x)$  defined on a convex set  $\Gamma \subset \mathbf{C}^n$  (for all  $x \in \Gamma$ ,  $f(x) \in \mathbf{R}$ ), is called a *concave functional* if for all  $x_1, x_2 \in \Gamma$  and  $\alpha \in \mathbf{R}$ ,  $\alpha \in [0, 1]$ ,

$$(1 - \alpha)f(x_1) + \alpha f(x_2) \leq f((1 - \alpha)x_1 + \alpha x_2).$$

Similarly, the functional  $f(x)$  is *strictly concave* if for all  $x_1, x_2 \in \Gamma$  and  $\alpha \in \mathbf{R}$ ,  $\alpha \in (0, 1)$ ,

$$(1 - \alpha)f(x_1) + \alpha f(x_2) < f((1 - \alpha)x_1 + \alpha x_2).$$

A quadratic form  $x^*Ax$ ,  $x \in \Gamma \subset \mathbf{C}^n$ , where  $A$  is Hermitian ( $A^* = A$ ), is *positive definite* if for all  $x \in \Gamma$ ,  $x \neq 0$ ,  $x^*Ax > 0$ .

The above quadratic form is *positive semidefinite* if for all  $x \in \Gamma$ ,  $x \neq 0$ ,  $x^*Ax \geq 0$ .

For a twice differentiable functional  $f(x)$  defined on  $\Gamma \subset \mathbf{C}^n$ , the symmetric matrix of second partial derivatives is known as the Hessian and is denoted here by  $H[f(x)]$ :

$$H[f(x)] = \begin{bmatrix} \frac{\partial^2 f}{\partial x_1^2}(x) & \dots & \frac{\partial^2 f}{\partial x_1 \partial x_n}(x) \\ \vdots & \ddots & \vdots \\ \frac{\partial^2 f}{\partial x_n \partial x_1}(x) & \dots & \frac{\partial^2 f}{\partial x_n^2}(x) \end{bmatrix}.$$

For notational simplicity it is assumed that  $\dim(\Gamma) = n$ . Note that in the case of a quadratic form  $x^*Ax$ , where  $A$  is Hermitian, the Hessian  $H[x^*Ax] = 2A$ .

The following lemmas relate the positive definiteness (or semidefiniteness) of the Hessian to the convexity of the functional.

#### Lemma 4.1

*A twice differentiable functional  $f(x)$ , defined on an open set  $\Gamma \subset \mathbf{C}^n$ , is convex iff the Hessian  $H(x)$  is positive semidefinite.*

#### Lemma 4.2

*For a twice differentiable functional  $f(x)$ , defined on an open set  $\Gamma \subset \mathbf{C}^n$ , if  $H(x)$  is positive definite, then  $f(x)$  is strictly convex on  $\Gamma$ .*

## 4.2 Optimization Problems

The generic optimization problem will be formulated as

$$\min_{x \in \Gamma} f(x) \quad \text{subject to} \quad g_i(x) \leq 0, \quad i = 1, \dots, m. \quad (4.1)$$

where  $f(x)$  is referred to as the *objective functional* and the  $g_i(x)$  are the *constraints*.

The following terms will be used. The *feasible region* of the optimization problem (Equation 4.1), denoted here by  $F$ , is

$$F = \left\{ x \mid g_i(x) \leq 0, x \in \Gamma, i = 1, \dots, m \right\}.$$

This is simply the region of  $\Gamma$  where the constraints of the optimization problem are satisfied.

If there exists  $\bar{x}$  such that

$$f(\bar{x}) = \min_{x \in \Gamma} f(x), \quad \text{subject to} \quad g_i(x) \leq 0, i = 1, \dots, m, \quad (4.2)$$

then  $f(\bar{x})$  is called the *global minimum* of the optimization problem (Equation 4.1).

Finding the global minimum is the goal of the optimization. However, it is usually only possible to find a local minimum:

If there exists an open ball  $B_\delta(\hat{x})$  about  $\hat{x}$ , with radius  $\delta > 0$  where

$$f(\hat{x}) = \min_{x \in B_\delta(\hat{x}) \cap \Gamma} f(x), \quad \text{subject to} \quad g_i(x) \leq 0, \quad i = 1, \dots, m,$$

then  $f(\hat{x})$  is a *local minimum* of the optimization problem (Equation 4.1).

The following lemmas relate the various minima to conditions involving convexity. They are presented without proof.

### Lemma 4.3

*If  $f(x)$  is convex then all local minima to the problem*

$$\min_{x \in \Gamma} f(x)$$

*are also global minima.*

### Lemma 4.4

*If  $f(x)$  is strictly convex, then there is a unique global minimum to the problem*

$$\min_{x \in \Gamma} f(x).$$

Clearly, convexity is a powerful property in optimization problems.

### 4.3 Lagrange Multipliers

Constrained optimization problems can be studied with Lagrange multipliers. Given the standard problem of Equation 4.1, referred to as the primal problem,

$$\min_{x \in \Gamma} f(x) \quad \text{subject to} \quad g_i(x) \leq 0, \quad i = 1, \dots, m.$$

form the Lagrangian, defined for  $\lambda_i \geq 0 \quad i = 1, \dots, m$ , as

$$L(x, \lambda) = f(x) + \sum_{i=1}^m \lambda_i g_i(x)$$

where  $\lambda = [\lambda_1, \dots, \lambda_m]^T$ . The constraint that  $\lambda_i > 0$  (or  $\lambda_i \geq 0$ ) will be abbreviated to  $\lambda > 0$  (or respectively  $\lambda \geq 0$ ). A dual function  $h(\lambda)$  is now defined as

$$h(\lambda) = \min_x L(x, \lambda).$$

This provides a lower bound on the primal problem solution; for  $\lambda \geq 0$ ,

$$h(\lambda) \leq f(\bar{x}),$$

where  $\bar{x}$ , as defined in Equation 4.2 achieves the minimum subject to the  $m$  constraints. The dual problem can be considered as tightening this bound. More formally, the dual problem is

$$\max_{\lambda \geq 0} h(\lambda). \tag{4.3}$$

A saddlepoint is a  $(x, \lambda)$  pair, denoted here by  $(\bar{x}, \bar{\lambda})$ , such that for all  $x \in \Gamma$  and for all  $\lambda \geq 0$ ,

$$L(\bar{x}, \lambda) \leq L(\bar{x}, \bar{\lambda}) \leq L(x, \bar{\lambda}). \tag{4.4}$$

Kuhn and Tucker [24] give an alternative but equivalent characterization of the saddlepoint for differentiable functions  $f(x)$  and  $g(x)$ . The term Kuhn-Tucker saddlepoint will often be used synonymously with saddlepoint, particularly when the discussion requires the definition of the form given in the following theorem.

**Theorem 4.5**

A point  $(\bar{x}, \bar{\lambda})$  with  $\bar{\lambda} \geq 0$  is a saddlepoint of the Lagrangian  $L(x, \lambda)$  iff the following conditions are satisfied.

- i)  $\bar{x}$  minimizes  $L(x, \bar{\lambda})$  over all  $x$ .
- ii)  $g_i(\bar{x}) \leq 0$ , for all  $i = 1, \dots, m$ .
- iii)  $\bar{\lambda}_i g_i(\bar{x}) = 0$ , for all  $i = 1, \dots, m$ .

Notice that condition *i* requires a global minimization of the Lagrangian. This may be difficult to verify for a nonconvex problem.

**Proof of Theorem 4.5:** Assume that  $(\bar{x}, \bar{\lambda})$  is a saddlepoint, defined by Equation 4.4.

Condition *i* is simply a restatement of the right hand inequality of Equation 4.4. To see that conditions *ii* and *iii* must also hold, consider the left hand inequality of Equation 4.4,

$$L(\bar{x}, \lambda) \leq L(\bar{x}, \bar{\lambda}).$$

Using the definition of the Lagrangian gives

$$f(\bar{x}) + \sum_{i=1}^m \lambda_i g_i(\bar{x}) \leq f(\bar{x}) + \sum_{i=1}^m \bar{\lambda}_i g_i(\bar{x})$$

which implies that

$$\sum_{i=1}^m (\lambda_i - \bar{\lambda}_i) g_i(\bar{x}) \leq 0 \quad \text{for all } \lambda_i \geq 0. \quad (4.5)$$

Clearly  $g_i(\bar{x}) \leq 0$  for all  $i = 1, \dots, m$ . If for any  $i$  this were not so, then a sufficiently large choice of the corresponding  $\lambda_i$  would violate Equation 4.5. Therefore, the point  $\bar{x}$  satisfies the constraints of the optimization, and condition *ii* of the theorem is satisfied.

Now choose  $\lambda_i = 0$  in Equation 4.5 giving

$$- \sum_{i=1}^m \bar{\lambda}_i g_i(\bar{x}) \leq 0 \quad \text{for all } \lambda_i \geq 0. \quad (4.6)$$

Noting that  $g_i(\bar{x}) \leq 0$  for  $i = 1, \dots, m$ , it is clear that Equation 4.6 can only be satisfied if

$$\bar{\lambda}_i g_i(\bar{x}) = 0, \quad \text{for } i = 1, \dots, m \quad (4.7)$$

which is condition *iii*.

To prove the converse, assume that  $\bar{x}$  satisfies conditions *i*, *ii*, and *iii* of Theorem 4.5.

Condition *i* immediately implies the right hand inequality; for all  $x$ ,

$$L(\bar{x}, \bar{\lambda}) \leq L(x, \bar{\lambda}).$$

The left hand inequality is obtained by considering

$$\begin{aligned} L(\bar{x}, \lambda) &= f(\bar{x}) + \sum_{i=1}^m \lambda_i g_i(\bar{x}) \\ &\leq f(\bar{x}) \quad \text{as } \lambda_i \geq 0 \text{ and condition } ii \text{ implies that } g_i(\bar{x}) \leq 0 \\ &= f(\bar{x}) + \sum_{i=1}^m \bar{\lambda}_i g_i(\bar{x}) \quad \text{as condition } iii \text{ implies that } \bar{\lambda}_i g_i(\bar{x}) = 0 \\ &= L(\bar{x}, \bar{\lambda}). \end{aligned}$$

►

Finding a saddlepoint leads to a sufficient condition for the solution of the primal problem.

#### Theorem 4.6

*If the point  $(\bar{x}, \bar{\lambda})$  is a saddlepoint of the Lagrangian  $L(x, \lambda)$  then  $\bar{x}$  solves the primal problem:*

$$f(\bar{x}) = \min_{x \in \Gamma} f(x) \quad \text{subject to } g_i(x) \leq 0, \quad i = 1, \dots, m.$$

**Proof of Theorem 4.6:** Consider the right hand inequality of Equation 4.4

$$f(\bar{x}) + \sum_{i=1}^m \bar{\lambda}_i g_i(\bar{x}) \leq f(x) + \sum_{i=1}^m \bar{\lambda}_i g_i(x)$$

which reduces to

$$f(\bar{x}) \leq f(x) + \sum_{i=1}^m \bar{\lambda}_i g_i(x)$$

by condition *iii*. Now for any  $x$  satisfying  $g_i(x) \leq 0$ , for  $i = 1, \dots, m$ ,

$$f(\bar{x}) \leq f(x).$$

The following result indicates why it is often easier to attempt to solve the dual problem rather than the primal problem. For the dual problem, Equation 4.3, define a domain  $D$  by

$$D = \left\{ \lambda \mid \lambda \geq 0, h(\lambda) \text{ is finite} \right\}.$$

Linearity of the Lagrangian with respect to  $\lambda$  leads to the following theorem.

**Theorem 4.7**

*The dual function  $h(\lambda)$  is concave over any convex subset of its domain  $D$ .*

**Proof of Theorem 4.7:** Consider  $\lambda_1, \lambda_2$  in  $E$ , a convex subset of  $D$ , and the dual function

$$h(\alpha\lambda_1 + (1 - \alpha)\lambda_2) \quad \text{for } \alpha \in [0, 1].$$

As  $(\alpha\lambda_1 + (1 - \alpha)\lambda_2) \in E$ ,

$$\begin{aligned} h(\alpha\lambda_1 + (1 - \alpha)\lambda_2) &= \min_{x \in \Gamma} L(x, \alpha\lambda_1 + (1 - \alpha)\lambda_2) \\ &= \min_{x \in \Gamma} \alpha L(x, \lambda_1) + (1 - \alpha)L(x, \lambda_2) \\ &\geq \alpha \min_{x \in \Gamma} L(x, \lambda_1) + (1 - \alpha) \min_{x \in \Gamma} L(x, \lambda_2) \\ &\geq \alpha h(\lambda_1) + (1 - \alpha)h(\lambda_2). \end{aligned}$$

In certain model validation problems it will be shown that the domain of  $h(\lambda)$  where the dual function is finite,  $D$ , is always convex. Theorem 4.7 can then be used to show that on this domain the maximization of the dual is a well behaved problem.



## Chapter 5

# Application of Lagrange Techniques to the Model Validation Problem

The Lagrange multiplier techniques outlined in Chapter 4 will be applied to the minimum  $\|w\|$  model validation problem (Problem 3.5). The Lagrangian is formulated for two closely related problems; the first is Problem 3.5 with the restriction that  $x \in \mathcal{X}_e$  dropped:

$$\min_x f(x) \quad \text{subject to } g_i(x) \leq 0, \quad i = 1, \dots, m,$$

where

$$f(x) = x^* \begin{bmatrix} 0 & 0 \\ 0 & I \end{bmatrix} x \tag{5.1}$$

and

$$\begin{aligned} g_i(x) &= x^* \begin{bmatrix} T_i & 0 \\ 0 & 0 \end{bmatrix} x \\ &\quad - \begin{bmatrix} x^* & u^* \end{bmatrix} P^* \begin{bmatrix} T_i & 0 \\ 0 & 0 \end{bmatrix} P \begin{bmatrix} x \\ u \end{bmatrix}. \end{aligned} \tag{5.2}$$

The second Lagrangian to be considered is that for the problem of interest (Problem 3.6):

$$\min_{x_e} f_e(x_e) \quad \text{subject to } g_{ei}(x_e) \leq 0, \quad i = 1, \dots, m,$$

where

$$f_e(x_e) = (x_0^* + x_e^* V^*) \begin{bmatrix} 0 & 0 \\ 0 & I \end{bmatrix} (x_0 + V x_e). \quad (5.3)$$

and

$$\begin{aligned} g_{ei}(x_e) &= (x_0^* + x_e^* V^*) \begin{bmatrix} T_i & 0 \\ 0 & 0 \end{bmatrix} (x_0 + V x_e) \\ &\quad - \begin{bmatrix} x_0^* + x_e^* V^* & u^* \end{bmatrix} P^* \begin{bmatrix} T_i & 0 \\ 0 & 0 \end{bmatrix} P \begin{bmatrix} x_0 + V x_e \\ u \end{bmatrix}. \end{aligned} \quad (5.4)$$

The dropping of the equality constraint allows certain properties of the Lagrangians to be shown more easily. The Lagrange multipliers associated with the first Lagrangian have a very strong relationship to the  $D \in \mathcal{D}$  used in the calculation of the upper bound to  $\mu$  (Equation 2.15). This leads to the fact that  $\sigma$ -stable models always have a region of  $\lambda$  space on which the dual function is finite. More specifically, it will be shown that this finite region is also convex.

The concavity of the dual function then leads to some desirable optimization properties. If the maximization of the dual occurs at a  $\lambda$  value inside this region, then a saddlepoint has been found and the solution to the primal problem (Problem 3.6) immediately follows.

Difficulties arise when the maximization of the dual function leads to the boundary of the region on which the dual function is finite. In this case it is possible that no saddlepoint exists but the Lagrangian has a nontrivial kernel. A further search in this kernel will always yield a saddlepoint in the single perturbation block problem.

The details now follow.

## 5.1 Formulation of the Lagrangians

Consider the Lagrangian for Problem 3.5 without the constraint  $x \in \mathcal{X}_e$ .

$$L(x, \lambda) = f(x) + \sum_{i=1}^m \lambda_i g_i(x), \quad \lambda_i \geq 0.$$

The associated dual function  $h(\lambda)$  is defined, for  $\lambda \geq 0$ , as

$$h(\lambda) = \min_x L(x, \lambda).$$

Introducing the notation

$$A_i = \begin{bmatrix} T_i - P_{11}^* T_i P_{11} & -P_{11}^* T_i P_{12} \\ -P_{12}^* T_i P_{11} & -P_{12}^* T_i P_{12} \end{bmatrix}$$

and

$$B = \begin{bmatrix} 0 & 0 \\ 0 & I \end{bmatrix}$$

allows the Equations 5.1 and 5.2 of the optimization problem (Problem 3.5) to be expressed as

$$f(x) = x^* B x$$

and

$$g_i(x) = x^* A_i x - 2 \operatorname{Re} \left\{ x^* \begin{bmatrix} P_{11}^* \\ P_{12}^* \end{bmatrix} T_i P_{13} u \right\} - u^* P_{13}^* T_i P_{13} u.$$

Section 5.1.1 will study the properties of this Lagrangian in detail.

Now consider the inclusion of the constraint  $x \in \mathcal{X}_e$ . The Lagrangian is now formulated for Problem 3.6. Using the notation introduced above Equations 5.3 and 5.4 become

$$f_e(x_e) = x_e^* V^* B V x_e + 2 \operatorname{Re} \{ x_0^* B V x_e \} + x_0^* B x_0$$

and

$$\begin{aligned} g_{ei}(x_e) &= x_e^* V^* A_i V x_e \\ &\quad + 2 \operatorname{Re} \left\{ x_e^* V^* A_i x_0 - x_e^* V^* \begin{bmatrix} P_{11}^* \\ P_{12}^* \end{bmatrix} T_i P_{13} u \right\} \\ &\quad - 2 \operatorname{Re} \left\{ x_0^* \begin{bmatrix} P_{11}^* \\ P_{12}^* \end{bmatrix} T_i P_{13} u \right\} + x_0^* A_i x_0 - u^* P_{13}^* T_i P_{13} u. \end{aligned}$$

The Lagrangian, denoted by  $L_e(x_e, \lambda)$  to emphasize the inclusion of the equality constraint, associated with the above is

$$\begin{aligned} L_e(x_e, \lambda) &= f_e(x_e) + \sum_{i=1}^m \lambda_i g_{ei}(x_e), \quad \lambda_i \geq 0. \\ &= x_e^* V^* (B + \sum_{i=1}^m \lambda_i A_i) V x_e + 2 \operatorname{Re} \{ x_0^* C_e(\lambda) \} + d_e(\lambda) \end{aligned} \tag{5.5}$$

where

$$C_e(\lambda) = V^* B x_0 + \sum_{i=1}^m \lambda_i \left[ V^* A_i x_0 - V^* \begin{bmatrix} P_{11}^* \\ P_{12}^* \end{bmatrix} T_i P_{13} u \right] \tag{5.6}$$

and

$$d_e(\lambda) = x_0^* B x_0 + \sum_{i=1}^m \lambda_i [x_0^* A_i x_0 - 2 \operatorname{Re} \{ x_0^* \begin{bmatrix} P_{11}^* \\ P_{12}^* \end{bmatrix} T_i P_{13} u \} - u^* P_{13}^* T_i P_{13} u].$$

Note that in this formulation  $x_e$  is unconstrained. The dual function, denoted by  $h_e(\lambda)$ , is now defined for  $\lambda \geq 0$  by

$$h_e(\lambda) = \min_{x_e} L_e(x_e, \lambda).$$

The Lagrangian  $L_e(x_e, \lambda)$  is the one of interest in solving Problem 3.6. However, a study of the properties of  $L(x, \lambda)$  will aid in understanding the equality constrained case.

### 5.1.1 Properties of the Lagrangian: $L(x, \lambda)$ , The Unconstrained Case

Define  $\Lambda$  as the region of  $\lambda$  space upon which the Hessian of  $L(x, \lambda)$  is positive definite. Lagrange multipliers are generally defined with components  $\lambda_i \geq 0$ . Here they will be taken to be  $\lambda_i > 0$  with  $\lambda_i = 0$  treated as a special case.

Now the property that the Hessian of the Lagrangian is strictly positive definite is shown to be equivalent to a maximum singular value test. Consider the Lagrangian for  $\lambda \in \Lambda$ .

Clearly, it suffices to consider the positive definiteness of  $\frac{1}{2}H[L(x, \lambda)]$ . This is done for notational simplicity. Now

$$\begin{aligned} \frac{1}{2}H[L(x, \lambda)] &= B + \sum_{i=1}^m \lambda_i A_i \\ &= B + \sum_{i=1}^m \begin{bmatrix} \lambda_i T_i - P_{11}^* \lambda_i T_i P_{11} & -P_{11}^* \lambda_i T_i P_{12} \\ -P_{12}^* \lambda_i T_i P_{11} & -P_{12}^* \lambda_i T_i P_{12} \end{bmatrix}. \end{aligned}$$

Define  $D$  by

$$\begin{aligned} \sum_{i=1}^m \lambda_i T_i &= \begin{bmatrix} \lambda_1 I_1 & & & \\ & \lambda_2 I_2 & & \\ & & \ddots & \\ & & & \lambda_m I_m \end{bmatrix} \\ &= \begin{bmatrix} d_1^2 I_1 & & & \\ & d_2^2 I_2 & & \\ & & \ddots & \\ & & & d_m^2 I_m \end{bmatrix} \end{aligned}$$

$$= D^T D = D^* D = D^2, \quad (5.7)$$

where  $d_i > 0$ . Only  $\lambda_i > 0$  are being considered so  $D^{-1}$  is well defined. Note also that  $D$  defined above is an element of  $\mathcal{D}$  defined by Equation 2.13. Now

$$\begin{aligned} \frac{1}{2}H[L(x, \lambda)] &= B + \begin{bmatrix} D^2 - P_{11}^* D^2 P_{11} & -P_{11}^* D^2 P_{12} \\ -P_{12}^* D^2 P_{11} & -P_{12}^* D^2 P_{12} \end{bmatrix} \\ &= \begin{bmatrix} D^2 - P_{11}^* D^2 P_{11} & -P_{11}^* D^2 P_{12} \\ -P_{12}^* D^2 P_{11} & I - P_{12}^* D^2 P_{12} \end{bmatrix}. \end{aligned}$$

The problem is to find  $D$ , and consequently  $\lambda_i$ , such that the above is positive definite. Equivalently, using  $\gamma_{\min}$  and  $\gamma_{\max}$  to denote the minimum and maximum eigenvalue respectively,

$$\begin{aligned} \gamma_{\min} \begin{bmatrix} D^2 - P_{11}^* D^2 P_{11} & -P_{11}^* D^2 P_{12} \\ -P_{12}^* D^2 P_{11} & I - P_{12}^* D^2 P_{12} \end{bmatrix} &> 0 \\ \Leftrightarrow \gamma_{\max} \begin{bmatrix} P_{11}^* D^2 P_{11} - D^2 & P_{11}^* D^2 P_{12} \\ P_{12}^* D^2 P_{11} & P_{12}^* D^2 P_{12} - I \end{bmatrix} &< 0. \end{aligned}$$

Premultiplying and postmultiplying by a symmetric matrix does not change the inertia of the above matrix. As the above has all eigenvalues less than zero, the condition is equivalent to the following.

$$\begin{aligned} \gamma_{\max} \left\{ \begin{bmatrix} D^{-1} & 0 \\ 0 & I \end{bmatrix} \begin{bmatrix} P_{11}^* D^2 P_{11} - D^2 & P_{11}^* D^2 P_{12} \\ P_{12}^* D^2 P_{11} & P_{12}^* D^2 P_{12} - I \end{bmatrix} \begin{bmatrix} D^{-1} & 0 \\ 0 & I \end{bmatrix} \right\} &< 0 \\ \Leftrightarrow \gamma_{\max} \begin{bmatrix} D^{-1} P_{11}^* D^2 P_{11} D^{-1} - I & D^{-1} P_{11}^* D^2 P_{12} \\ P_{12}^* D^2 P_{11} D^{-1} & P_{12}^* D^2 P_{12} - I \end{bmatrix} &< 0 \\ \Leftrightarrow \gamma_{\max} \begin{bmatrix} D^{-1} P_{11}^* D^2 P_{11} D^{-1} & D^{-1} P_{11}^* D^2 P_{12} \\ P_{12}^* D^2 P_{11} D^{-1} & P_{12}^* D^2 P_{12} \end{bmatrix} &< 1 \\ \Leftrightarrow \gamma_{\max} \left\{ \begin{bmatrix} D^{-1} P_{11}^* D \\ P_{12}^* D \end{bmatrix} [D P_{11} D^{-1} \ D P_{12}] \right\} &< 1 \\ \Leftrightarrow \sigma_{\max}[D P_{11} D^{-1} \ D P_{12}] &< 1 \quad (5.8) \\ \Leftrightarrow \sigma_{\max} \left\{ \begin{bmatrix} D & 0 \\ 0 & I \end{bmatrix} \begin{bmatrix} P_{11} & P_{12} \\ 0 & 0 \end{bmatrix} \begin{bmatrix} D & 0 \\ 0 & I \end{bmatrix}^{-1} \right\} &< 1. \end{aligned}$$

This condition is reminiscent of that for the upper bound to  $\mu$ ,

$$\inf_{D \in \mathcal{D}} \sigma_{\max}(D M D^{-1}) < 1.$$

This is formally stated in the following theorem, relating the sufficient test for robust stability (Equation 2.15) to the existence of Lagrange multipliers. In essence it says that the Lagrange multipliers giving a positive definite Hessian of the Lagrangian exist if and only if the model is  $\sigma$ -stable.

**Theorem 5.1**

*There exist  $D \in \mathcal{D}$  with  $d_i > 0$  such that*

$$\sigma_{\max}(DP_{11}D^{-1}) < 1$$

*iff there exist  $\lambda_i > 0$ , such that*

$$(B + \sum_{i=1}^m \lambda_i A_i)$$

*is positive definite.*

**Proof of Theorem 5.1:** Assume there exist  $D \in \mathcal{D}$  such that

$$\sigma_{\max}(DP_{11}D^{-1}) = \beta < 1 \text{ and } \sigma_{\max}(DP_{12}) = \eta.$$

Note that the  $D$  contains a free parameter. In other words

$$\sigma_{\max}(\alpha DP_{11}(\alpha D)^{-1}) = \sigma_{\max}(DP_{11}D^{-1}) = \beta < 1.$$

Now as  $\alpha \rightarrow 0$

$$\sigma_{\max}[\alpha DP_{11}(\alpha D)^{-1} \alpha DP_{12}] \leq \beta + \alpha \eta$$

which for  $\alpha \in (0, (1 - \beta)/\eta)$  is less than 1. The condition of Equation 5.8 is now satisfied for  $\alpha D$ . By appropriate choice of  $\lambda$  from Equation 5.7, the Hessian of the Lagrangian is positive definite.

For the converse finding  $\lambda$  such that the Hessian of the Lagrangian is positive definite is equivalent to finding a  $D$  such that

$$\sigma_{\max}[DP_{11}D^{-1} DP_{12}] = \beta < 1,$$

which must necessarily satisfy

$$\sigma_{\max}(DP_{11}D^{-1}) \leq \beta < 1.$$



Packard [10] points out that there is no loss of generality in restricting  $D$  to be positive and real. This translates exactly into the same requirements on  $\lambda$ .

### 5.1.2 Properties of the Lagrangian: $L_e(x_e, \lambda)$ , The Constrained Case

Now define  $\Lambda_e$  as the region of  $\lambda$  space in which the Hessian of the Lagrangian  $L_e(x_e, \lambda)$  is positive definite and  $\lambda_i > 0$ . It will be shown for  $\lambda \in \Lambda_e$ ,  $h_e(\lambda)$  is finite and concave. The following lemma relates  $\Lambda_e$  to  $\Lambda$ .

#### Lemma 5.2

$$\Lambda \subseteq \Lambda_e$$

**Proof of Lemma 5.2:** For every  $\lambda \in \Lambda$  and for all  $x \neq 0$ ,

$$x^*(B + \sum_{i=1}^m \lambda_i A_i)x > 0. \quad (5.9)$$

Now consider, for all  $x_e \neq 0$ ,

$$x_e^* V^*(B + \sum_{i=1}^m \lambda_i A_i) V x_e.$$

Note that for each  $x_e$  there exists an  $x$ , given by  $x = V x_e$ , and from Equation 5.9, for all  $x_e \neq 0$ ,

$$x_e^* V^*(B + \sum_{i=1}^m \lambda_i A_i) V x_e > 0.$$

Therefore  $\lambda \in \Lambda_e$ . ▶

It can now be shown that the existence of  $D \in \mathcal{D}$  giving a sufficient condition for robust stability is sufficient to guarantee the existence of  $\lambda$  such that the Hessian of  $L_e(x_e, \lambda)$  is positive definite. This is expressed in the following theorem.

#### Theorem 5.3

*If there exist  $D \in \mathcal{D}$  with  $d_i > 0$  such that*

$$\sigma_{\max}(D P_{11} D^{-1}) < 1,$$

*then there exist  $\lambda_i > 0$  such that*

$$V^*(B + \sum_{i=1}^m \lambda_i A_i) V$$

*is positive definite.*

**Proof of Theorem 5.3:** This follows immediately from Theorem 5.1 and Lemma 5.2. ▶

Theorem 5.3 shows that  $\sigma$ -stable models always have a region of  $\lambda$  space upon which  $h_e(\lambda)$  is finite. Chapter 7 will establish a stronger relationship between robust stability ( $\mu(P_{11}) < 1$ ) and the existence of a solution to the model validation problem.

### 5.1.3 Properties of the Sets $\Lambda$ and $\Lambda_e$

The previous sections have shown that for models which meet the sufficient condition for robust stability, the sets  $\Lambda$  and  $\Lambda_e$  are not empty. This section gives some results regarding these sets.

Packard [10] points out that the region of  $\mathcal{D}$  such that for  $D \in \mathcal{D}$ ,

$$\sigma_{\max}(DM D^{-1}) < 1,$$

is a convex region. It is not surprising then that  $\Lambda$  and  $\Lambda_e$  are also convex regions.

**Lemma 5.4** *The set  $\Lambda_e$  consisting of all  $\lambda$  such that the Hessian of the Lagrangian,*

$$H[L_e(x_e, \lambda)] = 2V^*(B + \sum_{i=1}^m \lambda_i A_i)V, \quad (5.10)$$

*is positive semidefinite, is a convex set.*

**Proof of Lemma 5.4:** Consider  $\eta$  and  $\xi$ , elements of  $\lambda$  space such that for all  $x_e$ ,

$$x_e^* V^*(B + \sum_{i=1}^m \eta_i A_i)V x_e \geq 0 \quad \text{and} \quad x_e^* V^*(B + \sum_{i=1}^m \xi_i A_i)V x_e \geq 0.$$

Examine the positive definiteness of  $\frac{1}{2}H[L_e(x_e, \lambda)]$  for all convex combinations of  $\eta$  and  $\xi$ . For all  $x_e$  and  $\alpha \in [0, 1]$ ,

$$\begin{aligned} x_e^* V^*(B + \sum_{i=1}^m (\alpha \eta_i + (1 - \alpha) \xi_i) A_i)V x_e &= \alpha x_e^* V^*(B + \sum_{i=1}^m \eta_i A_i)V x_e \\ &\quad + (1 - \alpha) x_e^* V^*(B + \sum_{i=1}^m \xi_i A_i)V x_e \\ &\geq 0. \end{aligned}$$

▶

**Corollary 5.5**

$\Lambda_e$  is convex.



**Proof of Corollary 5.5:**  $\Lambda_e$  is simply the set of all  $\lambda > 0$  such that the Hessian of  $L_e(x_e, \lambda)$  is strictly positive definite. The proof is identical to that for Lemma 5.4 with strictly greater than signs replacing greater than or equal to signs in the equations. ▶

### Corollary 5.6

*$\Lambda$  is convex.*

**Proof of Corollary 5.6:** The proof is identical to that for Lemma 5.4 and Corollary 5.5 with  $x$  substituted for  $x_e$  and the removal of  $V$  from the equations. ▶

By Lemma 4.2,  $L_e(x_e, \lambda)$  is a strictly convex function of  $x_e$  for  $\lambda \in \Lambda_e$ . It is in fact a positive definite quadratic. Now for every  $\lambda \in \Lambda_e$ ,

$$h_e(\lambda) = \min_{x_e} L_e(x_e, \lambda)$$

is readily calculated as  $L_e(x_e, \lambda)$  has a unique global minimum.

The above shows that the Lagrangian is well behaved for  $\lambda$  contained within  $\Lambda_e$ . Unfortunately, maximizing the dual will sometimes lead to the boundary of  $\Lambda_e$ . The definition and some of the properties of the boundary are studied in the next section.

#### 5.1.4 The Boundary of $\Lambda_e$

The properties of the Lagrangian on the boundary of  $\Lambda_e$  are now studied. Two types of boundary are possible for the set  $\Lambda_e$ . Denote by  $\partial\Lambda_e$  the boundary of  $\Lambda_e$  such that the minimum eigenvalue of the Hessian of the Lagrangian is zero. As the multipliers in  $\Lambda_e$  are constrained to have components greater than zero, the hyperplanes defined by each component of  $\lambda_e$  being equal to zero also bound  $\Lambda_e$ . Denote these boundaries by  $\partial_0\Lambda_e$ .

It is possible that a point  $\lambda$  meets the definition for both  $\partial\Lambda_e$  and  $\partial_0\Lambda_e$ . Such points will be considered to be elements of  $\partial\Lambda_e$ . This will allow the space upon which it is always possible to solve the problem to be clearly defined.

Figure 5.1 gives a stylized example of the regions  $\Lambda_e$ ,  $\partial\Lambda_e$ , and  $\partial_0\Lambda_e$  in order to make this point clear. The region  $\partial_0\Lambda_e$  consists of the union of the two half open intervals  $[[0, a), 0]^T$  and  $[0, [0, b))^T$ . The points  $\lambda = [a, 0]^T$  and  $\lambda = [0, b]^T$  are defined to belong to the region  $\partial\Lambda_e$ .

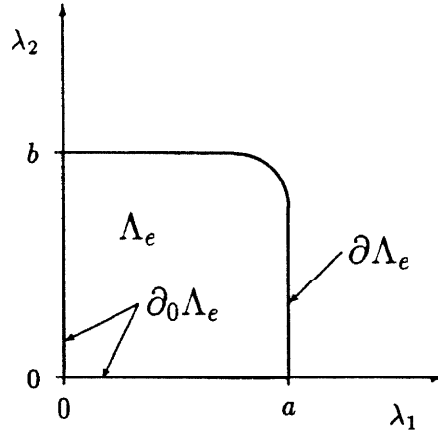


Figure 5.1: Example  $\lambda$  Space Illustrating  $\Lambda_e$ ,  $\partial\Lambda_e$ , and  $\partial_0\Lambda_e$

Two further facts are suggested by Figure 5.1; the point  $\lambda = 0$  is either a member of  $\partial_0\Lambda_e$  or a member of  $\partial\Lambda_e$ ; and the set  $\Lambda_e \cup \partial\Lambda_e \cup \partial_0\Lambda_e$  is convex. The first fact follows from observing that  $V^*BV$  is either positive definite or positive semidefinite. The second fact arises from noting that the set  $\Lambda_e \cup \partial\Lambda_e \cup \partial_0\Lambda_e$  is simply the intersection of the set  $\lambda \geq 0$  and the set where the Hessian of the Lagrangian is positive semidefinite. The convexity of this then comes directly from Lemma 5.4.

Now consider the eigenvalues of the Hessian of the Lagrangian for each part of the  $\lambda$  space where  $\lambda \geq 0$ . For  $\lambda \in \Lambda_e \cup \partial_0\Lambda_e$ , all the eigenvalues of

$$V^*(B + \sum_{i=1}^m \lambda_i A_i)V$$

are strictly greater than zero. For  $\lambda \in \partial\Lambda_e$ ,

$$V^*(B + \sum_{i=1}^m \lambda_i A_i)V$$

has at least one zero eigenvalue. For  $\lambda \geq 0$  and  $\lambda \notin \Lambda_e \cup \partial\Lambda_e$ ,

$$V^*(B + \sum_{i=1}^m \lambda_i A_i)V$$

has a negative eigenvalue and selecting  $x_e$  as the associated eigenvector allows the quadratic term to dominate  $h_e(\lambda)$ . Consequently  $h_e(\lambda) = -\infty$ . In searching for a maximum of  $h_e(\lambda)$ , for  $\lambda \geq 0$ , it suffices to study  $\Lambda_e$ ,  $\partial\Lambda_e$  and  $\partial_0\Lambda_e$ .

### 5.1.5 Properties of the Dual Function: $h_e(\lambda)$

It is well known (refer to Wismer and Chattergy [20] for example) that the dual function is concave over convex regions of the domain on which it is finite. This is explicitly stated in the context of this problem in the following theorem.

#### Theorem 5.7

*For all  $\lambda \in \Lambda_e$ , the dual function*

$$h_e(\lambda) = \min_{x_e} L_e(x_e, \lambda)$$

*is concave.*

**Proof of Theorem 5.7:** The proof is identical to that of Theorem 4.7. ▶

## 5.2 Solving the Model Validation Problem

The properties of the space  $\Lambda_e$  and the dual function  $h_e(\lambda)$  can give a solution to the model validation problem by finding a Kuhn-Tucker saddlepoint. It will be shown here that if the solution to the dual problem occurs away from the boundary  $\partial\Lambda_e$ , then it also solves the primal problem and hence the model validation problem. In the case where the maximization leads to the boundary  $\partial\Lambda_e$ , it may not be possible to find a Kuhn-Tucker saddlepoint. In these cases it is possible to bound the solution to the primal problem. This is examined in Section 5.2.2.

### 5.2.1 Solution via the Dual Problem

#### Theorem 5.8

*If*

$$\max_{\lambda \geq 0} h_e(\lambda) = L_e(\bar{x}_e, \bar{\lambda}) \quad \text{with } \bar{\lambda} \notin \partial\Lambda_e,$$

*then  $\bar{x} = x_0 + V\bar{x}_e$  solves Problem 3.5:*

$$\begin{aligned} f(\bar{x}) = \min_x f(x) \quad \text{subject to} \quad & g_i(x) \leq 0, \quad i = 1, \dots, m \\ & \text{and} \quad g_e(x) = 0. \end{aligned}$$

**Proof of Theorem 5.8:** The proof of this theorem will proceed by establishing each of the three conditions given in the Kuhn-Tucker Saddlepoint theorem (Theorem 4.5).  $h_e(\lambda)$  is concave over  $\Lambda_e \cup \partial_0 \Lambda_e$  so every local maximum is also global. As  $L_e(x_e, \lambda)$  is convex for  $\lambda \in \Lambda_e \cup \partial_0 \Lambda_e$ , the calculation of  $h_e(\bar{\lambda})$  does in fact give a global minimization of  $L_e(x_e, \bar{\lambda})$  over all  $x_e$ . The first condition of Theorem 4.5 is therefore satisfied.

The second and third conditions are established for the case where  $\bar{\lambda} \in \Lambda_e$ . At  $\bar{\lambda}$

$$\left. \frac{\partial h_e(\lambda)}{\partial \lambda} \right|_{\lambda=\bar{\lambda}} = 0.$$

By the construction of the Lagrangian

$$\frac{\partial h_e(\lambda)}{\partial \lambda} = \frac{\partial L_e(x_e, \lambda)}{\partial \lambda} + \frac{\partial L_e(x_e, \lambda)}{\partial x_e} \frac{\partial x_e}{\partial \lambda}.$$

But for  $\bar{x}_e$  chosen to minimize  $L_e(x_e, \bar{\lambda})$ ,

$$\frac{\partial L_e(x_e, \lambda)}{\partial x_e} = 0$$

giving

$$\left. \frac{\partial h_e(\lambda)}{\partial \lambda} \right|_{\lambda=\bar{\lambda}} = \left. \frac{\partial L_e(\bar{x}_e, \lambda)}{\partial \lambda} \right|_{\lambda=\bar{\lambda}} = \begin{bmatrix} g_{e1}(\bar{x}_e) \\ \vdots \\ g_{em}(\bar{x}_e) \end{bmatrix}$$

so  $g_{ei}(\bar{x}_e) = 0$  for  $i = 1, \dots, m$  satisfying both conditions *ii* and *iii* of Theorem 4.5.

It only remains to consider the case where  $\bar{\lambda} \in \partial_0 \Lambda_e$ . Define  $I_n$  as the set of indices  $i$  where  $\lambda_i = 0$ . For  $i = 1, \dots, m, i \notin I_n$ ,

$$\left. \frac{\partial L_e(\bar{x}_e, \lambda)}{\partial \lambda_i} \right|_{\lambda=\bar{\lambda}} = 0 \text{ implying that } g_{ei}(x_e) = 0.$$

And for  $i \in I_n$ ,

$$\left. \frac{\partial L_e(\bar{x}_e, \lambda)}{\partial \lambda_i} \right|_{\lambda=\bar{\lambda}} \leq 0 \text{ implying that } g_{ei}(x_e) \leq 0.$$

If this were not so, then there exists  $\epsilon > 0$  such that for  $\lambda_i = \epsilon$ ,

$$h_e(\lambda) > h_e(\bar{\lambda}),$$

contradicting the fact that  $h_e(\bar{\lambda})$  is the maximum. For  $i \notin I_n$  condition *iii* is satisfied by  $g_{ei}(x_e) = 0$ . For  $i \in I_n$  it is satisfied by  $\lambda_i = 0$ .

The three conditions of Theorem 4.5 are satisfied and so  $(\bar{x}_e, \bar{\lambda})$  is a Kuhn-Tucker saddlepoint. By Theorem 4.6  $\bar{x}_e$  solves Problem 3.6 and consequently  $\bar{x} = x_0 + V\bar{x}_e$  solves Problem 3.5. ►

### 5.2.2 Bounds on a Solution to the Model Validation Problem

A detailed examination of the dual function on the boundary is postponed until Section 5.3. The result of interest here is that it is always possible to solve the single perturbation block case (Section 5.3.3). This allows the calculation of a lower bound on the minimum  $\|w\|$  required to account for the observed datum.

If the structure of the perturbation block  $\Delta$  is ignored, a simpler problem can be posed. This is equivalent to simply setting  $m = 1$ . Denote an admissible  $(w, \Delta)$  for this problem as  $(w_l, \Delta_l)$ .

#### Theorem 5.9

*There exist no admissible  $(w, \Delta)$  for the model validation problem (Problem 3.4) with  $\|w\| < \|w_l\|$ .*

**Proof of Theorem 5.9:** This follows immediately from the fact that every  $\Delta$  structure with  $m > 1$  is contained within the set of unstructured ( $m = 1$ )  $\Delta$ . Every solution to the model validation problem (Problem 3.4) meets the constraints of the  $m = 1$  case and therefore satisfies

$$x^* \begin{bmatrix} 0 & 0 \\ 0 & I \end{bmatrix} x \geq x_l^* \begin{bmatrix} 0 & 0 \\ 0 & I \end{bmatrix} x_l$$

which is simply

$$\|w\|^2 \geq \|w_l\|^2.$$

►

Solution via the dual problem involves finding  $x$  such that the constraints  $g_{ei}(x)$  are met exactly ( $g_{ei}(x) = 0$ ) or the constraint is satisfied and inactive at the solution ( $\lambda_i = 0$ ). In the case where the maximization of the dual leads to the boundary  $\partial\Lambda_e$ , it may not be possible to find a Kuhn-Tucker saddlepoint. Any  $x$ , denoted here by  $x_u$ , such that  $g_{ei}(x_u) \leq 0$  for  $i = 1, \dots, m$  is a feasible point of the minimization and as such  $\sqrt{f(x_u)}$  ( $= \|w_u\|$  say) is an upper bound of the minimum  $\|w\|$  solving the model validation optimization.

The Lagrange multiplier approach leads to the possibility of a gap in the solution of the model validation problem. In the case where a solution is found on the interior of

$\Lambda_e$  or on  $\partial_0\Lambda_e$ , the minimum  $\|w\|$  meeting the constraints is found. In the case where  $m = 1$  and  $\lambda \in \partial\Lambda_e$ , the minimum  $\|w\|$  is still found. This allows the model validation question *Can the model account for the observed datum?*, to be answered in a yes/no manner.

If  $m \geq 3$  (or  $m = 2$  and  $\dim(V) = 1$ )<sup>1</sup> and  $\lambda \in \partial\Lambda_e$  maximizes the dual function, it is possible to have a gap in the answer to the model validation question. By this it is meant that the Lagrange methods do not yield the solution and  $\|w_u\| > \|w_l\|$ . This is analogous to the gap between the upper and lower bounds in the calculation of  $\mu$ . It will be proven in Chapter 7 that if  $m = 1$  or  $m = 2$  and  $\dim(V) > 1$ , then the gap cannot occur.

Even though a gap exists it may still be possible to answer the model validation question. If  $\|w_l\| > 1$ , then by Theorem 5.9 there is no vector  $x$  meeting all of the constraints of the model. Alternatively, if  $\|w_u\| \leq 1$  there does exist a vector meeting all of the constraints of the model ( $x_u$  is such a vector). However, if  $\|w_l\| < 1$  and  $\|w_u\| > 1$ , there is no conclusive statement that can be made with regard to the model validation question.

### 5.3 The Dual Function at the Boundary: $\partial\Lambda_e$

Section 5.2.1 showed that a saddlepoint can always be found if the maximum of the dual function occurs for  $\lambda \in \Lambda_e$  or  $\lambda \in \partial_0\Lambda_e$ . The remaining case, the maximum occurring on the boundary  $\partial\Lambda_e$ , can only occur if  $h_e(\lambda)$  is finite on  $\partial\Lambda_e$ . To see this note that for  $\lambda \in \Lambda_e$ , the quadratic term is always positive definite and so  $h_e(\lambda) > -\infty$ . For  $\lambda \in \partial\Lambda_e$ ,  $h_e(\lambda)$  may be finite or may be equal to negative infinity. If the maximum of  $h_e(\lambda)$  is to occur for some  $\bar{\lambda} \in \partial\Lambda_e$ , then  $h_e(\bar{\lambda})$  must be finite.

The properties of  $h_e(\lambda)$  for  $\lambda \in \partial\Lambda_e$  are now studied. For  $\lambda$  close to the boundary  $\partial\Lambda_e$ , the Hessian of the Lagrangian

$$H[L_e(x_e, \lambda)] = 2V^*(B + \sum_{i=1}^m \lambda_i A_i)V$$

---

<sup>1</sup>Refer to Section 8.3.2 for an example where  $m = 3$  and no saddlepoint exists. Section 7.5 discusses the case where  $m = 2$  and  $\dim(V) = 1$ .

has an eigenvalue close to zero. In general, the  $x_e$  achieving the minimum of  $L_e(x_e, \lambda)$  will become larger in norm as  $\lambda$  approaches the boundary. This happens as the linear term dominates and can be made large and negative with a sufficiently large  $x_e$ . This is not always the case, and the next section will give necessary and sufficient conditions under which  $h_e(\lambda)$  is finite on the boundary.

### 5.3.1 When is $h_e(\lambda)$ finite on $\partial\Lambda_e$ ?

For  $\lambda \in \partial\Lambda_e$  the Hessian of the Lagrangian has a zero eigenvalue. Whether or not the minimum of  $L_e(x_e, \lambda)$  for  $\lambda \in \partial\Lambda_e$  is finite depends on the associated eigenvector and the linear term of the Lagrangian;  $C_e(\lambda)$ . For  $\bar{\lambda} \in \partial\Lambda_e$ , define

$$\bar{\lambda}A = \sum_{i=1}^m \bar{\lambda}_i A_i.$$

#### Theorem 5.10

$h_e(\bar{\lambda}) = -\infty$  for  $\bar{\lambda} \in \partial\Lambda_e$  iff there exists  $x_{ek} \in \text{Ker}[V^*(B + \bar{\lambda}A)V]$  for which  $\text{Re}\{C_e(\bar{\lambda})^* x_{ek}\} \neq 0$ .

**Proof of Theorem 5.10:** Assume there exists

$$x_{ek} \in \text{Ker}[V^*(B + \bar{\lambda}A)V]$$

and

$$\text{Re}\{C_e(\bar{\lambda})^* x_{ek}\} = \beta \neq 0.$$

Take  $x_e = \alpha x_{ek}$ .

$$\begin{aligned} h_e(\bar{\lambda}) \leq L_e(\alpha x_{ek}, \bar{\lambda}) &= \alpha^2 x_{ek}^* V^*(B + \bar{\lambda}A)V x_{ek} + 2\alpha\beta + d_e(\bar{\lambda}) \\ &= 2\alpha\beta + d_e(\bar{\lambda}). \end{aligned}$$

Pick  $\alpha$  such that  $2\alpha\beta < 0$  and as  $|\alpha| \rightarrow \infty$ ,

$$h_e(\bar{\lambda}) \leq L_e(\alpha x_{ek}, \bar{\lambda}) \rightarrow -\infty.$$

For the converse assume  $h_e(\bar{\lambda}) = -\infty$  but for all  $x_{ek} \in \text{Ker}[V^*(B + \bar{\lambda}A)V]$ ,  $\text{Re}\{C_e(\bar{\lambda})^* x_{ek}\} = 0$ . Partition  $x_e$  as  $x_e = x_{ek} \oplus x_{ek}^\perp$ , then

$$\begin{aligned} h_e(\bar{\lambda}) &= \min_{x_{ek} \oplus x_{ek}^\perp} L_e(x_{ek} \oplus x_{ek}^\perp, \bar{\lambda}) \\ &= \min_{x_{ek}^\perp} x_{ek}^{\perp*} V^*(B + \bar{\lambda}A)V x_{ek}^\perp + 2 \text{Re}\{C_e(\bar{\lambda})^* x_{ek}^\perp\} + d_e(\bar{\lambda}). \end{aligned} \quad (5.11)$$

But

$$x_{ek}^\perp{}^* V^*(B + \overline{\lambda A}) V x_{ek}^\perp > 0 \quad (5.12)$$

for all  $x_{ek}^\perp$ , and if  $h_e(\bar{\lambda}) = -\infty$ , then there must be a  $x_{ek}^\perp$  of infinite norm achieving this. From Equation 5.12 the quadratic term is always positive implying that  $h_e(\bar{\lambda}) = \infty$  which is a contradiction. ▶

**Corollary 5.11**

*$h_e(\bar{\lambda})$  is finite for  $\bar{\lambda} \in \partial\Lambda_e$  iff for every  $x_{ek} \in \text{Ker}[V^*(B + \overline{\lambda A})V]$ ,  $\text{Re}\{C_e(\bar{\lambda})^* x_{ek}\} = 0$ .*

The above gives necessary and sufficient conditions for the value of  $h_e(\lambda)$  to be finite on the boundary of  $\Lambda_e$ . If the above condition is satisfied it is possible that

$$\max_{\lambda \geq 0} h_e(\lambda)$$

occurs for  $\bar{\lambda} \in \partial\Lambda_e$ . However, it is not necessarily true that

$$\left. \frac{\partial h_e(\lambda)}{\partial \lambda} \right|_{\lambda=\bar{\lambda}} \leq 0.$$

Although condition *i* of Theorem 4.5 is satisfied, conditions *ii* and *iii* may not be, and it is no longer guaranteed that  $(\bar{x}_e, \bar{\lambda})$  is a Kuhn-Tucker saddlepoint.

### 5.3.2 Finding a Kuhn-Tucker Saddlepoint on the Boundary

The previous section demonstrated that on the boundary  $\partial\Lambda_e$  where  $h_e(\lambda)$  is finite, there exists  $x_{ek}$  such that

$$x_{ek}^* V^*(B + \overline{\lambda A}) V x_{ek} = 0,$$

and for every such  $x_{ek}$ ,

$$\text{Re}\{C_e(\bar{\lambda})^* x_{ek}\} = 0.$$

$x_{ek}$  is therefore in the kernel of the Lagrangian  $L_e(x_e, \lambda)$  and can be considered as an additional degree of freedom that can be exploited in attempting to find a saddlepoint.

This is now discussed more formally.

If



$$\max_{\lambda} h_e(\lambda) = L_e(\bar{x}_e, \bar{\lambda})$$

with  $\bar{\lambda} \in \partial\Lambda_e$ , then for every vector  $x_{ek}$  in the kernel of  $V^*(B + \bar{\lambda}A)V$ ,

$$L_e(\bar{x}_e + x_{ek}, \bar{\lambda}) = L_e(\bar{x}_e, \bar{\lambda}). \quad (5.13)$$

The choice of  $x_{ek}$  gives an additional degree of freedom in finding a Kuhn-Tucker saddlepoint. Consider the constraint

$$\begin{aligned} g_{ei}(x_e) &= x_e^* V^* A_i V x_e \\ &+ 2 \operatorname{Re} \left\{ x_e^* V^* A_i x_0 - x_e^* V^* \begin{bmatrix} P_{11}^* \\ P_{12}^* \end{bmatrix} T_i P_{13} u \right\} \\ &- 2 \operatorname{Re} \left\{ x_0^* \begin{bmatrix} P_{11}^* \\ P_{12}^* \end{bmatrix} T_i P_{13} u \right\} + x_0^* A_i x_0 - u^* P_{13}^* T_i P_{13} u, \end{aligned}$$

and examine the effect of adding  $x_{ek}$  to  $x_e$ .

$$\begin{aligned} g_{ei}(x_e + x_{ek}) &= x_{ek}^* V^* A_i V x_{ek} \\ &+ 2 \operatorname{Re} \{ x_{ek}^* V^* A_i (x_0 + V x_e) \} - 2 \operatorname{Re} \left\{ x_{ek}^* V^* \begin{bmatrix} P_{11}^* \\ P_{12}^* \end{bmatrix} T_i P_{13} u \right\} \\ &+ g_{ei}(x_e). \end{aligned}$$

This in effect defines another problem. Does there exist  $x_{ek} \in \operatorname{Ker}[V^*(B + \bar{\lambda}A)V]$ , such that, for  $i = 1, \dots, m$ , the following equation is satisfied.

$$\begin{aligned} x_{ek}^* V^* A_i V x_{ek} + 2 \operatorname{Re} \{ x_{ek}^* V^* A_i (x_0 + V x_e) \} \\ - 2 \operatorname{Re} \left\{ x_{ek}^* V^* \begin{bmatrix} P_{11}^* \\ P_{12}^* \end{bmatrix} T_i P_{13} u \right\} \\ + g_{ei}(x_e) = 0. \end{aligned} \quad (5.14)$$

The following section will show that this problem can be solved in the single perturbation block case.

### 5.3.3 The Single Perturbation Block Case

If  $\sigma_{\max}(P_{11}) < 1$  and  $\lambda$  is a scalar, then  $\Lambda_e$  is an open interval on the real line:  $(0, \partial\Lambda_e)$ . It will be shown that in this case it is always possible to solve the boundary problem of Equation 5.14.

Consider  $\bar{x}_e$ , corresponding to a solution of the Lagrangian on the boundary:

$$h_e(\bar{\lambda}) = \min_{x_e} L_e(x_e, \bar{\lambda}) = L_e(\bar{x}_e, \bar{\lambda}), \quad \bar{\lambda} = \partial\Lambda_e.$$

The choice of  $\bar{x}_e$  is not unique. To aid in the proof of the Lemmas that follow, choose  $\bar{x}_e$  as the limit of a sequence of solution vectors  $\hat{x}_e$  as the boundary is approached from within  $\Lambda_e$ .

More formally,

$$\bar{x}_e = \lim_{\|\epsilon\| \rightarrow 0} \hat{x}_e \tag{5.15}$$

where

$$H[L_e(x_e, \bar{\lambda} - \epsilon)] > 0,$$

and

$$L_e(\hat{x}_e, \bar{\lambda} - \epsilon) = \min_{x_e} L_e(x_e, \bar{\lambda} - \epsilon).$$

Note that in the single perturbation block case,  $\lambda$ , and consequently  $\epsilon$ , is a scalar. Furthermore for  $\epsilon > 0$ , the Hessian of the Lagrangian is positive definite, and  $\hat{x}_e$  is unique. At  $\lambda = \bar{\lambda}$ ,  $x_{ek} \in \text{Ker}[V^*(B + \bar{\lambda}A)V]$ , giving

$$L_e(\bar{x}_e + \alpha x_{ek}, \bar{\lambda}) = L_e(\bar{x}_e, \bar{\lambda}), \quad \alpha \in \mathbb{C}.$$

The vector  $x_{ek}$  will be considered as a free variable to be searched over in an attempt to find a saddlepoint. The following two lemmas give the properties required for a solution of Equation 5.14 in the case where  $m = 1$ .

### Lemma 5.12

*For  $m = 1$  and  $\bar{x}_e$  defined by Equation 5.15,*

$$g_{ei}(\bar{x}_e) \geq 0.$$

**Proof of Lemma 5.12:** Consider the derivative of  $h_e(\bar{\lambda})$  from the left:

$$\lim_{\epsilon \rightarrow 0} \frac{h_e(\bar{\lambda}) - h_e(\bar{\lambda} - \epsilon)}{\epsilon}.$$

Note that  $\hat{x}_e$  has been defined such that

$$\frac{\partial h_e(\bar{\lambda} - \epsilon)}{\partial \lambda} = g_{ei}(\hat{x}_e).$$

As  $\bar{x}_e$  has been chosen as the limit of the  $\hat{x}_e$ ,  $g_{ei}(\bar{x}_e)$  is the derivative of  $h_e(\bar{\lambda})$  from the left.

$$g_{ei}(\bar{x}_e) = \lim_{\epsilon \rightarrow 0} \frac{h_e(\bar{\lambda}) - h_e(\bar{\lambda} - \epsilon)}{\epsilon}.$$

If  $g_{ei}(\bar{x}_e) < 0$ , then  $h_e(\bar{\lambda} - \epsilon) > h_e(\bar{\lambda})$  contradicting the fact that the maximum occurs on the boundary. ▶

**Lemma 5.13**

$$x_{ek}^* V^* A V x_{ek} < 0.$$

**Proof of Lemma 5.13:** On the boundary  $x_{ek}^* V^* (B + \overline{\lambda A}) V x_{ek} = 0$ .

As  $x_{ek} V^* B V x_{ek} \geq 0$ ,  $x_{ek}^* V^* A V x_{ek} \leq 0$ . Equality cannot occur; if it did, then there would exist a zero eigenvalue for all  $\lambda$ , making  $\Lambda_e$  empty and contradicting  $\sigma_{\max}(P_{11}) < 1$ . ▶

Now, for  $\bar{x}_e$  minimizing the Lagrangian on the boundary, there is an extra degree of freedom. For  $\alpha \in \mathbb{C}$ ,

$$\begin{aligned} g(x_e) = g(\bar{x}_e + \alpha x_{ek}) &= \alpha^* \alpha (x_{ek}^* V^* A V x_{ek}) \\ &+ 2 \operatorname{Re} \{ \alpha^* x_{ek}^* V^* A (x_0 + V \bar{x}_e) \} \\ &- 2 \operatorname{Re} \left\{ \alpha^* x_{ek}^* V^* \begin{bmatrix} P_{11}^* \\ P_{12}^* \end{bmatrix} T_i P_{13} u \right\} \\ &+ g(\bar{x}_e). \end{aligned}$$

The above is simply a quadratic in  $\alpha$ . By Lemma 5.13 it is negative definite, and by Lemma 5.12, for  $\alpha = 0$ , Equation 5.14 has a non-negative value. Therefore, there exists  $\alpha$  such that

$$g(x_e) = g(\bar{x}_e + \alpha x_{ek}) = 0.$$

All three conditions of Theorem 4.5 are now satisfied, and  $x_e$  is therefore a solution of the primal problem.

## Chapter 6

### Skewed $\mu$

This Chapter considers the  $\mu$  problem in more detail and develops a generalization of the perturbation blocks. The results and methods of proof presented here are simple extensions of those of Fan and Tits [9, 8] and Doyle [7]. The notation developed here will allow the model validation problem to be considered in a simpler form in Chapter 7.

#### 6.1 Motivation for a Generalization of $\mu$

This chapter will consider the general problem with  $m$  perturbation blocks. Again each of the  $m$  blocks will be assumed to be a full complex matrix. Consider the system illustrated in Figure 6.1. As in Section 2.1.2, the block structure is an  $m$ -tuple of integers  $(k_1, \dots, k_m)$  and  $\Delta$  is defined by

$$\Delta = \left\{ \text{diag} (\Delta_1 \dots \Delta_m) \mid \dim(\Delta_i) = k_i \right\}.$$

Recall, from Section 2.2.2, the definition of  $\mathbf{B}_\delta \Delta$  and  $\mu$ :

$$\mathbf{B}_\delta \Delta := \left\{ \Delta \mid \Delta \in \Delta, \sigma_{\max}(\Delta_i) \leq \delta \right\}. \quad (6.1)$$

$$\mu(M) := \begin{cases} 0 & \text{if no } \Delta \in \Delta \text{ solves } \det(I + M\Delta) = 0 \\ \text{otherwise} & \\ \left[ \min_{\Delta \in \Delta} \left\{ \delta \mid \exists \Delta \in \mathbf{B}_\delta \Delta \text{ such that } \det(I + M\Delta) = 0 \right\} \right]^{-1}. & \end{cases} \quad (6.2)$$

Also recall the definition of  $R_i$  (Equation 3.3):

$$R_i = \text{block row}(0_1, \dots, 0_{i-1}, I_i, 0_{i+1}, \dots, 0_m),$$

where  $\dim(0_j) = k_j \times k_j$ ,  $\dim(I_i) = k_i \times k_i$ .

Note that the  $m$   $\Delta$  blocks are the only constraints to be considered in this problem. Therefore, the use of  $R_i$  is sufficient to select the desired components of both  $x$  and  $Mx$ .

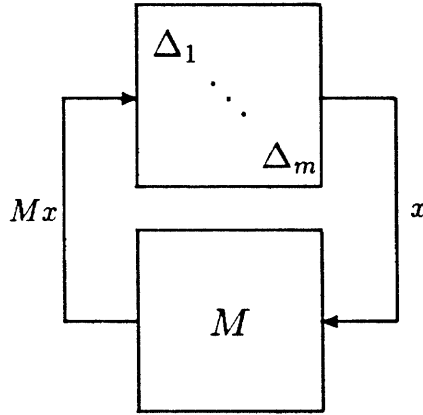


Figure 6.1: System to be Considered for  $\mu$  Problems

The following theorem (due to Fan and Tits [8]) states that  $\mu$  is equivalent to a maximization problem over the unit sphere. For details of the proof, refer to [8].

**Theorem 6.1**

$$\begin{aligned} \mu(M) &= \max_{\gamma, \|x\|=1} \left\{ \gamma \mid \|R_i x\| \gamma = \|R_i Mx\|, i = 1, \dots, m \right\} \\ &= \max_{\gamma, \|x\|=1} \left\{ \gamma \mid \|R_i x\| \gamma \leq \|R_i Mx\|, i = 1, \dots, m \right\}. \end{aligned}$$

The above illustrates that the  $\mu$  can be considered as a maximization with a series of norm constraints on  $x$  and  $Mx$ . This is reminiscent of the constraints imposed for the model validation problem. For the  $\mu$  problem the variable to be maximized,  $\gamma$ , affects all constraints uniformly.

It is easy to imagine a similar maximization where the  $\gamma$  dependence was not present in every constraint. In other words, for certain perturbation blocks  $\gamma$  is replaced by a fixed scaling. A physical motivation for this problem arises from the following.

Consider a model of the form  $F_u(M, \Delta)$  with inputs  $w$  and outputs  $e$  as in Figure 2.2. For the convenience of the reader, Figure 2.2 has been repeated here as Figure 6.2. It is assumed that  $\|\Delta\| \leq 1$  and the following question is posed: *What is the worst case  $\|e\|_2$ , for any signal  $w \in \text{BL}_2$ ?* This is not strictly speaking a  $\mu$  problem. If  $\mu(M) = \alpha$ , then it is possible to say that for  $\|\Delta\| \leq 1/\alpha$ , the worst case norm of the error  $e$  is less than or equal to  $1/\alpha$ . Note the uniformity of the scaling in the answer that  $\mu$  provides.

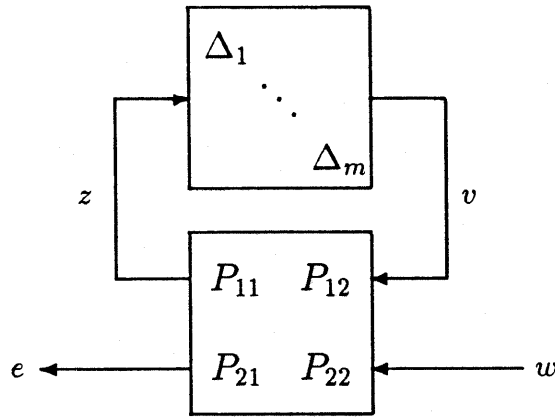


Figure 6.2: Generic Model Structure Including Uncertainty

Although the results of this chapter provide a means of directly answering the worst case error question, the same answer can be trivially obtained by an iterative procedure using the standard  $\mu$  problem formulation. Consider a scaling of the output  $e$  by  $\eta e$ , and absorb this scaling into the system  $M$ . Now find  $\eta$  such that the scaled system, denoted  $M_s$ , has  $\mu(M_s) = 1$  and the worst case error is then  $1/\eta$ . Assuming that  $\mu(M_s)$  can be calculated, a simple bisection technique will be able to accomplish this iteration.

So the results of this chapter do not provide anything that is fundamentally new. They do, however, allow considerable notational and conceptual simplification of the more general problem to be considered in Chapter 7.

## 6.2 Skewed $\mu$ : $\mu_s$

Consider the integers  $1, \dots, m$  to be divided into two disjoint sets:  $I_s$  and  $\bar{I}_s$  where  $I_s$  may be empty. It will now be assumed that for  $i \in I_s$ ,  $\|\Delta_i\| \leq 1$ . Define a ball in which

only certain of the  $\Delta$  blocks are allowed to vary in size:

$$\mathbf{B}_s^\delta \Delta := \left\{ \Delta \mid \Delta \in \Delta, \begin{array}{l} \sigma_{\max}(\Delta_i) \leq 1, i \in I_s \\ \sigma_{\max}(\Delta_i) \leq \delta, i \in \bar{I}_s \end{array} \right\}. \quad (6.3)$$

Now define “skewed  $\mu$ ”, denoted  $\mu_s$ , by the following:

$$\mu_s(M) := \begin{cases} 0 & \text{if no } \Delta \in \mathbf{B}_s^\infty \Delta \text{ solves } \det(I + M\Delta) = 0 \\ \text{otherwise} & \\ \left[ \min_{\Delta \in \mathbf{B}_s^\infty \Delta} \left\{ \delta \mid \exists \Delta \in \mathbf{B}_s^\delta \Delta \text{ such that } \det(I + M\Delta) = 0 \right\} \right]^{-1} & \end{cases}. \quad (6.4)$$

Two maximization problems are now introduced:

$$\hat{\mu}_s(M) := \max_{\gamma, \|x\|=1} \left\{ \gamma \mid \begin{array}{l} \|R_i x\| = \|R_i M x\|, i \in I_s \\ \|R_i x\| \gamma = \|R_i M x\|, i \in \bar{I}_s \end{array} \right\} \quad (6.5)$$

and

$$\bar{\mu}_s(M) := \max_{\gamma, \|x\|=1} \left\{ \gamma \mid \begin{array}{l} \|R_i x\| \leq \|R_i M x\|, i \in I_s \\ \|R_i x\| \gamma \leq \|R_i M x\|, i \in \bar{I}_s \end{array} \right\}. \quad (6.6)$$

Note that it is not necessary to restrict  $x$  to be on the unit sphere ( $\|x\| = 1$ ) as for any  $x$  meeting the above constraints,  $\alpha x$ ,  $\alpha \in (0, \infty)$ , also meets the constraints. However, the restriction to the unit sphere, and the compactness of the unit sphere, makes it clear that the maximum is achieved.

For a finite matrix  $M$ ,  $\mu(M)$  is also finite. This is no longer true for  $\mu_s(M)$ . If the  $\Delta_i$  blocks with  $i \in \bar{I}_s$  do not play a role in the equation  $\det(I + M\Delta) = 0$ , then  $\mu_s(M)$  will be infinite. In other words there is a choice of  $\Delta_i$  with  $i \in I_s$ ,  $\|\Delta_i\| \leq 1$ , such that  $\det(I + M\Delta) = 0$  irrespective of the size of the  $\Delta_i$  for  $i \in \bar{I}_s$ . An example will be presented at the end of this section in which this pathology arises.

In the case where  $\mu_s(M)$  is finite, the above maximizations are indeed equivalent. This is proven in a manner similar to that used by Fan and Tits [8] for the analogous  $\mu(M)$  maximization problems.

**Theorem 6.2**

If  $\mu_s(M)$  is finite, then

$$\mu_s(M) = \hat{\mu}_s(M) = \bar{\mu}_s(M).$$

The proof of Theorem 6.2 will proceed via two preliminary lemmas. The first concerns the properties of the smallest zero of a polynomial in  $\mathbf{C}^m$ . This lemma is due to Doyle [7], but the formulation given here more closely resembles that of Packard [10].

Consider the zeros of a polynomial  $p : \mathbf{C}^m \rightarrow \mathbf{C}$ . If  $z \in \mathbf{C}^m$ , define

$$\|z\|_\infty = \max_{i \leq m} |z_i|.$$

Now define  $\beta$  as the norm of the smallest zero of the polynomial.

$$\beta = \min \left\{ \|z\|_\infty \mid p(z) = 0 \right\}. \quad (6.7)$$

**Lemma 6.3**

Let  $p$  be a polynomial from  $\mathbf{C}^m \rightarrow \mathbf{C}$  and define  $\beta$  by Equation 6.7. Then there exists a  $z \in \mathbf{C}^m$  such that  $|z_i| = \beta$  for all  $i = 1, \dots, m$  and  $p(z) = 0$ .

In other words, there exists a minimizing solution with every component equal in magnitude. Doyle [7] and Packard [10] use this result to prove that  $\mu$  is always equal to its lower bound (Equation 2.15). Here it will play a similar role, but the existence of blocks that do not scale complicates the issue. This complication is removed with the following lemma.

**Lemma 6.4**

If

$$\delta_0 = \min_{\Delta \in \mathbf{B}_s^\infty \Delta} \left\{ \delta \mid \exists \Delta \in \mathbf{B}_s^\delta \Delta \text{ such that } \det(I + M\Delta) = 0 \right\},$$

then there exists  $\Delta \in \mathbf{B}_s^{\delta_0} \Delta$  such that

$$|\Delta_i| = \begin{cases} 1, & i \in I_s \\ \delta_0, & i \in \bar{I}_s \end{cases}$$

and  $\det(I + M\Delta) = 0$ .



**Proof of Lemma 6.4:** By hypothesis there exists  $\Delta \in \mathbf{B}_8^{\delta_0} \Delta$  such that  $\det(I + M\Delta) = \det(I + \Delta M) = 0$ ,

$$|\Delta_i| \leq \begin{cases} 1, & i \in I_s \\ \delta_0, & i \in \overline{I}_s, \end{cases}$$

and for at least one  $i \in \overline{I}_s$ ,  $|\Delta_i| = \delta_0$ . Performing a singular value decomposition of this  $\Delta$  and factoring out a scaling matrix gives

$$\Delta = U\Sigma_s \Sigma V^*, \quad U, V \in \mathcal{Q} \quad (\mathcal{Q} \text{ is defined by Equation 2.14})$$

with

$$\begin{aligned} \Sigma &= \text{diag}(d_1 I_1, \dots, d_m I_m), & \dim(I_i) &= k_i \times k_i \\ \Sigma_s &= \text{diag}(\hat{d}_1 I_1, \dots, \hat{d}_m I_m), & \dim(I_i) &= k_i \times k_i \end{aligned}$$

where  $\Sigma_s$  is a scaling matrix defined by

$$\hat{d}_i = \begin{cases} 1/\delta_0, & i \in I_s \\ 1, & i \in \overline{I}_s. \end{cases}$$

Therefore each element of  $\Sigma$  is bounded in magnitude by  $\delta_0$ ,

$$\max_i |d_i| = \delta_0.$$

Now

$$\det(I + U\Sigma_s \Sigma V^* M) = 0$$

can be considered as a polynomial in the  $m$  real variables,  $d_i$ . Denote this polynomial as  $p(d)$ , then

$$\delta_0 = \min \left\{ \|d\|_\infty \mid p(d) = 0 \right\}.$$

By Lemma 6.3 there exists  $\bar{d}$ , with elements  $\bar{d}_i$ , such that  $p(\bar{d}) = 0$  and  $|\bar{d}_i| = \delta_0$ . This is equivalent to the existence of a  $\Sigma$  such that

$$\begin{aligned} \Sigma &= \text{diag}(\bar{d}_1 I_1, \dots, \bar{d}_m I_m) \\ &= \delta_0 Q, \quad Q \in \mathcal{Q} \end{aligned}$$

satisfying

$$\det(I + \delta_0 U \Sigma_s Q V^* M) = 0.$$

Choose  $\Delta$  to be

$$\Delta = \delta_0 U \Sigma_s Q V^* \in \mathbf{B}_s^{\delta_0} \Delta.$$

Note that this choice of  $\delta$  satisfies the requirements of the Lemma. ▶

**Proof of Theorem 6.2:** It will be shown that  $\mu_s(M) \geq \tilde{\mu}_s(M)$ . By definition  $\mu_s(M) \geq 0$ , and so if  $\tilde{\mu}_s(M) = 0$ , the claim is obviously true. Consider the case where  $\tilde{\mu}_s(M) \neq 0$ . Initially consider  $\tilde{\mu}_s(M)$  to be finite. With this assumption there exists  $\bar{x}$  and  $\gamma$  achieving  $\tilde{\mu}_s(M)$ . This  $\bar{x}$  and  $\gamma$  will be used to construct a  $\Delta \in \mathbf{B}_s^\gamma \Delta$  such that  $\det(I + M\Delta) = 0$ . Now  $\tilde{\mu}_s(M)$  is defined by

$$\tilde{\mu}_s(M) = \max_{\gamma, \|\bar{x}\|=1} \left\{ \gamma \left| \begin{array}{l} \|R_i \bar{x}\| \leq \|R_i M \bar{x}\|, i \in I_s \\ \|R_i \bar{x}\| \gamma \leq \|R_i M \bar{x}\|, i \in \bar{I}_s \end{array} \right. \right\}, \quad (6.8)$$

implying that there exist  $Q_i$ ,  $\dim(Q_i) = k_i \times k_i$ , with  $\sigma_{\max}(Q_i) \leq 1$  such that

$$\begin{aligned} -R_i \bar{x} &= Q_i R_i M \bar{x}, i \in I_s \\ -\tilde{\mu}_s(M) R_i \bar{x} &= Q_i R_i M \bar{x}, i \in \bar{I}_s. \end{aligned}$$

Stacking these equations into a block matrix form gives

$$-\eta \bar{x} = Q M \bar{x}$$

where

$$\eta = \text{diag}(\eta_1 I_1, \dots, \eta_m I_m), \quad \eta_i = \begin{cases} 1, & i \in I_s \\ \tilde{\mu}_s(M), & i \in \bar{I}_s, \end{cases}$$

and

$$Q = \text{block diag}(Q_1, \dots, Q_m).$$

Therefore

$$(\eta I + Q M) \bar{x} = 0 \implies (I + \eta^{-1} Q M) \bar{x} = 0.$$

Note that choosing  $\Delta$  as  $\Delta = \eta^{-1} Q$  gives

$$\Delta \in \mathbf{B}_s^{\tilde{\mu}_s(M)^{-1}} \Delta \quad \text{and} \quad \det(I + M\Delta) = 0.$$

The definition of  $\mu_s(M)$ ,

$$\frac{1}{\mu_s(M)} = \min_{\Delta \in \mathbf{B}_s^\infty} \left\{ \delta \mid \exists \Delta \in \mathbf{B}_s^\delta \Delta \text{ such that } \det(I + M\Delta) = 0 \right\},$$

implies that

$$\frac{1}{\mu_s(M)} \leq \tilde{\mu}_s(M)^{-1}$$

and consequently

$$\mu_s(M) \geq \tilde{\mu}_s(M).$$

Now return to the assumption that  $\tilde{\mu}_s(M)$  is finite. If this were not so, then there would exist  $\gamma$  and  $x$  meeting the constraints of Equation 6.8 with  $\gamma > \mu_s(M)$ . It should be noted that the statement of the theorem assumes that  $\mu_s(M)$  is finite. The above construction could then be used to obtain a  $\Delta \in \mathbf{B}_s^\gamma \Delta$  for which  $\det(I + M\Delta) = 0$ , contradicting  $\gamma > \mu_s(M)$ .

Now consider the claim that  $\hat{\mu}_s(M) \geq \mu_s(M)$ . By definition  $\hat{\mu}_s(M) \geq 0$ , and so if  $\mu_s(M) = 0$ , the claim is obviously true. Assume then that  $\mu_s(M) > 0$  and define  $\delta = 1/\mu_s(M)$ .  $\delta$  is finite and by the assumption that  $\mu_s(M)$  is finite  $\delta > 0$ . This implies that there exists

$$\Delta \in \mathbf{B}_s^\delta \Delta \text{ such that } \det(I + \Delta M) = 0$$

and for at least one  $i \in \bar{I}_s$ ,  $\sigma_{\max}(\Delta_i) = \delta$ . By Lemma 6.4 there exists a  $\Delta$  such that

$$|\Delta_i| = \begin{cases} 1, & i \in I_s \\ \delta, & i \in \bar{I}_s \end{cases}$$

and  $\det(I + M\Delta) = \det(I + \Delta M) = 0$ . Consequently, there exists  $\bar{x}$  such that for this choice of  $\Delta$ ,

$$(I + \Delta M)\bar{x} = 0,$$

implying that

$$\bar{x} = -\Delta M \bar{x}.$$

Now consider the norm relationships implied by the above equation for each partition  $R_i$ :

$$\begin{aligned}\|R_i \bar{x}\| &= \|R_i M \bar{x}\|, \quad i \in I_s \\ \|R_i \bar{x}\| 1/\delta &= \|R_i M \bar{x}\|, \quad i \in \bar{I}_s.\end{aligned}$$

$\bar{x}$  and  $1/\delta$  therefore satisfy the conditions of the  $\hat{\mu}_s(M)$  maximization giving

$$\hat{\mu}_s(M) \geq 1/\delta = \mu_s(M).$$

Combining the above claims gives the following inequalities.

$$\hat{\mu}_s(M) \geq \mu_s(M) \geq \tilde{\mu}_s(M).$$

But any  $x$  and  $\gamma$  achieving the maximum for  $\hat{\mu}_s(M)$  also satisfies the conditions of  $\tilde{\mu}_s(M)$ , and therefore

$$\tilde{\mu}_s(M) \geq \hat{\mu}_s(M).$$

►

In the  $\mu$  case no conditions on the solutions of the maximizations being finite are required. This is not so for  $\mu_s(M)$  as can be seen in the following example. If  $\mu_s(M)$  is not finite, the value of  $\mu_s(M)$  implied as a result of the maximizations can be arbitrarily bad. To illustrate this consider

$$M = \begin{bmatrix} a & 0 \\ 1 & 0 \end{bmatrix}, \quad a > 1$$

with block structure (1,1) and  $I_s = \{1\}$ ,  $\bar{I}_s = \{2\}$ . Define  $x = [x_1 \ x_2]^T$ . Consider the  $\hat{\mu}_s(M)$  maximization in this case:

$$\hat{\mu}_s(M) = \max_{\gamma, \|x\|=1} \left\{ \gamma \left| \begin{array}{l} \|x_1\| = \|ax_1\| \\ \|x_2\|\gamma = \|x_1\| \end{array} \right. \right\}$$

The only way to meet the first constraint is to make  $x_1 = 0$ . This implies then that  $\|x_2\| = 1$ . The only way to achieve the second constraint is to set  $\gamma = 0$ , implying that  $\hat{\mu}_s(M) = 0$ .

Consider  $\Delta \in \Delta$ ,

$$\Delta = \begin{bmatrix} \delta_1 & 0 \\ 0 & \delta_2 \end{bmatrix}$$

with  $|\delta_1| \leq 1$  giving  $\Delta \in \mathbf{B}_g^\infty \Delta$ . Examine the condition  $\det(I + M\Delta) = 0$  for this  $\Delta$ .

$$\begin{aligned} \det(I + M\Delta) &= \det \left( I + \begin{bmatrix} a & 0 \\ 1 & 0 \end{bmatrix} \begin{bmatrix} \delta_1 & 0 \\ 0 & \delta_2 \end{bmatrix} \right) \\ &= \det \left( \begin{bmatrix} 1 + \delta_1 a & 0 \\ \delta_2 & 1 \end{bmatrix} \right) \\ &= 0 \end{aligned} \tag{6.9}$$

If  $\delta_1 = -1/a$ ,  $|\delta_1| < 1$  and Equation 6.9 is satisfied for any value of  $\delta_2$ , including  $\delta_2 = 0$ , implying that  $\mu_s(M) = \infty$ .

Now consider  $\tilde{\mu}_s(M)$  for this example. The first constraint of Equation 6.6 will be met for every  $x_1$ , and by choosing  $x_2 = 0$  the second can be met for any  $\gamma$  implying that  $\tilde{\mu}_s(M) = \infty$ .

This example will be reconsidered in Section 6.5.2 in light of the following geometric interpretation.

### 6.3 A Geometric Interpretation

The numerical range, or field of values, of a Hermitian matrix  $N$  is defined as the set

$$\{x^* N x \mid \|x\| = 1\}. \tag{6.10}$$

A generalization of the numerical range is the following. Consider  $m$  Hermitian matrices  $N_i$ ,  $i = 1, \dots, m$  of dimension  $n \times n$ . Define a vector valued function of  $x$  where each component of the vector  $\nu$  is given by

$$\nu_i = x^* N_i x.$$

Define as the generalized numerical range, the range of this function when the domain is restricted to  $\|x\| = 1$ :

$$W(N_1, \dots, N_m) = \{\nu \mid \nu_i = x^* N_i x, \|x\| = 1\}.$$

The following lemma is proven by Fan and Tits [25, 26].

#### Lemma 6.5

*If  $m < 3$ , or  $m = 3$  and  $n > 2$ , then  $W(N_1, \dots, N_m)$  is a convex set.*

The convexity of the  $m = 2$  case was proven by Doyle [7], and in a different context, by Householder [27]. The proof of the  $m = 1$  case is due to Hausdorff [28], and dates from the introduction of the numerical range by Toeplitz [29].

Now consider the application of the numerical range to the  $\mu_s(M)$  problem. Define

$$N(\alpha) = \begin{bmatrix} N_1(\alpha) \\ \vdots \\ N_m(\alpha) \end{bmatrix}$$

where  $\alpha \in \mathbf{R}$ ,  $\alpha \geq 0$ , and

$$N_i(\alpha) = \begin{cases} R_i^T R_i - M^* R_i^T R_i M, & i \in I_s \\ \alpha R_i^T R_i - M^* R_i^T R_i M, & i \in \bar{I}_s. \end{cases}$$

Note that each  $N_i(\alpha)$  is still Hermitian. The numerical range of  $N(\alpha)$  is defined as  $W(\alpha)$ :

$$W(\alpha) = \left\{ \nu \mid \nu_i = x^* N_i(\alpha) x, \|x\| = 1 \right\}.$$

For each  $\alpha$ ,  $W(\alpha)$  is a set in  $\mathbf{R}^m$ . For  $m \leq 3$  this set is convex as the above construction guarantees that  $n \geq m$ . Define  $c(\alpha)$  as the minimum distance between  $W(\alpha)$  and the origin.

$$c(\alpha) = \min \left\{ \|\nu\| \mid \nu \in W(\alpha) \right\}$$

**Lemma 6.6**

*If  $\mu_s(M)$  is finite,  $c(\mu_s(M)^2) = 0$ , and for all  $\alpha > \mu_s(M)^2$ ,  $c(\alpha) > 0$ .*

**Proof of Lemma 6.6:** Assume  $\bar{x}$  is a solution to the  $\mu_s(M)$  maximization of Equation 6.5. Then

$$\begin{aligned} \|R_i \bar{x}\| &= \|R_i M \bar{x}\|, & i \in I_s \\ \|R_i \bar{x}\| \mu_s(M) &= \|R_i M \bar{x}\|, & i \in \bar{I}_s. \end{aligned}$$

Now

$$\begin{aligned} c(\mu_s(M)^2) &= \min_{\|x\|=1} \left\{ \|\nu\| \mid \nu_i = x^* N_i(\mu_s(M)^2) x \right\} \\ &= \min_{\|x\|=1} \left\{ \left( \sum_{i=1}^m (x^* N_i(\mu_s(M)^2) x)^2 \right)^{1/2} \right\} \\ &\leq \left( \sum_{i=1}^m (\bar{x}^* N_i(\mu_s(M)^2) \bar{x})^2 \right)^{1/2}. \end{aligned}$$

However,

$$\begin{aligned} \bar{x}^* N_i(\mu_s(M)^2) \bar{x} &= \begin{cases} \|R_i \bar{x}\|^2 - \|R_i M \bar{x}\|^2, & i \in I_s \\ \|R_i \bar{x}\|^2 \mu_s(M)^2 - \|R_i M \bar{x}\|^2, & i \in \bar{I}_s \end{cases} \\ &= 0 \end{aligned} \quad (6.11)$$

and so  $c(\mu_s(M)^2) = 0$ . To prove the second part of the lemma, assume that for a particular  $\alpha$ ,  $0 \in W(\alpha)$ . This implies that there exists an  $x$ , denoted here by  $\hat{x}$ , such that

$$\hat{x}^* N_i(\alpha) \hat{x} = 0, \quad i = 1, \dots, m.$$

Therefore,

$$\begin{aligned} \|R_i \hat{x}\|^2 - \|R_i M \hat{x}\|^2 &= 0, \quad i \in I_s \\ \|R_i \hat{x}\|^2 \alpha - \|R_i M \hat{x}\|^2 &= 0, \quad i \in \bar{I}_s \end{aligned}$$

which implies that

$$\begin{aligned} \|R_i \hat{x}\| &= \|R_i M \hat{x}\|, \quad i \in I_s \\ \|R_i \hat{x}\| \alpha^{1/2} &= \|R_i M \hat{x}\|, \quad i \in \bar{I}_s. \end{aligned}$$

$\alpha^{1/2}$  is a feasible point of the  $\mu_s(M)$  maximization of Equation 6.5 and so

$$\alpha^{1/2} \leq \mu_s(M) \implies \alpha \leq \mu_s(M)^2.$$

►

### Corollary 6.7

If  $\mu_s(M)$  is finite,

$$\mu_s(M) = \inf_{\alpha} \left\{ \alpha^{1/2} \mid 0 \notin W(\beta) \text{ for all } \beta > \alpha \right\}.$$

The calculation of  $\mu_s(M)$  can be formulated as a search over  $\alpha$ . Before proceeding with an algorithm, it is necessary to investigate several properties of  $c(\alpha)$ .

### Lemma 6.8

$c(\alpha)$  is continuous and for all  $\alpha \in \mathbf{R}$ ,  $s \in \mathbf{R}$ , with  $s \geq 0$ ,

$$c(\alpha + s) \leq c(\alpha) + s.$$

**Proof of Lemma 6.8:** Define  $\phi(x, \alpha)$  as a vector valued function of  $x$  and  $\alpha$ :

$$\phi_i(x, \alpha) = x^* N_i(\alpha) x, \|x\| = 1, \alpha \in \mathbf{R} \quad i = 1, \dots, m$$

Then

$$c(\alpha) = \min_x \|\phi(x, \alpha)\|.$$

The norm is a continuous function of its argument,  $\phi(x, \alpha)$  is also continuous, and as the domain  $x, \|x\| = 1$ , is compact,  $c(\alpha)$  is continuous.

Consider

$$c(\alpha + s) = \min_{\|x\|=1} \left\{ \left( \sum_{i=1}^m (x^* N_i(\alpha + s) x)^2 \right)^{1/2} \right\}.$$

Define the vector valued functions  $A(x, \alpha)$  and  $B(x)$  by

$$A_i(x, \alpha) = x^* N_i(\alpha) x$$

and

$$B_i(x) = x^* \delta(i) T_i x \quad \text{where } \delta(i) = \begin{cases} 0, & i \in I_s \\ 1, & i \in \bar{I}_s. \end{cases}$$

Then

$$x^* N_i(\alpha + s) x = A_i(x, \alpha) + B_i(x)$$

and

$$\begin{aligned} c(\alpha + s) &= \min_{\|x\|=1} \|A(x, \alpha) + sB(x)\| \\ &\leq \min_{\|x\|=1} \{\|A(x, \alpha)\| + s\|B(x)\|\}. \end{aligned}$$

Note that

$$\|B(x)\| \leq \|x\| = 1,$$

implying that

$$\begin{aligned} c(\alpha + s) &\leq \min_{\|x\|=1} \{\|A(x, \alpha)\| + s\} \\ &= \min_{\|x\|=1} \{\|A(x, \alpha)\|\} + s \\ &= c(\alpha) + s. \end{aligned}$$





## 6.4 An Algorithm for $\mu_s(M)$

Corollary 6.7 and Lemma 6.8 suggest an algorithm for the calculation of  $\mu_s(M)$ . This is the same algorithm as that presented by Fan and Tits [9]. The proof of convergence is also identical but is included here for completeness. This algorithm actually calculates  $\hat{\mu}_s(M)$ . The assumption that  $\mu_s(M)$  is finite is disguised in step *i*.

### 6.4.1 Outline of the $\mu_s(M)$ Algorithm

**Algorithm 6.9** ( $\mu_s(M)$ )

- i*) Set  $\alpha_0 \geq \mu_s(M)^2$ .
- ii*)  $\alpha_{j+1} = \alpha_j - c(\alpha_j)$ .
- iii*)  $j = j + 1$ . Go to step *ii*.

**Theorem 6.10**

*The sequence  $\{\alpha_j\}$  generated by Algorithm 6.9 is monotonic nonincreasing and*

$$\lim_{j \rightarrow \infty} \alpha_j = \mu_s(M)^2.$$

**Proof of Theorem 6.10:** If  $\alpha_j \geq \mu_s(M)^2$ , then  $\alpha_{j+1} \geq \mu_s(M)^2$ . To show this, consider the means of obtaining  $\alpha_{j+1}$  (step *ii* of Algorithm 6.9).

$$\begin{aligned} \alpha_{j+1} &= \alpha_j - c(\alpha_j) \\ &= \alpha_j - c(\alpha_j - \mu_s(M)^2 + \mu_s(M)^2) \\ &\geq \alpha_j - c(\mu_s(M)^2) + \mu_s(M)^2 - \alpha_j \quad \text{by Lemma 6.8} \\ &\geq \mu_s(M)^2 \quad \text{as } c(\mu_s(M)^2) = 0. \end{aligned}$$

Given, by step *i* of the algorithm,  $\alpha_0 \geq \mu_s(M)^2$ , then  $\alpha_j \geq \mu_s(M)^2$  for all  $j$ . The sequence is monotonic nonincreasing as  $c(\alpha) \geq 0$  for all  $\alpha \in \mathbf{R}$ . The algorithm therefore converges to a limit, denoted here by  $\bar{\alpha}$ , satisfying

$$\bar{\alpha} \geq \mu_s(M)^2. \tag{6.12}$$

Taking the limit of step *ii*, and noting from Lemma 6.8 that  $c(\alpha)$  is continuous, gives

$$\bar{\alpha} = \bar{\alpha} - c(\bar{\alpha}).$$

This implies that  $c(\bar{\alpha}) = 0$  which by Lemma 6.6 implies that  $\bar{\alpha} \leq \mu_s(M)^2$ . Combining this with the inequality of Equation 6.12 gives the desired result.  $\blacktriangleright$

It should be noted that for  $\alpha < \mu_s(M)^2$  it is not necessarily true that  $0 \in W(\alpha)$ . This may make the choice of  $\alpha_0$  difficult. In the case where  $I_s = \emptyset$ ,  $\mu_s(M) = \mu(M)$ , and the obvious choice is the upper bound:  $\alpha_0 = \sigma_{\max}(M)^2$ .

When  $\mu_s(M)$  is not finite, it is not possible to choose  $\alpha_0$ . If  $\alpha_0 < \mu_s(M)^2$ , the algorithm may converge to an incorrect finite value. The examples demonstrated in Section 6.5.2 have this unfortunate property.

Algorithm 6.9 disguises the difficulties in the calculation of  $\mu_s(M)$ . These difficulties are identified in the next section.

#### 6.4.2 On the Calculation of $c(\alpha)$

Critical to Algorithm 6.9 is the calculation of  $c(\alpha)$ . This is still an unsolved problem. It is, however, easy to calculate the following:

$$c'(\alpha) = \min \left\{ \|\nu\| \mid \nu \in \text{co}[W(\alpha)] \right\}.$$

The following algorithm, due to Gilbert [30], will calculate  $c'(\alpha)$ . This algorithm is discussed by Doyle [7] and Packard [10], both of whom provide a proof of convergence. In the discussion below the index  $j$  will denote iteration number.

##### Algorithm 6.11 ( $c'(\alpha)$ )

- i) Select any  $\nu_0 \in \text{co}[W(\alpha)]$ . Any choice of  $x_0$ ,  $\|x_0\| = 1$ , will give a suitable  $\nu_0$  by  $\nu_i = x_0^* N_i(\alpha) x_0$ .
- ii) Given  $\nu_j \in \text{co}[W(\alpha)]$ , find  $\bar{\nu}_j \in W(\alpha)$  minimizing  $\langle \nu_j, \bar{\nu}_j \rangle$ .
- iii)  $\nu_{j+1} = \min\{\text{co}[\nu_j, \bar{\nu}_j]\}$ . Clearly  $\nu_{j+1} \in \text{co}[W(\alpha)]$ .
- iv)  $j = j + 1$ . Go to step ii.

Step *ii* of the algorithm is now considered in greater detail. The iteration index  $j$  is dropped for clarity. The index  $i$  will be used to denote the  $i^{\text{th}}$  component of  $\nu$ :  $\nu_i = x^* N_i(\alpha) x$ .

$$\begin{aligned} \min_{\|x\|=1} \langle \nu, \bar{\nu} \rangle &= \min_{\|x\|=1} \sum_{i=1}^m \nu_i \bar{\nu}_i \\ &= \min_{\|x\|=1} \sum_{i=1}^m \nu_i \bar{x}^* N_i(\alpha) \bar{x} \\ &= \min_{\|x\|=1} \bar{x}^* \left( \sum_{i=1}^m \nu_i N_i(\alpha) \right) \bar{x}. \end{aligned}$$

This is achieved for any unit norm  $x$  corresponding to the minimum eigenvalue:

$$\gamma_{\min} \left( \sum_{i=1}^m \nu_i N_i(\alpha) \right).$$

Unfortunately for  $0 \in \text{co}[W(\alpha)]$ ,

$$\lim_{j \rightarrow \infty} \nu_j = 0 \implies \lim_{j \rightarrow \infty} \left( \sum_{i=1}^m \nu_i N_i(\alpha) \right) = 0.$$

As  $j \rightarrow \infty$ , and  $\alpha$  approaches  $\mu_s(M)^2$ , the algorithm requires finding the eigenvector corresponding to the minimum eigenvalue of a matrix which is itself approaching zero. This is numerically poorly conditioned, and this algorithm will not reliably give  $x_j$  as  $j \rightarrow \infty$ .

### 6.4.3 An Imperfect Algorithm

Using  $c'(\alpha)$  instead of  $c(\alpha)$  gives the following algorithm.

#### Algorithm 6.12

- i*) Set  $\alpha_0 \geq \mu_s(M)^2$ .
- ii*)  $\alpha_{j+1} = \alpha_j - c'(\alpha_j)$ .
- iii*)  $j = j + 1$ . Go to step *ii*.

In certain cases this will still yield the correct value of  $\mu_s(M)$ . The following results are immediate.

**Theorem 6.13**

If  $\mu_s(M)$  is finite and  $c'(\alpha) = c(\alpha)$  for all  $\alpha \in \mathbf{R}$ , then Algorithm 6.12 converges to  $\mu_s(M)^2$ .

**Proof of Theorem 6.13:** Substitution of  $c(\alpha)$  for  $c'(\alpha)$  in Algorithm 6.13 gives Algorithm 6.9. Theorem 6.10 then gives the result. ▶

**Lemma 6.14**

If  $W(\alpha)$  is convex, then  $c'(\alpha) = c(\alpha)$  for all  $\alpha \in \mathbf{R}$ .

**Proof of Lemma 6.14:** If  $W(\alpha)$  is convex, then  $\text{co}[W(\alpha)] = W(\alpha)$ . ▶

**Lemma 6.15**

If  $\mu_s(M)$  is finite and  $m \leq 3$ , Algorithm 6.12 converges to  $\mu_s(M)^2$ .

**Proof of Lemma 6.15:** By Lemma 6.5, if  $m \leq 3$ , then  $W(\alpha)$  is convex. Lemma 6.14 and Theorem 6.13 then give the result. ▶

The above supports Doyle's [7] result that  $\mu(M)$  can easily be calculated for  $m \leq 3$ . The fact that this is also true for  $\mu_s(M)$  is hardly surprising as  $\mu_s(M)$  can be iteratively calculated from  $\mu(M)$ . Note that a particular type of nonconvexity is required in order for Algorithm 6.12 to fail to yield  $\mu_s(M)^2$ . More specifically, Algorithm 6.12 will converge to a value strictly greater than  $\mu_s(M)^2$  only if there exists  $\alpha > \mu_s(M)^2$  for which  $0 \in \text{co}[W(\alpha)]$ .

Fan and Tits [9] show that in the  $\mu(M)$  case, the existence of a halfspace containing  $W(\mu(M)^2)$  is equivalent to the existence of  $D \in \mathcal{D}$  such that

$$\inf_{D \in \mathcal{D}} \sigma_{\max}(DM D^{-1}) = \mu(M).$$

Section 7.5.1 will give a similar result relating the existence of the halfspace to the existence of a saddlepoint of the Lagrangian for the model validation problem.

## 6.5 Numerical Examples

### 6.5.1 A Geometric Example of $\mu(M)$ and $\mu_s(M)$

To illustrate some of the geometric concepts consider the following system.

$$M = \begin{bmatrix} 0.05 - 0.5i & 1.0 + i & -0.1 + 0.25i \\ 0.5 & 0.75 + 0.5i & 0.5i \\ 1.0 - 0.25i & 1.0 & -0.5 + i \end{bmatrix} \quad (6.13)$$

and a block structure of (1,2). Two cases are considered:

- i)  $I_s = \emptyset$ .  $\bar{I}_s = \{1, 2\}$ . This is simply  $\mu(M)$ .
- ii)  $I_s = \{1\}$ .  $\bar{I}_s = \{2\}$ .

The boundaries of  $W(\alpha)$  for  $\alpha = 0, 1, 5.6, 15,$  and  $20$  are plotted in each of the figures. The algorithm for plotting the boundaries of  $W(\alpha)$ , for  $m = 2$ , is given in the next section. Figure 6.3 shows these boundaries for the first case. In this example  $\mu(M)^2 = 5.6$  and, as expected, the curve labeled  $W(5.6)$  passes through the origin.

Figure 6.4 shows the boundaries for the second case. Note that for  $I_s = \{1\}$ ,  $\mu_s(M)^2 = 15$ , and the curve labeled  $W(15)$  passes through the origin. The  $\alpha = 1$  curve is actually identical on both plots as for  $I_s \neq \emptyset$  the assumed scaling is one. This is difficult to see as Figures 6.3 and 6.4 use different axis scales.

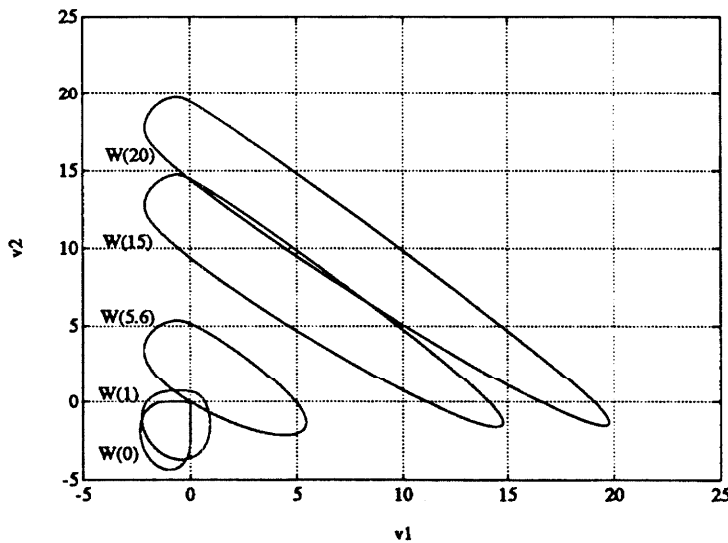


Figure 6.3: Boundaries of  $W(\alpha)$  for  $\alpha = 0, 1, 5.6, 15,$  and  $20$ .  $I_s = \emptyset$ . ( $\mu(M)$ )

### 6.5.2 The Pathological Example Revisited

Consider again

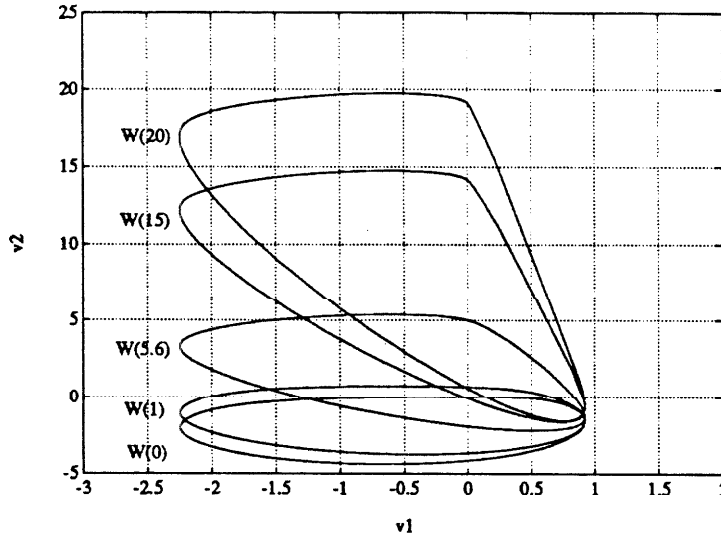


Figure 6.4: Boundaries of  $W(\alpha)$  for  $\alpha = 0, 1, 5.6, 15,$  and  $20$ .  $I_s = \{1\}$

$$M = \begin{bmatrix} a & 0 \\ 1 & 0 \end{bmatrix}, \quad a > 1$$

with a block structure  $(1,1)$  and  $I_s = \{1\}$ . For this example the sets  $W(\alpha)$  are simply intervals.  $W(\alpha)$  will be examined for  $a = 2$ . Figure 6.5 shows the boundary of  $W(\alpha)$  plotted for  $\alpha = 0, 1,$  and  $5$ . Note that  $0 \in W(0)$  and for  $\alpha > 0, 0 \notin W(\alpha)$ . The  $\nu_2 = 0$  axis gives all solutions meeting the second ( $\bar{I}_s$ ) constraint with equality. Note that for all  $\alpha > 0$ , this axis intersects  $W(\alpha)$  in a region where  $\nu_1 < 0$ . The  $x$  giving these points satisfy the first constraint ( $I_s$ ) with a strict inequality. Observe that such a region can always be found. As  $\alpha \rightarrow \infty$  the only  $\nu$  in  $W(\alpha)$  with  $\nu_2 = 0$  is the point  $\nu = [-3 \ 0]^T$ .

### 6.5.3 Algorithm to Plot the Boundaries of $W(\alpha)$

The algorithm to plot the boundaries of  $W(\alpha)$  when  $m = 2$  is that used by Fan and Tits [9]. It is given here for completeness.

#### Algorithm 6.16 ( $W(\alpha)$ Boundary)

- i) Set  $\theta = 0$  and choose  $K$  to be a large integer.
- ii) Select  $x$ , any unit norm eigenvector corresponding to

$$\gamma_{\min} [\cos \theta N_1(\alpha) + \sin \theta N_2(\alpha)].$$

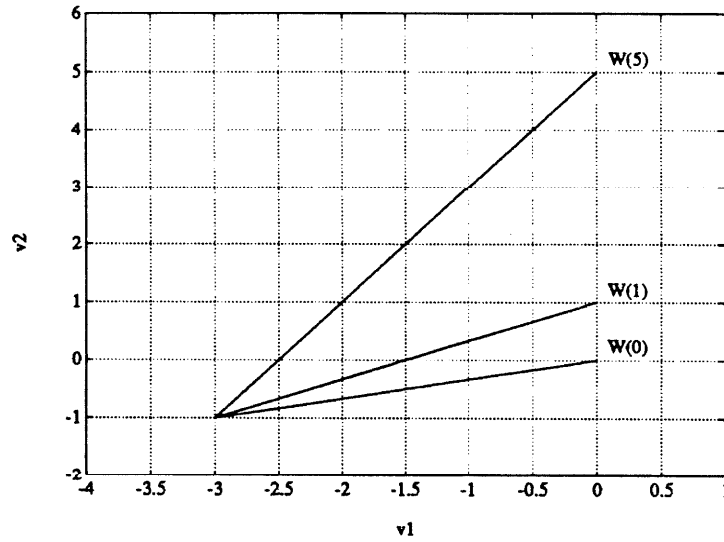


Figure 6.5: Boundaries of  $W(\alpha)$  for  $\alpha = 0, 1,$  and  $5$ .  $I_s = \{1\}$ . ( $a = 2$ )

iii) Set

$$\nu_2 = \begin{bmatrix} x^* N_1(\alpha) x \\ x^* N_2(\alpha) x \end{bmatrix}.$$

iv) If  $\theta \neq 0$  draw the line segment  $\overline{\nu_1 \nu_2}$ .

If  $\theta \geq 2\pi$  stop.

v) Set  $\nu_1 = \nu_2$ ,  $\theta = \theta + 2\pi/K$ . Go to step ii.

## Chapter 7

# A General Interconnection Structure

A more general  $(P, \Delta)$  interconnection structure, one in which known inputs and outputs are included, is now presented. Several problems can be posed with such a structure;  $\mu$ ,  $\mu_s$ , and model validation are examples. It is shown, by treating the model validation problem as an example, how the general problem can be reformulated using the generalized numerical range of Chapter 6. The convexity properties of the numerical range are then inherited by each of the subproblems. The geometric framework also gives an interpretation of the existence of a Kuhn-Tucker saddlepoint. For the model validation example, this framework is used to determine the conditions under which a saddlepoint will always exist.

The discussion of the interconnection structure and the resulting problems is applicable to general systems of matrix operators. However, the specific results applying to the model validation problem will assume a constant matrix problem with a minimum  $\|w\|$  objective.



## 7.1 Formulation of the General Problem

### 7.1.1 Interconnection Structure

Consider all possible classes of inputs and outputs used in both  $\mu$  and model validation problems. These are:

- $v$  Inputs from the  $\Delta$  block. These are signals internal to the model.
- $z$  Outputs to the  $\Delta$  block. Again these are internal to the model.
- $w$  Inputs to the system which are known to have bounded norm. These can have physical meaning: noise, disturbances, command inputs.
- $e$  Outputs from the system for which the norm is the quantity of interest. These can be errors, actuator outputs, and/or combinations of variables.
- $u$  Known or measured inputs to the system.
- $y$  Known or measured outputs from the system.

A general interconnection structure including all of the above listed inputs and outputs is shown in Figure 7.1. The notation  $N_{ij}$  is used to represent the elements of the interconnection structure in order to avoid confusion with the subblocks  $P_{ij}$  introduced in earlier chapters.

It is again assumed that each of the  $m$  perturbation blocks is a square norm-bounded matrix operator. In the discussion that follows, when both  $e$  and  $w$  are present in the model, it will be assumed that  $\dim(e) = \dim(w)$ . This is without loss of generality as the interconnection structure can be augmented with zero inputs or outputs.

Chapter 6 introduced the consideration of norm constrained problems in which certain of the norm relationships are fixed and others are allowed to scale in an optimization problem. The general problem presented here is simply the  $\mu_s$  problem with an additional constraint imposed by the input  $u$  and output  $y$ .

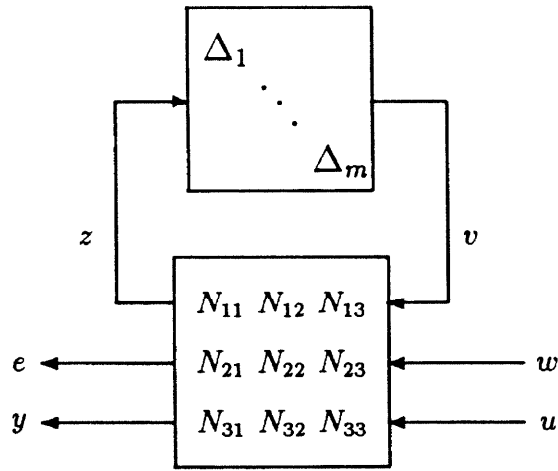


Figure 7.1: The General Interconnection Structure

Consider the norm relationships implied by Figure 7.1. Again the vector  $x$  is defined as  $x = [v^T \ w^T]^T$ .

$$\|v_i\|_{S_i} \leq \left\| \left( [N_{11} \ N_{12} \ N_{13}] \begin{bmatrix} x \\ u \end{bmatrix} \right)_i \right\|, \quad i = 1, \dots, m. \quad (7.1)$$

$$\|w\|_{S_{m+1}} \leq \left\| [N_{21} \ N_{22} \ N_{23}] \begin{bmatrix} x \\ u \end{bmatrix} \right\| \quad (7.2)$$

$$y = [N_{31} \ N_{32} \ N_{33}] \begin{bmatrix} x \\ u \end{bmatrix} \quad (7.3)$$

where  $S_i$  represents a general scaling.

The integers  $1, \dots, m+1$  are divided into two disjoint sets:  $I_s$  and  $\bar{I}_s$ , where  $I_s$  may be empty. As in Chapter 6 this will allow one of the norm relationships of Equation 7.1 or 7.2 to be considered as a maximization objective and the remaining norm relationships to be considered as constraints. For  $i \in I_s$ , the norm relationship is assumed to be fixed and, without loss of generality, is assumed to be unity. For  $i \in \bar{I}_s$ , the norm relationships will be scaled, and, consistent with Chapter 6, the variable  $\gamma$  will be used as the scaling. In terms of the general scaling  $S$  introduced above,

$$S_i = \begin{cases} 1 & \text{for } i \in I_s \\ \gamma & \text{for } i \in \bar{I}_s. \end{cases}$$

Again  $R_i$  is defined as the projection from  $x$  to the components of  $x$  corresponding to the  $i^{\text{th}}$   $\Delta$  block. However, in order to discuss the problem in the most general manner  $R_i$  is defined for  $i = 1, \dots, m + 1$ . Contrast this with the definition used throughout Chapter 3 (Equation 3.3). For the remainder of this chapter  $R_i$  is defined by

$$R_i = \text{block row}(0_1, \dots, 0_{i-1}, I_i, 0_{i+1}, \dots, 0_{m+1}),$$

where the row dimension of all blocks is  $k_i$  if  $i = 1, \dots, m$  and equal to  $\dim(w)$  if  $i = m + 1$ . The column dimension of the  $j^{\text{th}}$  block is equal to  $k_j$  for  $j = 1, \dots, m$  and  $\dim(e)$  for  $j = m + 1$ .

A two element vector notation, similar to that in Chapter 3, will again be adopted to identify certain components of  $[z \ e \ y]^T$ . The notation is as follows:

$$R_i x = v_i \quad \text{and} \quad \begin{bmatrix} R_i & 0 \end{bmatrix} N \begin{bmatrix} x \\ u \end{bmatrix} = z_i, \quad \text{for } i = 1, \dots, m,$$

$$R_i x = w \quad \text{and} \quad \begin{bmatrix} R_i & 0 \end{bmatrix} N \begin{bmatrix} x \\ u \end{bmatrix} = e, \quad \text{for } i = m + 1,$$

$$\text{and} \quad \begin{bmatrix} 0 & I \end{bmatrix} N \begin{bmatrix} x \\ u \end{bmatrix} = y.$$

As in the model validation problem, it is possible that there is no  $x$  such that

$$\begin{aligned} y &= \begin{bmatrix} 0 & I \end{bmatrix} N \begin{bmatrix} x \\ u \end{bmatrix} \\ &= \begin{bmatrix} N_{31} & N_{32} & N_{33} \end{bmatrix} \begin{bmatrix} x \\ u \end{bmatrix}. \end{aligned}$$

Define  $\mathcal{X}_e$  as the set of all  $x$  meeting this equality constraint:

$$\mathcal{X}_e := \left\{ x \mid y = \begin{bmatrix} 0 & I \end{bmatrix} N \begin{bmatrix} x \\ u \end{bmatrix} \right\}.$$

When this problem framework is applied to the model validation problem, this definition of  $\mathcal{X}_e$  will coincide with that of Equation 3.12. It will also be required that there exist an  $x \in \mathcal{X}_e$  such that the norm conditions corresponding to  $i \in I_s$  are satisfied. More formally,  $x$  will be called “feasible” if  $x \in \mathcal{X}_e$  and

$$\|R_i x\| \leq \left\| \begin{bmatrix} R_i & 0 \end{bmatrix} N \begin{bmatrix} x \\ u \end{bmatrix} \right\|, \quad i \in I_s.$$

The formulation of a meaningful optimization problem requires the existence of at least one feasible  $x$ .

The general problem to be considered is the following.

### Problem 7.1

*If there exists at least one feasible  $x$ , then compute the following quantity:*

$$\sup_{\gamma, x} \left\{ \gamma \left| \begin{array}{l} \|R_i x\| \leq \left\| \begin{bmatrix} R_i & 0 \end{bmatrix} N \begin{bmatrix} x & u \end{bmatrix}^T \right\|, i \in I_s \\ \|R_i x\| \gamma \leq \left\| \begin{bmatrix} R_i & 0 \end{bmatrix} N \begin{bmatrix} x & u \end{bmatrix}^T \right\|, i \in \bar{I}_s \\ y = \begin{bmatrix} 0 & I \end{bmatrix} N \begin{bmatrix} x & u \end{bmatrix}^T \end{array} \right. \right\}$$

If the input-output constraint of Equation 7.3 is dropped, then Problem 7.1 reminiscent of  $\mu_s(N)$ . The following section will discuss some of the problems that this framework can be used to address.

#### 7.1.2 Applicable problems

A series of problems can be posed for the structure depicted in Figure 7.1. The following distinctions and nomenclature are somewhat arbitrary but serve to illustrate the range of problems that this framework will address.

It is important to note the distinction between an input or output being equal to zero or being absent. For example  $y = 0$  imposes as much of a constraint on the problem as any other value of  $y$ . However,  $y$  being absent poses no constraint.

- i) *Given measured inputs  $u$ , outputs  $y$ , and  $\|\Delta\| \leq 1$ , what is the maximum gain from  $w$  to  $e$  ( $\|e\|/\|w\|$ )? This is Problem 7.1 with  $I_s = \{1, \dots, m\}$  and  $\bar{I}_s = \{m+1\}$ . Without the  $y$  and  $u$  constraints, it would be possible to assume that either  $\|e\| = 1$  or  $\|w\| = 1$  and pose the question as a worst case output or minimum norm input question. This may no longer be true in general.*
- ii) *The signal  $e$  is absent, and  $y$  are  $u$  are known outputs and inputs.  $w$  is known to be bounded. This is the model validation problem. Three cases serve to illustrate the range of possible subproblems.*

- (a)  $\|\Delta\| \leq 1$ . This is the minimum  $\|w\|$  problem considered in detail in Chapter 5. This can be formulated as Problem 7.1 where  $I_s = \{1, \dots, m\}$ .
- (b)  $\|w\| \leq 1$ . Again a Problem 7.1 arises with  $I_s = m + 1$ . All  $\Delta$  blocks scale equally and the minimum  $\|\Delta\|$  solution will be found.
- (c)  $I_s$  is any other subset of  $\{1, \dots, m + 1\}$ . The previous two cases can be considered as extremes of the more general problem. Considering the model validation problem as a constrained  $\mu_s$  problem allows the choice of the  $\|\Delta_i\| \leq 1$  assumption to be placed on any subset of  $\{1, \dots, m\}$ .

A particularly relevant subproblem is then, *given a selected  $\Delta_i$ , what is the minimum  $\|\Delta_i\|$  such that  $\|\Delta_j\| \leq 1, j \neq i, \|w\| \leq 1$ , and the observed datum is accounted for?* This is a powerful tool for the identification of systems modeled with  $F_u(P, \Delta)$  models.

- iii) The signal  $w$  is absent. *Given measured inputs ( $u$ ) and a measured part of the output ( $y$ ), what is the worst case  $e$  that can arise from  $\|\Delta\| \leq 1$ ?* This formulation can be used to study worst case internal variables given an observed input and output.
- iv) The signal  $y$  is absent. *Given a known part of the input ( $u$ ), and an unknown bounded part ( $w, \|w\| \leq 1$ ), what is the worst case  $e$ ?* This is simply a  $\mu$  problem (or more generally a  $\mu_s$  problem) with part of the input known.
- v) The signal  $u$  is absent. This is again a worst case error question where part of the output ( $y$ ) is constrained.
- vi) The signals  $u$  and  $y$  are both absent. This is the usual  $\mu$  (or  $\mu_s$ ) formulation.
- vii) Both  $e$  and  $w$  are absent. The problem becomes, *what is the minimum  $\|\Delta\|$  that can account for the observed datum ( $y$  and  $u$ )?*

The above list gives an idea of the type of problems that can be posed in this framework. It should be noted that whenever  $y$  and/or  $u$  are present, there is an equality constraint upon  $x$ . In the constant matrix case, the equality constraint will be reformulated to give a subspace constraint on  $x$ . Unfortunately, the subspace constraint alters

the characteristics of the associated optimization problem. In Chapter 6 it was shown that for finite  $\mu_s$ , the maximization problems  $\bar{\mu}_s$  and  $\hat{\mu}_s$  were equivalent. When a subspace constraint is imposed, this is no longer true. The norm inequalities arising from the  $\Delta$  blocks might not be met at their boundaries (for  $\|\Delta_i\| = 1$ ). It is for this reason that less than or equal to signs were used in the formulation of Problem 7.1. In the constant matrix case, Problem 7.1 is therefore more closely related to  $\bar{\mu}_s$  than to  $\mu_s$  itself.

In some cases certain of the signals are absent, the signal  $e$ , for example, in the model validation problem. This will often change the nature of the problem formulation. However, the techniques used here in considering the general problem will still be applicable. Section 7.3 demonstrates this for the case of model validation.

The next section will demonstrate a means of reformulating Problem 7.1 in order to replace the equality constraint by a subspace constraint. For the model validation case at least, this leads to a solution via the geometric framework of Chapter 6.

## 7.2 Reformulation of the General Problem

Problem 7.1 is similar to the  $\mu_s$  problem of Chapter 6. The differences are the imposition of the equality constraint and the inclusion of  $u$  in the norm constraints. This section will introduce a reformulation of the problem which will allow the geometric analysis of Chapter 6 to be applied to the model validation problem.

Consider the equality constraint imposed by  $y$  and  $u$ .

$$y = \begin{bmatrix} N_{31} & N_{32} & N_{33} \end{bmatrix} \begin{bmatrix} x \\ u \end{bmatrix}. \quad (7.4)$$

This vector constraint will be replaced by a subspace constraint plus a scalar equality constraint. The method used is similar to the reparametrization of Section 3.2.1. The details presented here are applicable to constant matrix problems; however, the principles used in this formulation can be applied to more general systems.

Denote by  $V$  an orthonormal matrix of basis vectors for the kernel of  $[N_{31} \ N_{32}]$ . Choose  $x_0$  as the solution to Equation 7.4 with  $x_0$  orthogonal to  $V$ . Define the subspace  $\mathcal{X}$  by

$$\mathcal{X} = \text{span}\{x_0, V\},$$

then  $x$  satisfies Equation 7.4 if and only if  $x \in \mathcal{X}$  and  $\langle x_0, x \rangle = \|x_0\|^2$ . These constraints will now be applied to the problem.

Now consider the system shown in Figure 7.2. Note that  $\dim(\hat{y}) = 1$  and  $\dim(\hat{u}) = 1$ . Furthermore, if  $\hat{y} = 1$ , then  $\langle x_0, x \rangle = \|x_0\|^2$ . If in addition  $x \in \mathcal{X}$ , then the output equality constraint is satisfied. Note also that if  $\hat{u} = 1$ , then  $N_{13}u\hat{u} = N_{13}u$  (and similarly for  $N_{23}u$ ) and the effect of the input on  $z$  and  $e$  is correct.

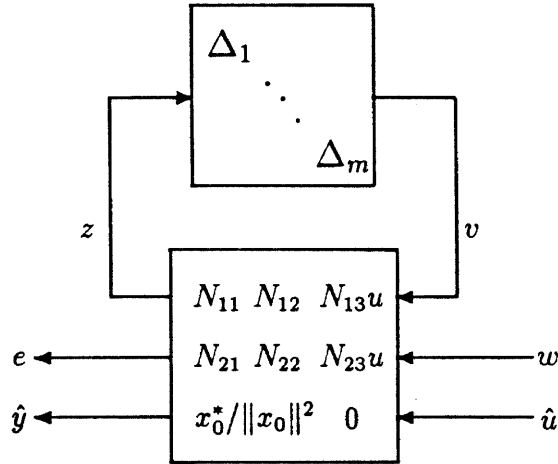


Figure 7.2: The Generic System with a Reparametrization to give Scalar Constraints

It is possible to at least guarantee that  $\hat{y} = \hat{u}$  by closing the loop from  $\hat{y}$  to  $\hat{u}$ . Doing this results in the following system:

$$\tilde{N} = \begin{bmatrix} N_{11} & N_{12} \\ N_{21} & N_{22} \end{bmatrix} + \frac{1}{\|x_0\|^2} \begin{bmatrix} N_{13}u x_0^* \\ N_{23}u x_0^* \end{bmatrix}$$

with inputs  $v$  and  $w$  and outputs  $z$  and  $e$ . This allows Problem 7.1 to be cast into the following problem. Note that the equality constraint has been replaced by a subspace constraint and an equality constraint on  $x$ , and that  $u$  no longer enters the norm constraints directly.

**Problem 7.2**

If there exists at least one feasible  $x$ , then compute the following quantity:

$$\sup_{\gamma, x} \left\{ \gamma \left| \begin{array}{l} \|R_i x\| \leq \|R_i \tilde{N} x\|, i \in I_s \\ \|R_i x\| \gamma \leq \|R_i \tilde{N} x\|, i \in \bar{I}_s \end{array} \right. \right\}$$

subject to  $x \in \mathcal{X}$  and  $\langle x_0, x \rangle = \|x_0\|^2$ .

Although the constraint  $\langle x_0, x \rangle = \|x_0\|^2$  appears to be as restrictive as the original constraint, it will subsequently be seen that it is only important that  $\langle x_0, x \rangle \neq 0$ .

The equivalence of Problems 7.1 and 7.2 is formally stated and proven in the following theorem.

**Theorem 7.3**

*Problem 7.1 is equivalent to Problem 7.2.*

**Proof of Theorem 7.3:** Consider every feasible  $x$  for Problem 7.2:  $x \in \mathcal{X}$ ,  $\langle x_0, x \rangle = \|x_0\|^2$ , and

$$\begin{aligned} \|R_i x\| &\leq \|R_i \tilde{N} x\| \\ &= \left\| R_i \left( \begin{bmatrix} N_{11} & N_{12} \\ N_{21} & N_{22} \end{bmatrix} x + \frac{1}{\|x_0\|^2} \begin{bmatrix} N_{13} u x_0^* \\ N_{23} u x_0^* \end{bmatrix} x \right) \right\| \\ &= \left\| R_i \left( \begin{bmatrix} N_{11} & N_{12} & N_{13} \\ N_{21} & N_{22} & N_{23} \end{bmatrix} \begin{bmatrix} x \\ u \end{bmatrix} \right) \right\| \\ &= \left\| \begin{bmatrix} R_i & 0 \end{bmatrix} N \begin{bmatrix} x \\ u \end{bmatrix} \right\|. \end{aligned}$$

Note that  $x \in \mathcal{X}_e$  iff  $x \in \mathcal{X}$  and  $\langle x_0, x \rangle = \|x_0\|^2$  and so every feasible  $x$  for Problem 7.2 is also feasible for Problem 7.1. The converse is true as the right hand sides of the norm inequalities shown above are in fact equal. Furthermore, by the same manipulations,

$$\sup_{x \text{ feasible}} \left\{ \gamma \mid \|R_i x\| \gamma \leq \|R_i \tilde{N} x\| \right\} = \sup_{x \text{ feasible}} \left\{ \gamma \mid \|R_i x\| \gamma \leq \left\| \begin{bmatrix} R_i & 0 \end{bmatrix} N \begin{bmatrix} x \\ u \end{bmatrix} \right\| \right\},$$

and so a candidate  $(\gamma, x)$  for one problem is also a candidate for the other.  $\blacktriangleright$

A function  $\psi_s(M, \mathcal{X})$  is defined and used to attempt to solve Problem 7.2.  $\psi_s(M, \mathcal{X})$  is simply the  $\tilde{\mu}_s(M)$  maximization (or supremum in the general case) with the additional constraint that  $x \in \mathcal{X}$ .

Define



$$\psi_s(M, \mathcal{X}) := \begin{cases} 0 & \text{if } \{x \mid x \in \mathcal{X}, \|R_i x\| \leq \|R_i M x\|, i \in I_s\} = \emptyset \\ \text{otherwise} \\ \sup_{\substack{\gamma, \|x\|=1 \\ x \in \mathcal{X}}} \left\{ \gamma \mid \begin{array}{l} \|R_i x\| \leq \|R_i M x\|, i \in I_s \\ \|R_i x\| \gamma \leq \|R_i M x\|, i \in \bar{I}_s \end{array} \right\}. \end{cases} \quad (7.5)$$

The function  $\psi_s(M, \mathcal{X})$  has been defined such that  $\psi_s(\tilde{N}, \mathcal{X})$  is a bound on the solution to Problem 7.1 or Problem 7.2. The following theorem states this and also gives sufficient conditions for the bound to be exact.

For notational convenience define  $\gamma_0$  as the solution to Problem 7.2 in the case that a feasible  $x$  exists:

$$\gamma_0 := \sup_{\substack{\gamma, x \in \mathcal{X} \\ \langle x_0, x \rangle = \|x_0\|^2}} \left\{ \gamma \mid \begin{array}{l} \|R_i x\| \leq \|R_i \tilde{N} x\|, i \in I_s \\ \|R_i x\| \gamma \leq \|R_i \tilde{N} x\|, i \in \bar{I}_s \end{array} \right\}.$$

#### Theorem 7.4

*If there exists a feasible  $x$  for Problem 7.2, then*

$$\psi_s(\tilde{N}, \mathcal{X}) \geq \gamma_0.$$

*Furthermore, if there exists an  $x$  achieving the supremum for  $\psi_s(\tilde{N}, \mathcal{X})$  defined in Equation 7.5 such that  $\langle x_0, x \rangle \neq 0$ , then*

$$\psi_s(\tilde{N}, \mathcal{X}) = \gamma_0.$$

**Proof of Theorem 7.4:** By the hypotheses of the theorem there exists a sequence  $x_k, k = 1, \dots$  giving the supremum of Problem 7.2 such that  $x_k \in \mathcal{X}, \langle x_0, x_k \rangle = \|x_0\|^2$ , and

$$\|R_i x_k\| \leq \|R_i \tilde{N} x_k\|, \quad i \in I_s.$$

Define

$$\gamma_k(x_k) = \sup_{\gamma} \left\{ \gamma \mid \|R_i x_k\| \gamma \leq \|R_i \tilde{N} x_k\|, i \in I_s \right\},$$

then, for this particular sequence  $x_k$ ,

$$\lim_{k \rightarrow \infty} \gamma_k(x_k) = \gamma_0.$$

Now define a sequence  $x_k^s$ ,  $k = 1, \dots$  by

$$x_k^s = \frac{x_k}{\|x_k\|}.$$

Then  $\|x_k^s\| = 1$ ,  $x_k^s \in \mathcal{X}$ , and

$$\|R_i x_k^s\| \leq \|R_i \tilde{N} x_k^s\|, \quad i \in I_s.$$

The sequence  $x_k^s$  therefore satisfies the constraints of the  $\psi_s(\tilde{N}, \mathcal{X})$  optimization and

$$\begin{aligned} & \lim_{k \rightarrow \infty} \sup_{\gamma} \left\{ \gamma \mid \|R_i x_k^s\| \gamma \leq \|R_i \tilde{N} x_k^s\|, \quad i \in I_s \right\} \\ &= \lim_{k \rightarrow \infty} \sup_{\gamma} \left\{ \gamma \mid \|R_i x_k\| \gamma \leq \|R_i \tilde{N} x_k\|, \quad i \in I_s \right\} \\ &= \lim_{k \rightarrow \infty} \gamma_k(x_k) = \gamma_0. \end{aligned}$$

Therefore,  $(x_k^s, \gamma_k(x_k))$  is a candidate sequence for the  $\psi_s(\tilde{N}, \mathcal{X})$  optimization, giving the same supremum ( $\gamma_0$ ), implying that

$$\psi_s(\tilde{N}, \mathcal{X}) \geq \gamma_0.$$

To prove the second part of the theorem, consider the  $x$  achieving the supremum of  $\psi_s(\tilde{N}, \mathcal{X})$ . By hypothesis  $x \in \mathcal{X}$ ,  $\|x\| = 1$ ,  $\langle x_0, x \rangle = \theta \neq 0$ , and

$$\begin{aligned} \|R_i x\| &\leq \|R_i \tilde{N} x\|, \quad i \in I_s \\ \|R_i x\| \psi_s(\tilde{N}, \mathcal{X}) &\leq \|R_i \tilde{N} x\|, \quad i \in \bar{I}_s. \end{aligned}$$

Choose  $x_s$  as

$$x_s = x \frac{\|x_0\|^2}{\theta}$$

then  $x_s \in \mathcal{X}$ ,  $\langle x_0, x_s \rangle = \|x_0\|^2$ , and  $x_s$  still meets the above norm constraints.  $x_s$  is therefore a feasible  $x$  for Problem 7.2, and  $(x_s, \psi_s(\tilde{N}, \mathcal{X}))$  is a candidate  $(x, \gamma)$  pair for the optimization of Problem 7.2 implying that

$$\psi_s(\tilde{N}, \mathcal{X}) \leq \gamma_0.$$

►

It will be seen that when this framework is applied to the constant matrix problem, the sufficient conditions of Theorem 7.4 ( $x$  achieves the supremum for  $\psi_s(\tilde{N}, \mathcal{X})$ ) and

$\langle x_0, x \rangle \neq 0$ ) will always be met. A large part of the reason is the restriction to the constant matrix, and hence finite dimensional, case.

In many problem applications some of the signals shown in the general interconnection structure (Figure 7.1) are not present. In the model validation problem, for example, there is no signal  $e$ . Without this signal the number of block inputs is not equal to the number of block outputs. A fictitious input or output (in the case of model validation) must be included to formulate the problem in the manner described here.

An additional problem can arise in the method of finding a solution to the general problem. The function  $\psi_s$  has been defined as the solution to an optimization problem. It will subsequently be seen that, in the constant matrix case,  $\psi_s$  is ideally suited to calculation via the geometric framework presented in Chapter 6. However, calculation of  $\psi_s$  may yield a maximizing  $\bar{x}$  such that  $\langle x_0, \bar{x} \rangle = 0$ . In this case  $\psi_s$  is only an upper bound to the desired  $\gamma_0$  of Problem 7.1 or Problem 7.2.

In at least the case of model validation there is a choice of fictitious output which will always ensure that  $\langle x_0, \bar{x} \rangle \neq 0$  if the problem does indeed have a finite solution.

### 7.3 Application to the Model Validation Problem

In this section the general interconnection structure and reformulation of Section 7.2 will be applied to the constant matrix minimum  $\|w\|$  problem.

As discussed above, a fictitious output must be added to the interconnection structure before the model validation problem can be considered in the general framework.

The general interconnection structure is defined by the following.

$$\begin{aligned} [N_{11} \ N_{12} \ N_{13}] &= [P_{11} \ P_{12} \ P_{13}] \\ [N_{21} \ N_{22} \ N_{23}] &= \left[ \begin{array}{c} x_0^*/\|x_0\|^2 \\ Z \end{array} \right] 0 \\ [N_{31} \ N_{32} \ N_{33}] &= [P_{21} \ P_{22} \ P_{23}] \end{aligned}$$

where  $Z$  is a block of zeros of dimension  $\dim(w) - 1 \times \dim(x)$ . The first element of the output  $e$  in the general interconnection structure is now made equal to  $\hat{y}$  of Figure 7.2. The block of zeros  $Z$  is simply appended to satisfy the assumption that  $\dim(e) = \dim(w)$ .

The removal of the equality constraint by the reparametrization to form  $\hat{y}$  and  $\hat{u}$  and then closing the loop between  $\hat{y}$  and  $\hat{u}$  results in the following system.

$$\tilde{N} = \begin{bmatrix} P_{11} & P_{12} \\ x_0^*/\|x_0\|^2 & Z \end{bmatrix} + \frac{1}{\|x_0\|^2} \begin{bmatrix} P_{13}ux_0^* \\ 0 \end{bmatrix}. \quad (7.6)$$

Now consider the minimum  $\|w\|$  problem studied in detail in Chapter 5. For the equivalent  $\psi_s$  problem choose  $I_s = \{1, \dots, m\}$  and  $\bar{I}_s = \{m+1\}$ . The main result is given in the following theorem. The terms “ $(w, \Delta)$  is feasible” or “ $x$  is feasible” will both be taken to mean that the  $x$  (and equivalently the associated  $w$  and  $\Delta$ ) satisfy the norm constraints arising from the  $\Delta$  blocks:

$$\|R_i x\| \leq \|R_i \tilde{N} x\|, \quad i = 1, \dots, m$$

and the equality constraint

$$y = \begin{bmatrix} N_{31} & N_{32} & N_{33} \end{bmatrix} \begin{bmatrix} x \\ u \end{bmatrix}.$$

This definition of “ $x$  is feasible” is consistent with that used in Problems 7.1 and 7.2.

### Theorem 7.5

Consider the minimum  $\|w\|$  model validation problem (Problem 3.3). Consider also  $\psi_s(\tilde{N}, \mathcal{X})$  where  $\tilde{N}$  is defined by Equation 7.6,  $I_s = \{1, \dots, m\}$ , and  $\bar{I}_s = \{m+1\}$ .

If  $\mu(P_{11}) < 1$  and  $\psi_s(\tilde{N}, \mathcal{X}) = 0$ ,

then no feasible  $(w, \Delta)$  exists.

If  $\mu(P_{11}) < 1$  and  $\psi_s(\tilde{N}, \mathcal{X}) > 0$ ,

$$\text{then } \min_{x \text{ feasible}} \|w\| = \frac{1}{\psi_s(\tilde{N}, \mathcal{X})}.$$

The proof of Theorem 7.5 will require a preliminary lemma. Before considering the lemma or the proof, some points are noted in the following remarks.

Note that as robust stability of the model is assumed ( $\mu(P_{11}) < 1$ ), the above theorem covers all cases of interest.

In the constant matrix case considered here that for each  $i \in I_s$ , the set of  $x$  meeting the constraint

$$\|R_i x\| \leq \|R_i \tilde{N} x\|$$

is a closed set. The set of all feasible  $x$  is therefore a finite union of closed sets and consequently is itself closed and bounded ( $\|x\| = 1$ ). Therefore, there will always be a feasible  $x$  achieving the supremum of the  $\psi_s(\tilde{N}, \mathcal{X})$  optimization.

Although the maximizing  $x$  will always be feasible, it may still occur that  $\psi_s(\tilde{N}, \mathcal{X}) = \infty$ . Clearly, this will happen if and only if there exists a feasible  $x$  such that

$$\|R_i x\| = 0 \quad \text{for all } i \in \overline{I}_s.$$

In the model validation problem this simply, says that there exists a  $(w, \Delta)$  pair satisfying the constraints with  $w = 0$ . In other words, the perturbation uncertainty alone can account for the observed input-output datum.

Recall from Theorem 7.4 that  $\psi_s$  will solve the general problem (Problem 7.1) if there exists a feasible  $x$  achieving the supremum of  $\psi_s(\tilde{N}, \mathcal{X})$  with  $\langle x_0, x \rangle \neq 0$ . The consideration of the constant matrix case has guaranteed that the maximizing  $x$  exists. The following lemma will show that the construction of  $\tilde{N}$  for the model validation problem guarantees  $\langle x_0, x \rangle \neq 0$  for every feasible  $x$  for which

$$\|R_i x\| < \|R_i \tilde{N} x\|, \quad i \in \overline{I}_s.$$

This argument will be made more rigorous in the proof of Theorem 7.5.

### Lemma 7.6

*In the case where  $\mu(P_{11}) < 1$  and  $\psi_s(\tilde{N}, \mathcal{X}) > 0$ , if  $x \in \mathcal{X}$  satisfies the norm constraints,*

$$\|R_i x\| \leq \|R_i \tilde{N} x\|, \quad i = 1, \dots, m \tag{7.7}$$

$$\|R_i x\| \gamma \leq \|R_i \tilde{N} x\|, \quad i = m + 1, \gamma > 0, \tag{7.8}$$

*then  $\langle x_0, x \rangle \neq 0$ .*

**Proof of Lemma 7.6:** Assume the contrary: consider a feasible  $x$  for the model validation optimization ( $x \in \mathcal{X}$  and Equation 7.7 satisfied) for which  $\langle x_0, x \rangle = 0$ . Equation 7.8 implies that

$$\|w\|\gamma \leq \left\| \begin{bmatrix} \frac{\langle x_0, x \rangle}{\|x_0\|^2} \\ 0 \\ \vdots \\ 0 \end{bmatrix} \right\|.$$

By assumption  $\gamma > 0$ , implying that  $w = 0$ . Note that in this case  $\psi_s(\tilde{N}, \mathcal{X})$ , which is bounded below by the supremum of the above over all  $\gamma$ , would be infinite.

Consider the resulting input-output relationship for  $\tilde{N}$  with this choice of  $x$ .

$$\begin{aligned} \begin{bmatrix} z \\ 0 \end{bmatrix} &= \left( \begin{bmatrix} P_{11} & P_{12} \\ x_0^*/\|x_0\|^2 & Z \end{bmatrix} + \frac{1}{\|x_0\|^2} \begin{bmatrix} P_{13}u x_0^* \\ 0 \end{bmatrix} \right) x \\ &= \begin{bmatrix} P_{11} & P_{12} \\ x_0^*/\|x_0\|^2 & Z \end{bmatrix} x \quad \text{as } \langle x_0, x \rangle = 0 \\ &= \begin{bmatrix} P_{11}v \\ 0 \end{bmatrix} \quad \text{as } x = \begin{bmatrix} v \\ w \end{bmatrix} = \begin{bmatrix} v \\ 0 \end{bmatrix} \end{aligned}$$

This implies that there exists  $v$  such that

$$\|R_i v\| \leq \|R_i P_{11} v\| \quad \text{for all } i = 1, \dots, m$$

which contradicts the stability assumption for  $P_{11}$ :  $\mu(P_{11}) < 1$ . ►

The reason for the choice of  $x_0^*/\|x_0\|^2$  as the only nonzero component of the fictitious output is now clear. This choice ensures that  $\langle x_0, x \rangle \neq 0$  satisfying the sufficient condition for  $\psi_s(\tilde{N}, \mathcal{X})$  to solve the general problem. The details of this are now presented for the model validation problem.

**Proof of Theorem 7.5:** Consider the case where  $\psi_s(\tilde{N}, \mathcal{X}) > 0$ . To show that

$$\min \|w\| \leq \frac{1}{\psi_s(\tilde{N}, \mathcal{X})}$$

consider  $x \in \mathcal{X}$ ,  $\|x\| = 1$ , meeting the constraints

$$\|R_i x\| \leq \|R_i \tilde{N} x\|, \quad i = 1, \dots, m \tag{7.9}$$

$$\|R_i x\| \psi_s(\tilde{N}, \mathcal{X}) \leq \|R_i \tilde{N} x\|, \quad i = m + 1. \tag{7.10}$$

Now

$$\|R_{m+1} \tilde{N} x\| = \frac{|\langle x_0, x \rangle|}{\|x_0\|^2}$$

and by Lemma 7.6, all feasible  $x$  meeting the constraints of Equations 7.9 and 7.10,

$$\frac{\langle x_0, x \rangle}{\|x_0\|^2} = \theta \neq 0.$$

Define

$$x_s = \frac{1}{\theta} x, \quad \text{and } w_s = R_{m+1} x_s.$$

Then  $\langle x_0, x_s \rangle = \|x_0\|^2$ ,  $x_s \in \mathcal{X}$ , and, as the norm constraints of Equation 7.9 are invariant to a scaling,  $x_s$  is feasible. Therefore,  $w_s$  and an associated  $\Delta$  are also feasible.

Now from Equation 7.10, which is satisfied for  $x_s$ ,

$$\|R_{m+1} x_s\| \psi_s(\tilde{N}, \mathcal{X}) = \|w_s\| \psi_s(\tilde{N}, \mathcal{X}) \leq \|R_{m+1} \tilde{N} x_s\| = \frac{\langle x_0, x_s \rangle}{\|x_0\|^2} = 1. \quad (7.11)$$

If  $\psi_s(\tilde{N}, \mathcal{X}) = \infty$  then  $\|w_s\| = 0$ , directly implying that

$$\min_{x \text{ feasible}} \|w\| = 0.$$

This is consistent with the formulation used in the theorem;

$$\min_{x \text{ feasible}} \|w\| = \frac{1}{\psi_s(\tilde{N}, \mathcal{X})}.$$

If, on the other hand,  $\psi_s(\tilde{N}, \mathcal{X}) < \infty$ , then Equation 7.10 and consequently Equation 7.11 is satisfied with equality. If this were not so, then there would exist  $\epsilon > 0$  such that  $\psi_s(\tilde{N}, \mathcal{X}) + \epsilon$  still meets the constraint of Equation 7.10, contradicting the definition of  $\psi_s(\tilde{N}, \mathcal{X})$ .

Therefore, noting that by assumption  $\psi_s(\tilde{N}, \mathcal{X}) > 0$ ,

$$\|w_s\| = \frac{1}{\psi_s(\tilde{N}, \mathcal{X})}$$

and consequently

$$\min_{x \text{ feasible}} \|w\| \leq \frac{1}{\psi_s(\tilde{N}, \mathcal{X})}.$$

Now to show that for  $\psi_s(\tilde{N}, \mathcal{X})$  finite,

$$\min \|w\| \geq \frac{1}{\psi_s(\tilde{N}, \mathcal{X})}$$

assume that there exists a feasible  $(w, \Delta)$ . This implies that there exists an  $x$  such that

$$\|R_i x\| \leq \|R_i ([P_{11} \ P_{12}] x + P_{13} u)\|$$

and

$$y - P_{23}u = [P_{21} P_{22}]x.$$

Consequently,  $x \in \mathcal{X}$  and  $\langle x_0, x \rangle = \|x_0\|^2$ . Now consider  $\tilde{N}x$ .

$$\begin{bmatrix} z \\ \hat{y} \\ 0 \end{bmatrix} = \left( \begin{bmatrix} P_{11} & P_{12} \\ x_0^*/\|x_0\|^2 & Z \end{bmatrix} + \frac{1}{\|x_0\|^2} \begin{bmatrix} P_{13}u x_0^* \\ 0 \end{bmatrix} \right) x$$

As

$$z = [P_{11} P_{12}]x + P_{13}u,$$

the norm constraint imposed by the  $\Delta$  blocks becomes

$$\|R_i x\| \leq \|R_i \tilde{N}x\|, \quad \text{for } i = 1, \dots, m.$$

Furthermore,

$$\hat{y} = \frac{\langle x_0, x \rangle}{\|x_0\|^2} = 1$$

which implies that

$$\|R_{m+1} \tilde{N}x\| = 1$$

and

$$\|R_{m+1}x\| \frac{1}{\|w\|} = 1 = \|R_{m+1} \tilde{N}x\|.$$

Therefore,  $x$  satisfies the norm constraints for a  $\psi_s(\tilde{N}, \mathcal{X})$  problem with  $\gamma = 1/\|w\|$ .  $x$  can be scaled without changing the norm constraints allowing it to also satisfy  $\|x\| = 1$  and  $x \in \mathcal{X}$ . Consequently,

$$\frac{1}{\|w\|} \leq \psi_s(\tilde{N}, \mathcal{X}) \tag{7.12}$$

implying that

$$\|w\| \geq \frac{1}{\psi_s(\tilde{N}, \mathcal{X})}$$

for all feasible  $w$  and so

$$\min \|w\| \geq \frac{1}{\psi_s(\tilde{N}, \mathcal{X})}.$$



Combining the two claims gives, for the  $\psi_s(\tilde{N}, \mathcal{X})$  case, the result that

$$\min \|w\| = \frac{1}{\psi_s(\tilde{N}, \mathcal{X})}.$$

To show that if  $\psi_s(\tilde{N}, \mathcal{X}) = 0$ , then no feasible  $(w, \Delta)$  exists, refer to Equation 7.12. The argument preceding this equation gives a construction of a candidate  $x$  and  $\gamma$  for the  $\psi_s(\tilde{N}, \mathcal{X})$  optimization. Equation 7.12 then applies giving the conclusion that if a feasible  $(w, \Delta)$  exists, then  $\psi_s(\tilde{N}, \mathcal{X}) \neq 0$ .  $\blacktriangleright$

Theorem 7.5 shows that  $\psi_s$  has been defined such that  $1/\psi_s(M, \mathcal{X})$  is the answer to the model validation problem. The following lemma shows that  $\psi_s$  can be bounded by  $\mu_s$ .

**Lemma 7.7**

$$\psi_s(M, \mathcal{X}) \leq \mu_s(M).$$

**Proof of Lemma 7.7:** If  $\psi_s(M, \mathcal{X}) = 0$  or  $\mu_s(M) = \infty$ , then the lemma is obviously true, albeit vacuous. Therefore, assume  $\psi_s(M, \mathcal{X}) > 0$  and  $\mu_s(M) < \infty$ . The first argument presented will assume that  $\psi_s(M, \mathcal{X}) < \infty$ . Consider any  $\gamma$  and  $x$  meeting the constraints of the  $\psi_s$  definition. Then

$$\|R_i x\| \leq \|R_i M x\|, \quad i \in I_s$$

$$\|R_i x\| \gamma \leq \|R_i M x\|, \quad i \in \bar{I}_s$$

with  $x \in \mathcal{X}$ .  $\gamma$  and  $x$  then meet the requirements of the  $\bar{\mu}_s(M)$  maximization which is equal to  $\mu_s(M)$  if  $\mu_s(M)$  is finite. This is true for all  $\gamma$  and therefore for  $\psi_s(M, \mathcal{X})$ .

Now consider the case when  $\psi_s(M, \mathcal{X}) = \infty$ . The norm conditions imply that there exists  $x$  and  $Q_i$  such that

$$-R_i x = Q_i M x$$

where

$$\|Q_i\| \leq 1, \quad i \in I_s$$

$$\|Q_i\| \leq \gamma^{-1}, \quad i \in \bar{I}_s.$$

Choosing  $\Delta$  such that  $\Delta_i = Q_i$  and stacking up each of the above equations into block matrix form gives

$$(I + \Delta M)x = 0.$$

But for  $\psi_s(M, \mathcal{X}) = \infty$ , the  $\Delta$  such that  $\det(I + \Delta M) = 0$  is an element of  $\mathbf{B}_s^0 \Delta$  implying that  $\mu_s(M) = \infty$ . ▶

## 7.4 A Geometric Interpretation

The previous section introduced the function  $\psi_s$  and showed its relationship to the model validation problem. As in the  $\mu$  and  $\mu_s$  cases, a numerical range function can be defined and used to develop a geometric approach to the problem. The convexity properties of the generalized numerical range then apply.

### 7.4.1 A Numerical Range Function

The  $\psi_s(M, \mathcal{X})$  problem (Equation 7.5) is considered for a general matrix  $M$  and subspace  $\mathcal{X}$ . It will be assumed in the notation used in this section that the general problem has  $m + 1$  norm constraints; in other words  $I_s \cup \overline{I}_s = \{1, \dots, m + 1\}$ . To further avoid a surfeit of notation, assume that  $V_{\mathcal{X}}$  is an orthonormal matrix of basis vectors for the subspace  $\mathcal{X}$ , and for all  $x \in \mathcal{X}$  there exists  $x_{\mathcal{X}}$  given by

$$x = V_{\mathcal{X}} x_{\mathcal{X}}. \tag{7.13}$$

Note that for all  $\|x_{\mathcal{X}}\| = 1$ ,  $x$  defined by Equation 7.13 has the properties  $\|x\| = 1$  and  $x \in \mathcal{X}$ . Define

$$N'(\alpha) = \begin{bmatrix} N'_1(\alpha) \\ \vdots \\ N'_{m+1}(\alpha) \end{bmatrix}$$

where

$$N'_i(\alpha) = \begin{cases} V_{\mathcal{X}}^* R_i^T R_i V_{\mathcal{X}} - V_{\mathcal{X}}^* M^* R_i^T R_i M V_{\mathcal{X}}, & i \in I_s \\ \alpha V_{\mathcal{X}}^* R_i^T R_i V_{\mathcal{X}} - V_{\mathcal{X}}^* M^* R_i^T R_i M V_{\mathcal{X}}, & i \in \overline{I}_s. \end{cases}$$

The numerical range of  $N'(\alpha)$  is defined as  $W'(\alpha)$ :

$$W'(\alpha) = \left\{ \nu \mid \nu_i = x_{\mathcal{X}}^* N'_i(\alpha) x_{\mathcal{X}}, \|x_{\mathcal{X}}\| = 1 \right\}$$

The following lemma is immediate from Lemma 6.5 by noting that the numerical range function  $W'(\alpha)$  is defined by  $m + 1$  Hermitian matrices.

**Lemma 7.8**

*If  $m = 1$ , or  $m \leq 2$  and  $\dim(x_{\mathcal{X}}) > 2$ , then  $W'(\alpha)$  is convex.*

**7.4.2 Properties of  $W'(\alpha)$**

In the  $\mu$  and  $\mu_s$  cases, it was sufficient to consider the relationship between the numerical range function and the origin. In the  $\psi_s$  case the maximization problem may only have a solution with a strict inequality on one of the constraints. Consideration of the origin is no longer sufficient; the quadrant where all components of  $\nu$  are negative must also be included.

Therefore, define

$$\nu_- = \{ \nu \mid \nu_i \leq 0 \}.$$

A lemma, analogous to Lemma 6.6 for the  $\mu_s$  case, can now be proven.

**Lemma 7.9**

*For all  $\alpha \leq \psi_s(M, \mathcal{X})^2$ ,*

$$W'(\alpha) \cap \nu_- \neq \emptyset,$$

*and for all  $\alpha > \psi_s(M, \mathcal{X})^2$ ,*

$$W'(\alpha) \cap \nu_- = \emptyset.$$

**Proof of Lemma 7.9:** Assume that  $\bar{x}$  is a solution to the  $\psi_s$  maximization. Then  $x \in \mathcal{X}$  and

$$\|R_i \bar{x}\| \leq \|R_i M \bar{x}\|, \quad i \in I_s$$

$$\|R_i \bar{x}\| \psi_s(M, \mathcal{X}) \leq \|R_i M \bar{x}\|, \quad i \in \bar{I}_s.$$

As  $x \in \mathcal{X}$  there exists  $\bar{x}_{\mathcal{X}}$  given by  $\bar{x} = V_{\mathcal{X}} \bar{x}_{\mathcal{X}}$ . Now consider  $\bar{\nu}$  where

$$\bar{\nu}_i = \bar{x}_{\mathcal{X}}^* N'_i(\psi_s(M, \mathcal{X})^2) \bar{x}_{\mathcal{X}}.$$

For  $i \in I_s$ ,

$$\begin{aligned}\bar{\nu}_i &= \bar{x}_\mathcal{X}^* V_\mathcal{X}^* R_i^T R_i V_\mathcal{X} \bar{x}_\mathcal{X} - \bar{x}_\mathcal{X}^* V_\mathcal{X}^* M R_i^T R_i M V_\mathcal{X} \bar{x}_\mathcal{X} \\ &= \|R_i \bar{x}\|^2 - \|R_i M \bar{x}\|^2 \\ &\leq 0.\end{aligned}$$

Similarly, for the  $i \in \bar{I}_s$  case,

$$\begin{aligned}\bar{\nu}_i &= \|R_i \bar{x}\|^2 \psi_s(M, \mathcal{X})^2 - \|R_i M \bar{x}\|^2 \\ &\leq 0\end{aligned}$$

and so  $\bar{\nu} \in \nu_-$ . In the case where  $\psi_s(M, \mathcal{X}) = \infty$ ,  $\bar{\nu}_i = -\|R_i M \bar{x}\|^2$ , and the above argument holds. This argument also holds for any  $\alpha < \psi_s(M, \mathcal{X})^2$  as the same  $\bar{x}$  can be chosen.

For the second part of the lemma, consider  $\alpha$  such that there exists  $\nu \in W'(\alpha) \cap \nu_-$ . This implies that there exists  $x_\mathcal{X}$  such that

$$x_\mathcal{X}^* N_i(\alpha) x_\mathcal{X} \leq 0, \quad i = 1, \dots, m+1.$$

Choosing  $x = V_\mathcal{X} x_\mathcal{X}$  gives

$$\begin{aligned}\|R_i x\|^2 - \|R_i M x\|^2 &\leq 0 \quad i \in I_s \\ \|R_i x\|^2 \alpha - \|R_i M x\|^2 &\leq 0 \quad i \in \bar{I}_s\end{aligned}$$

implying that

$$\begin{aligned}\|R_i x\| &\leq \|R_i M x\|, \quad i \in I_s \\ \|R_i x\| \alpha^{\frac{1}{2}} &\leq \|R_i M x\|, \quad i \in \bar{I}_s.\end{aligned}$$

By construction  $x \in \mathcal{X}$  and so  $x$  and  $\alpha^{1/2}$  are a feasible solution to the  $\psi_s(M, \mathcal{X})$  optimization. Therefore,  $\alpha \leq \psi_s(M, \mathcal{X})^2$ . ▶

**Corollary 7.10**

$$\psi_s(M, \mathcal{X}) = \inf_{\alpha \geq 0} \left\{ \alpha^{1/2} \mid W'(\beta) \cap \nu_- = \emptyset \text{ for all } \beta > \alpha \right\}$$

Lemma 7.9 is somewhat stronger than Lemma 6.6 in that it provides a means of determining if  $\alpha \leq \psi_s(M, \mathcal{X})^2$ . On the other hand Algorithm 6.9, which gives  $\mu_s$ , now only gives an upper bound for  $\psi_s(M, \mathcal{X})$ .

Using Algorithm 6.9 as a template, Corollary 7.10 could be used as the basis of an algorithm to calculate  $\psi_s(M, \mathcal{X})$ . To do this it is necessary to develop an algorithm to determine the minimum distance between  $W'(\alpha)$  and  $\nu_-$ . This will be a future research problem.

## 7.5 Relationship to the Lagrangian Formulation

Fan and Tits [9] show that the existence of a halfspace containing  $W(\mu(M)^2)$  is equivalent to the upper bound achieving  $\mu$ .

$$\inf_{D \in \mathcal{D}} \sigma_{\max}(DM D^{-1}) = \mu(M).$$

A similar relationship exists for the model validation problem. It will be assumed throughout that the model is robustly stable:  $\mu(P_{11}) < 1$ .

The numerical range function  $W'(\alpha)$ , defined in Section 7.4.1 for a general matrix  $M$  is now applied to  $\tilde{N}$  given by Equation 7.6. For the model validation problem  $I_s = \{1, \dots, m\}$  and  $\bar{I}_s = \{m+1\}$ . The subspace  $\mathcal{X}$  is parametrized by

$$V_{\mathcal{X}} = \begin{bmatrix} x_0 \\ \frac{x_0}{\|x_0\|} V \end{bmatrix}$$

where  $x_0$  and  $V$  are defined in Section 3.2.1.

The connection between the geometric formulation of  $\psi_s(\tilde{N}, \mathcal{X})$  and a Kuhn-Tucker saddlepoint for the model validation problem (Problem 3.6) is investigated in the following theorem.

### 7.5.1 The Existence of a Kuhn-Tucker Saddlepoint

#### Theorem 7.11

*If  $\psi_s(\tilde{N}, \mathcal{X}) > 0$ ,  $\psi_s(\tilde{N}, \mathcal{X}) < \infty$ , and  $W'(\psi_s(\tilde{N}, \mathcal{X})^2)$  is contained in a halfspace defined by  $\xi$ ,*

$$H(\xi) = \left\{ \nu \mid \langle \xi, \nu \rangle \geq 0, \xi_i \geq 0, \xi_{m+1} > 0 \right\},$$

then the Lagrangian,  $L_e(x_e, \lambda)$  (Equation 5.5), has a Kuhn-Tucker saddlepoint.

**Proof of Theorem 7.11:** This proof will proceed by deriving  $\lambda$  and  $x_e$  which will then be shown to satisfy conditions **i**, **ii**, and **iii** of Theorem 4.5.

$$\begin{aligned} \langle \xi, \nu \rangle &= \sum_{i=1}^{m+1} \xi_i \nu_i \\ &= \sum_{i=1}^{m+1} \xi_i x_{\mathcal{X}}^* N'_i(\psi_s(\tilde{N}, \mathcal{X})^2) x_{\mathcal{X}} \end{aligned}$$

But, using  $x = V_{\mathcal{X}} x_{\mathcal{X}}$ ,

$$\begin{aligned} x_{\mathcal{X}}^* N'_{m+1}(\psi_s(\tilde{N}, \mathcal{X})^2) x_{\mathcal{X}} &= \|R_{m+1} V_{\mathcal{X}} x_{\mathcal{X}}\|^2 \psi_s(\tilde{N}, \mathcal{X})^2 - \|R_{m+1} \tilde{N} V_{\mathcal{X}} x_{\mathcal{X}}\|^2 \\ &= \|w\|^2 \psi_s(\tilde{N}, \mathcal{X})^2 - \|\hat{y}\|^2, \end{aligned}$$

and so

$$\langle \xi, \nu \rangle = \xi_{m+1} (\|w\|^2 \psi_s(\tilde{N}, \mathcal{X})^2 - \|\hat{y}\|^2) + \sum_{i=1}^m \xi_i x_{\mathcal{X}}^* N'_i(\psi_s(\tilde{N}, \mathcal{X})^2) x_{\mathcal{X}}. \quad (7.14)$$

Define

$$\lambda_i = \frac{\xi_i}{\xi_{m+1} \psi_s(\tilde{N}, \mathcal{X})^2}. \quad (7.15)$$

This is well defined as by assumption both  $\psi_s(\tilde{N}, \mathcal{X})^2$  and  $\xi_{m+1}$  are greater than zero.

Then

$$\frac{\langle \xi, \nu \rangle}{\xi_{m+1} \psi_s(\tilde{N}, \mathcal{X})^2} = \|w\|^2 + \sum_{i=1}^m \lambda_i x_{\mathcal{X}}^* N'_i(\psi_s(\tilde{N}, \mathcal{X})^2) x_{\mathcal{X}} - \frac{\|\hat{y}\|^2}{\psi_s(\tilde{N}, \mathcal{X})^2}.$$

By Lemma 7.9 the sets  $\nu_-$  and  $W'(\psi_s(\tilde{N}, \mathcal{X})^2)$  have at least one element in common.

Denote one of these elements by  $\bar{\nu}$ . Then  $\bar{\nu}_i \leq 0$  but the condition that

$$\langle \xi, \nu \rangle = \sum_{i=1}^{m+1} \xi_i \nu_i \geq 0 \quad \text{for all } \nu \in W'(\psi_s(\tilde{N}, \mathcal{X})^2)$$

with  $\xi_i \geq 0$  for  $i = 1, \dots, m$  and  $\xi_{m+1} > 0$  can only be satisfied if for every  $\nu_i < 0$ , the corresponding  $\xi_i = 0$ . Furthermore, this leads to

$$\langle \xi, \bar{\nu} \rangle = 0.$$

Now denote by  $\bar{x}_{\mathcal{X}}$  the  $x_{\mathcal{X}}$  such that

$$\bar{\nu}_i = \bar{x}_\mathcal{X}^* N'_i(\psi_s(\tilde{N}, \mathcal{X})^2) \bar{x}_\mathcal{X}.$$

By Lemma 7.6

$$\frac{\langle x_0, V_\mathcal{X} \bar{x}_\mathcal{X} \rangle}{\|x_0\|^2} = \theta \quad \text{and } \theta \neq 0.$$

Define

$$\bar{x} = \frac{1}{\theta} V_\mathcal{X} \bar{x}_\mathcal{X}.$$

It is claimed that  $(\lambda, \bar{x})$  defined by the above is a saddlepoint of the Lagrangian. To prove this note that

$$\hat{y} = \frac{\langle x_0, \bar{x} \rangle}{\|x_0\|^2} = 1$$

implying that  $\bar{x}$  satisfies the equality constraint,  $\bar{x} = x_0 + V \bar{x}_e$ .

Now

$$\begin{aligned} L_e(x_e, \lambda) &= \|w\|^2 + \sum_{i=1}^m \lambda_i g_i(x_e) \\ &= \frac{\langle \xi, \nu \rangle}{\xi_{m+1} \psi_s(\tilde{N}, \mathcal{X})^2} + \frac{\|\hat{y}\|^2}{\psi_s(\tilde{N}, \mathcal{X})^2}. \end{aligned}$$

But  $x$  satisfies  $x = x_0 + V x_e$  if and only if  $\hat{y} = 1$  and  $x \in \mathcal{X}$  implying that

$$L_e(x_e, \lambda) = \frac{\langle \xi, \nu \rangle}{\xi_{m+1} \psi_s(\tilde{N}, \mathcal{X})^2} + \frac{1}{\psi_s(\tilde{N}, \mathcal{X})^2}.$$

For all  $x_e$  there exists a corresponding element of  $\mathcal{X}$ :  $x_\mathcal{X}$ . Although  $\|x_\mathcal{X}\|$  may not be equal to one, there exists a scaling  $\alpha \in \mathbf{R}$  such that  $\|\alpha x_\mathcal{X}\| = 1$  and the  $\nu$  corresponding to this  $\alpha x_\mathcal{X}$  is an element of  $W'(\psi_s(\tilde{N}, \mathcal{X})^2)$ . By the hypotheses of the theorem

$$\langle \xi, \nu \rangle \geq 0, \quad \text{where } \nu_i = \alpha^2 x_\mathcal{X}^* N'_i(\psi_s(\tilde{N}, \mathcal{X})^2) x_\mathcal{X}$$

and consequently

$$\langle \xi, \nu \rangle \geq 0, \quad \text{where } \nu_i = x_\mathcal{X}^* N'_i(\psi_s(\tilde{N}, \mathcal{X})^2) x_\mathcal{X}.$$

Noting that  $\psi_s(\tilde{N}, \mathcal{X})^2 > 0$  and  $\xi_{m+1} > 0$ ,

$$L_e(x_e, \lambda) \geq \frac{1}{\psi_s(\tilde{N}, \mathcal{X})^2}.$$

But  $\bar{x}_\mathcal{X}$  achieves  $\langle \xi, \nu \rangle = 0$  giving

$$L_e(\bar{x}_e, \lambda) = \frac{1}{\psi_s(\tilde{N}, \mathcal{X})^2}.$$

Therefore,  $\bar{x}_e$  minimizes  $L_e(x_e, \lambda)$  over all  $x_e$  satisfying condition *i* of Theorem 4.5.

Furthermore, for  $i = 1, \dots, m$ ,

$$\begin{aligned} \frac{1}{|\theta|^2} \nu_i &= \frac{1}{|\theta|^2} \bar{x}_x^* N_i'(\psi_s(\tilde{N}, \mathcal{X})^2) \bar{x}_x \\ &= \|R_i \bar{x}\|^2 - \|R_i \tilde{N} \bar{x}\|^2 \\ &= \|R_i \bar{x}\|^2 - \|R_i([P_{11} \ P_{12}]x + P_{13}u)\|^2 \\ &= g_i(\bar{x}) \\ &= g_{ei}(\bar{x}_e), \quad \text{for } \bar{x} = x_0 + V\bar{x}_e. \end{aligned}$$

Finally,  $\bar{\nu}_i \leq 0$  implying that  $g_{ei}(\bar{x}_e) \leq 0$  for  $i = 1, \dots, m$ . Condition *ii* of Theorem 4.5 is also satisfied.

To verify the complementary slackness condition (condition *iii*) of Theorem 4.5, consider  $\bar{\nu}_i$  for  $i$  such that  $g_{ei}(\bar{x}_e) < 0$ .

$$\begin{aligned} g_{ei}(\bar{x}_e) < 0 &\implies \frac{1}{|\theta|^2} \bar{x}_x^* N_i'(\psi_s(\tilde{N}, \mathcal{X})^2) \bar{x}_x < 0 \\ &\implies \bar{\nu}_i < 0 \\ &\implies \xi_i = 0 \\ &\implies \lambda_i = 0 \end{aligned}$$

All three conditions of Theorem 4.5 are satisfied implying that  $(\bar{x}, \lambda)$  is a saddlepoint of  $L_e(x_e, \lambda)$ . ▶

A possible source of complication is the requirement on the halfspace  $H(\xi)$  that  $\xi_{m+1} > 0$ . Note from Equation 7.14 that if  $\xi_{m+1} = 0$ , then the functional  $f(x) = \|w\|^2$  plays no part in the optimization. This case arises if  $x$  is specified by the constraints  $g_i(x)$  alone; there does not exist  $x$  such that  $g_i(x) < 0$ ,  $i = 1, \dots, m$ . This is a pathological condition which will always cause a problem for a Lagrangian formulation. The proof of Lemma 7.13 will illustrate the effect of this condition.

Theorem 7.11 requires that  $\psi_s(\tilde{N}, \mathcal{X}) > 0$ . By Theorem 7.5, if  $\psi_s(\tilde{N}, \mathcal{X}) = 0$ , then no feasible  $(w, \Delta)$  exists. This condition then imposes no additional restriction on the conditions under which a saddlepoint will exist.



The case where  $\psi_s(\tilde{N}, \mathcal{X}) = \infty$  must be treated separately. Fortunately this case is even less restrictive than that considered in Theorem 7.11, as is illustrated by the following theorem.

**Theorem 7.12**

*If  $\psi_s(\tilde{N}, \mathcal{X}) = \infty$ , then the Lagrangian  $L_e(x_e, \lambda)$  has a saddlepoint at  $\lambda = 0$ .*

**Proof of Theorem 7.12:** If  $\psi_s(\tilde{N}, \mathcal{X}) = \infty$ , then there exists a feasible  $x$  such that  $R_i x = 0$  for all  $i \in \bar{I}_s$ . In the model validation problem this implies that there exists a feasible  $x$ , denoted here by  $\bar{x}$ , with  $R_i \bar{x} = \bar{w} = 0$ . Define  $\bar{x}_e$  by  $\bar{x}_e = x_0 + V \bar{x}$ . It will now be demonstrated, by testing the three conditions of Theorem 4.5, that the point  $(\bar{x}_e, 0)$  is a saddlepoint.

Note that for  $\lambda = 0$ ,

$$L_e(x_e, \lambda) = \|w\|^2,$$

and for  $\bar{x}_e$ ,  $\|\bar{w}\|^2 = 0$ . Condition *i* is therefore satisfied. The fact that  $\bar{x}_e$  is feasible implies that  $g_{ei}(\bar{x}_e) \leq 0$ ,  $i = 1, \dots, m$ , satisfying condition *ii*. The choice of  $\lambda = 0$  is sufficient to satisfy condition *iii*. ▶

All possibilities for  $\psi_s(\tilde{N}, \mathcal{X})$  have therefore been covered by Theorems 7.11 and 7.12. For  $\psi_s(\tilde{N}, \mathcal{X}) = 0$  or  $\psi_s(\tilde{N}, \mathcal{X}) = \infty$ , the result is clear: no feasible  $(w, \Delta)$  exists and  $\min \|w\| = 0$  respectively.

For  $\psi_s(\tilde{N}, \mathcal{X}) \in (0, \infty)$  the existence of a Kuhn-Tucker saddlepoint depends on a separating hyperplane condition for  $W'(\alpha)$ . In certain cases, the convexity of  $W(\alpha)$  can be used to obtain a sufficient condition for the existence of a saddlepoint.

**Lemma 7.13**

*For the two perturbation block ( $m = 2$ ) model validation problem, if the feasible region defined by the inequality constraints has at least one interior point meeting the equality constraint (i.e., there exists  $x \in \mathcal{X}_e$  such that  $g_i(x) < 0$  for  $i = 1, \dots, m$ ) and the dimension of the kernel of  $[P_{21} P_{22}]$  is greater than one, then the Lagrangian  $L_e(x_e, \lambda)$  has a Kuhn-Tucker saddlepoint.*

**Proof of Lemma 7.13:** If the dimension of the kernel of  $[P_{21} P_{22}]$  is greater than one, then  $\dim(x_{\mathcal{X}}) > 2$ . For  $m = 2$ ,  $\dim(W'(\alpha)) = 3$ . By Lemma 6.5  $W'(\alpha)$  is convex.

The existence of  $x \in \mathcal{X}_e$  such that  $g_i(x) < 0$  for  $i = 1, \dots, m$  is sufficient to give a feasible  $(w, \Delta)$  which by Theorem 7.5 implies that  $\psi_s(\tilde{N}, \mathcal{X}) > 0$ . If  $\psi_s(\tilde{N}, \mathcal{X}) = \infty$ , then the saddlepoint exists by Theorem 7.12. Assume therefore that  $\psi_s(\tilde{N}, \mathcal{X}) < \infty$ .

Now consider  $\nu \in W'(\psi_s(\tilde{N}, \mathcal{X})^2) \cap \nu_-$ . Clearly  $\nu \in \partial W'(\psi_s(\tilde{N}, \mathcal{X})^2)$  and  $\nu \in \partial \nu_-$ . If this were not so, then there would exist  $x$  such that

$$\begin{aligned} \|R_i x\| &< \|R_i \tilde{N} x\|, \quad i = 1, \dots, m \\ \|R_{m+1} x\| \psi_s(\tilde{N}, \mathcal{X}) &< \|R_{m+1} \tilde{N} x\|, \end{aligned}$$

contradicting the definition  $\psi_s(\tilde{N}, \mathcal{X})$  (Equation 7.5). Both  $\nu_-$  and  $W'(\psi_s(\tilde{N}, \mathcal{X})^2)$  are convex nonoverlapping sets although they share at least one point in common on their boundaries. They can therefore be separated by a hyperplane. Note that every hyperplane separating  $\nu_-$  from any convex set such that  $\nu \notin \nu_-$  is of the form

$$\langle \xi, \nu \rangle = 0, \quad \xi_i \geq 0, \quad i = 1, \dots, m+1, \quad \xi \neq 0.$$

Therefore,  $W'(\psi_s(\tilde{N}, \mathcal{X})^2)$  is contained in a halfspace defined by

$$H(\xi) = \left\{ \nu \mid \langle \xi, \nu \rangle \geq 0, \xi_i \geq 0, i = 1, \dots, m+1, \xi \neq 0 \right\}.$$

Now consider  $\xi_{m+1}$ . By the hypotheses of the lemma, there exists  $\hat{x} \in \mathcal{X}$ ,  $\|\hat{x}\| = 1$  such that  $g_i(\hat{x}) < 0$ ,  $i = 1, \dots, m$ . Define  $\hat{x}_x$  by  $\hat{x} = V_x \hat{x}_x$  and  $\hat{\nu}$  by

$$\hat{\nu}_i = \hat{x}_x^* N_i'(\psi_s(\tilde{N}, \mathcal{X})^2) \hat{x}_x < 0.$$

Then for any  $\xi$  with  $\xi_i \geq 0$ ,  $i = 1, \dots, m$  and  $\xi_{m+1} = 0$ ,

$$\langle \xi, \hat{\nu} \rangle = \sum_{i=1}^{m+1} \xi_i \hat{\nu}_i = \sum_{i=1}^m \xi_i g_i(\hat{x}) < 0,$$

contradicting the fact that  $W'(\psi_s(\tilde{N}, \mathcal{X})^2)$  is bounded by a halfspace:  $\langle \xi, \nu \rangle \geq 0$ .

Therefore,  $\xi_{m+1} > 0$  and the halfspace is

$$H(\xi) = \left\{ \xi \mid \langle \xi, \nu \rangle \geq 0, \xi_i \geq 0, \xi_{m+1} > 0 \right\}.$$

Theorem 7.11 then implies that the Lagrangian  $L_e(x_e, \lambda)$  has a Kuhn-Tucker saddlepoint. ▶

## A Summary of the Application of $\psi_s(M, \mathcal{X})$ to the Model Validation Problem

A function  $\psi_s(M, \mathcal{X})$  has been defined and used to study the model validation problem from a geometric point of view. Section 7.3 showed that it was possible to reformulate the model validation problem as a  $\psi_s(M, \mathcal{X})$  problem. Theorem 7.5 then indicates that  $\psi_s(M, \mathcal{X})$  is the quantity of interest in solving the model validation problem. In particular

$$\min \|w\| = \frac{1}{\psi_s(\tilde{N}, \mathcal{X})}$$

or if no feasible  $(w, \Delta)$  exists, then  $\psi_s(\tilde{N}, \mathcal{X}) = 0$ .

Section 7.4.1 presented a generalized numerical range function and related its properties to  $\psi_s(M, \mathcal{X})$ . No algorithm is given for the calculation of  $\psi_s(M, \mathcal{X})$ ; a prerequisite is an algorithm to find the minimum distance between  $\nu_-$  and the numerical range function of  $\psi_s(M, \mathcal{X})$ .

However, the convexity properties of the generalized numerical range are used to establish the conditions under which a Kuhn-Tucker saddlepoint for the model validation optimization problem will always exist.

It is of interest to recap the means of bounding the model validation problem. Any upper bound to  $\psi_s(\tilde{N}, \mathcal{X})$  gives a lower bound on the minimum  $\|w\|$ . By Lemma 7.7  $\mu_s(\tilde{N})$  gives such a bound. As noted above, Algorithm 6.9 and Corollary 7.10 suggests a means of calculating  $\psi_s(\tilde{N}, \mathcal{X})$ . Judging by the difficulties associated with the application of Algorithm 6.9 to the  $\mu_s$  case, it is likely any such algorithm would only give an upper bound to  $\psi_s(\tilde{N}, \mathcal{X})$  when  $W'(\alpha)$  was not convex. The third means of obtaining a bound has been discussed in Section 5.2.2: solve the problem with Lagrange multipliers for the  $m = 1$  case. In the experimental example presented in Chapter 9, the minimum  $\|w\|$  problem is solved by a local search technique. The author has no experience with the calculation of bounds by any of the three techniques described above and, consequently, it is not known which will give the best results. It should be noted, however, that Algorithm 6.11, which in general calculates only an upper bound for  $\mu_s$ , is identical to the usual upper bound for  $\mu$  (Equation 2.15) when  $I_s = \emptyset$ . In practical applications this bound is very good, suggesting that the second method discussed above might lead to

the tightest bound on  $\psi_s(\tilde{N}, \mathcal{X})$ .

## Chapter 8

# A Study of Several Numerical Examples

This chapter will study several numerical examples to illustrate the relationship between the Lagrange multiplier approach of Chapter 5 and the geometric approach of Chapter 7.

Three single perturbation block cases are considered. The first shows the generic case where a solution to the Lagrange problem is found in the interior of  $\Lambda_\epsilon$ . In the second case  $\lambda = 0$  is the optimal solution. This illustrates the difference between the  $\mu_s$  and  $\psi_s$  formulations. The third case is studied for two different block structures: a single block problem and a three block problem. For both problems the Lagrange approach will encounter the boundary. In this single block problem, this becomes benign when considered from the geometric point of view. In the three block problem, it is proven that no saddlepoint exists.

### 8.1 Case 1

Consider the single perturbation block model described by

$$P = \left[ \begin{array}{ccc|cc} 0.1 - 0.1i & 0.2 - 0.2i & 0.1 + 0.0i & 0.6 - 0.4i & 0.6 - 0.6i \\ 0 & 0 & 0.1 + 0.1i & 0.7 - 0.1i & 0.4 - 0.2i \\ 0.2 + 0.2i & 0.0 - 0.1i & -0.1 + 0.1i & -0.4 - 0.1i & 0.6 + 0.5i \\ \hline 0.3 + 0.4i & -0.3 - 0.2i & -0.1 - 0.3i & 0.0 - 0.8i & -0.3 + 0.9i \\ -0.6 - 0.1i & 0.2 + 0.1i & 0.1 - 0.5i & 0.5 - 0.5i & -0.3 + 0.2i \\ -0.6 - 0.1i & 0.2 + 0.1i & -0.1 + 0.4i & 0.1 + 0.0i & -0.5 + 0.6i \end{array} \right]$$

where the solid divisions indicate the partitions  $P_{11}, \dots, P_{23}$ . The input  $u$  and the output  $y$  are:

$$u = \begin{bmatrix} 0.5 - 0.4i \end{bmatrix}$$

and

$$y = \begin{bmatrix} 0.4 + 0.0i \\ 0.3 - 0.6i \\ 0.1 - 1.1i \end{bmatrix}.$$

In this case the block structure is simply given by  $k_1 = 3$ .

Consider the reparametrization discussed in Section 3.2.1. In this example

$$x_0 = \begin{bmatrix} 0.5085 + 1.3140i \\ -0.8333 + 0.7643i \\ -2.1379 - 0.2296i \\ 2.2116 - 0.0191i \end{bmatrix}$$

and

$$V = \begin{bmatrix} -0.4749 + 0.0000i \\ -0.7477 + 0.2679i \\ 0.0476 + 0.2109i \\ 0.1952 - 0.2424i \end{bmatrix}.$$

It is a simple matter to verify that  $x_0$  is orthogonal to  $V$  and that

$$y - P_{23}u = [P_{21} \ P_{22}]x_0.$$

In this case the dimension of the search for  $x$  has been reduced to one.

Consider the constrained form of the Lagrangian:

$$\begin{aligned} L_e(x_e, \lambda) &= f_e(x_e) + \sum_{i=1}^m \lambda_i g_{ei}(x_e), \quad \lambda_i \geq 0 \\ &= x_e^* V^* (B + \sum_{i=1}^m \lambda_i A_i) V x_e + 2 \operatorname{Re}\{x_e^* C_e(\lambda)\} + d_e(\lambda) \end{aligned} \quad (8.1)$$

where

$$C_e(\lambda) = V^* B x_0 + \sum_{i=1}^m \lambda_i \left[ V^* A_i x_0 - V^* \begin{bmatrix} P_{11}^* \\ P_{12}^* \end{bmatrix} T_i P_{13} u \right]$$

and

$$d_e(\lambda) = x_0^* B x_0 + \sum_{i=1}^m \lambda_i [x_0^* A_i x_0 - 2 \operatorname{Re}\{x_0^* \begin{bmatrix} P_{11}^* \\ P_{12}^* \end{bmatrix} T_i P_{13} u\} - u^* P_{13}^* T_i P_{13} u].$$

In this case

$$B = \begin{bmatrix} 0 & 0 & 0 & 0 \\ 0 & 0 & 0 & 0 \\ 0 & 0 & 0 & 0 \\ 0 & 0 & 0 & 1 \end{bmatrix}$$

and

$$\begin{aligned} A_1 &= \begin{bmatrix} I - P_{11}^* P_{11} & -P_{11}^* P_{12} \\ -P_{12}^* P_{11} & -P_{12}^* P_{12} \end{bmatrix} \\ &= \begin{bmatrix} 0.90 + 0.00i & -0.02 + 0.02i & -0.01 - 0.05i & 0.00 - 0.08i \\ -0.02 - 0.02i & 0.91 + 0.00i & -0.01 - 0.01i & -0.21 + 0.00i \\ -0.01 + 0.05i & -0.01 + 0.01i & 0.95 + 0.00i & -0.15 + 0.07i \\ 0.00 + 0.08i & -0.21 - 0.00i & -0.15 - 0.07i & -1.19 + 0.00i \end{bmatrix}, \end{aligned}$$

making the quadratic term of the Lagrangian

$$x_e^* (0.0969 + 0.6821\lambda) x_e.$$

$C_e(\lambda)$  and  $d_e(\lambda)$  are given by

$$C_e(\lambda) = (-0.4363 + 0.5324i) + \lambda(1.2862 - 0.9478i)$$

and

$$d_e(\lambda) = 4.8916 + \lambda 2.2538.$$

Figure 8.1 shows the dual function plotted against  $\lambda$ . The maximum occurs in the interior of  $\Lambda_e$ ; at  $\lambda = 0.7610$ . At this point the value of the dual function is  $h(0.7610) = 6.0710$  implying that  $\|w\|^2 = 6.0710$  and consequently the minimum  $\|w\| = 2.4639$ . The value of  $x_e$  achieving this is  $x_e = -0.8808 + 0.3067i$  giving as an optimizing  $x$

$$x = \begin{bmatrix} 0.9268 + 1.1683i \\ 0.2569 + 0.2990i \\ -2.2444 - 0.4007i \\ 2.4579 + 0.1727i \end{bmatrix}.$$

It is easily verified that for this  $x$

$$[0 \ I]P \begin{bmatrix} x \\ u \end{bmatrix} = y,$$

$g(x) = 0$ , and  $\|w\| = 2.4639$ .

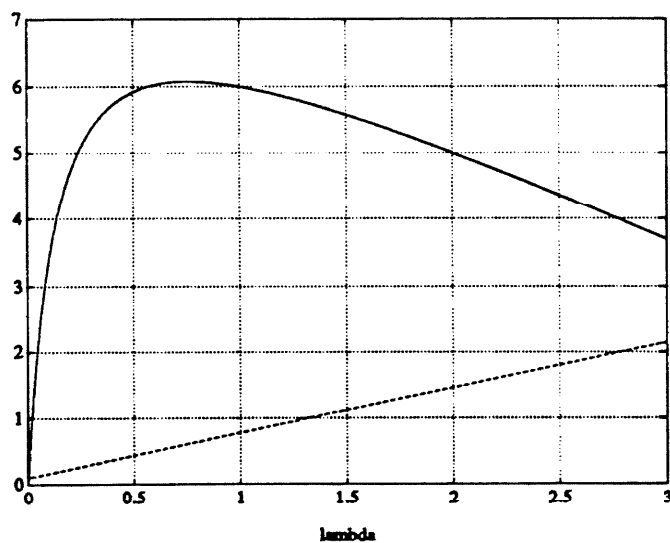


Figure 8.1: Case 1: Dual Function:  $h(\lambda)$  (solid line) and the minimum eigenvalue of the quadratic term:  $V^*(B + \lambda A)V$  (dashed line)

Now consider this problem from the geometric point of view. By Theorem 7.5, for a stable model  $P$ , finding  $\psi_s(\tilde{N}, \mathcal{X})$  (Equation 7.5) also yields the minimum  $\|w\|$ ;

$$\min \|w\| = \frac{1}{\psi_s(\tilde{N}, \mathcal{X})^2}.$$



$\psi_s(\tilde{N}, \mathcal{X})$  can be found by the optimization implied by

$$\psi_s(\tilde{N}, \mathcal{X}) = \inf_{\alpha \geq 0} \left\{ \alpha^{1/2} \mid W'(\beta) \cap \nu_- = \emptyset \text{ for all } \beta > \alpha \right\}.$$

For this problem  $I_s = \{1\}$  and  $\bar{I}_s = \{2\}$ . Using  $x_0$  and  $V$  given above  $\tilde{N}$  (Equation 7.6) is:

$$\tilde{N} = \begin{bmatrix} 0.0469 - 0.1277i & 0.1638 - 0.1684i & 0.0997 + 0.0914i & 0.6096 - 0.4935i \\ -0.0220 - 0.0227i & -0.0234 + 0.0098i & 0.0846 + 0.1457i & 0.7204 - 0.1452i \\ 0.2209 + 0.1490i & -0.0320 - 0.1306i & -0.1838 + 0.1073i & -0.3134 - 0.0990i \\ 0.0398 - 0.1028i & -0.0652 - 0.0598i & -0.1673 + 0.0189i & 0.1731 - 0.0015i \end{bmatrix}.$$

Figure 8.2 shows the set  $W'(\alpha)$  for  $\alpha = 0.165$ . Observe that  $0 \in W'(\alpha)$ . For all  $\alpha > 0.165$ ,  $W'(\alpha) \cap \nu_- = \emptyset$  implying that

$$\min \|w\| = \frac{1}{\psi_s(\tilde{N}, \mathcal{X})} = \frac{1}{\sqrt{0.165}} = 2.46.$$

This value agrees with that obtained via the Lagrange multiplier optimization.

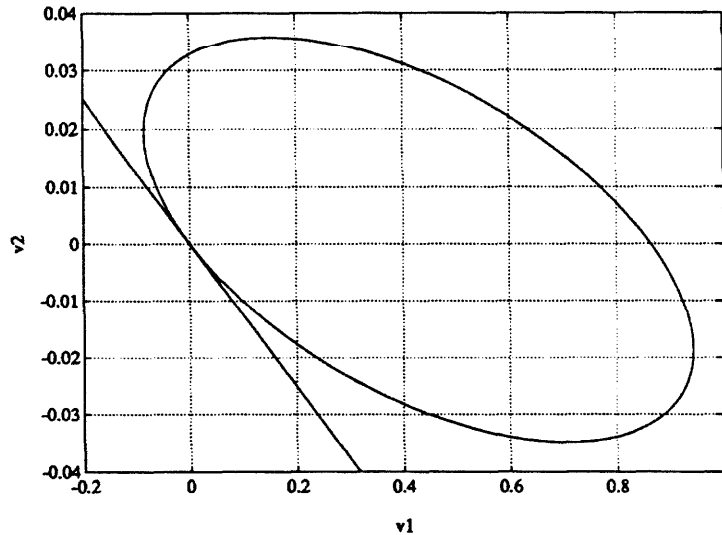


Figure 8.2: Case 1:  $W'(\alpha)$  for  $\alpha = 0.165$  and the supporting hyperplane defined by  $\langle \xi, \nu \rangle \geq 0$ ,  $\xi = [0.1256, 1]^T$

Furthermore,  $W'(\alpha)$ ,  $\alpha = 0.165$ , is contained in a halfspace  $H(\xi)$ :

$$H(\xi) = \{ \nu \mid \langle \xi, \nu \rangle \geq 0 \}$$

where

$$\xi = \begin{bmatrix} 0.1256 \\ 1 \end{bmatrix}.$$

The boundary of this halfspace is also shown in Figure 8.2.

By Theorem 7.11 the associated Lagrange optimization has a saddlepoint. Equation 7.15, in the proof of Theorem 7.11, gives the Lagrange multiplier as

$$\lambda = \frac{\xi_1}{\xi_{m+1} \psi_s(\bar{N}, \mathcal{X})^2} = \frac{0.1256}{1.0 \cdot 0.165} = 0.761.$$

Again this is in agreement with the results of the Lagrange multiplier optimization.

## 8.2 Case 2

Consider

$$P = \left[ \begin{array}{cc|cc} 0.6 + 0.5i & 0.0 + 0.2i & 0.8 + 0.2i & 0.3 + 0.8i \\ -0.9 - 0.4i & 0.3 + 0.0i & 0.5 - 0.4i & 0.0 + 0.4i \\ \hline 0.1 + 0.2i & -0.3 - 0.5i & 0.0 - 1.0i & -0.1 + 0.7i \end{array} \right]$$

with

$$y = \begin{bmatrix} 1.1 + 0.2i \\ -0.3 - 0.2i \end{bmatrix}$$

and

$$u = \begin{bmatrix} -0.3 - 0.2i \end{bmatrix}. \quad (8.2)$$

The block structure is (1).

Considering  $x$  as  $x = x_0 + Vx_e$  gives for  $x_0$  and  $V$

$$x_0 = \begin{bmatrix} -1.1536 + 0.1046i \\ 0.2826 - 0.3729i \\ -0.2397 - 0.0625i \end{bmatrix}$$

and

$$V = \begin{bmatrix} 0.3289 + 0.0000i \\ 0.7132 - 0.4429i \\ -0.1579 + 0.4025i \end{bmatrix}. \quad (8.3)$$

Consider the Lagrange multiplier approach, using the Lagrangian of Equation 8.1. The functional  $B$  and the quadratic term of the constraint constraint,  $A_1$ , are given by

$$B = \begin{bmatrix} 0 & 0 & 0 \\ 0 & 1 & 0 \\ 0 & 0 & 1 \end{bmatrix}$$

and

$$A_1 = \begin{bmatrix} 0.39 + 0.00i & -0.10 - 0.12i & -0.58 + 0.28i \\ -0.10 + 0.12i & -0.04 + 0.00i & -0.04 + 0.16i \\ -0.58 - 0.28i & -0.04 - 0.16i & -0.68 + 0.00i \end{bmatrix}.$$

The quadratic term of the Lagrangian is

$$x_e^*(0.8918 - 0.2551\lambda)x_e.$$

$C_e(\lambda)$  and  $d_e(\lambda)$  are given by

$$C_e(\lambda) = (0.3794 - 0.0344i) + \lambda(0.1933 - 0.3635i)$$

and

$$d_e(\lambda) = 0.2802 + \lambda 0.0029.$$

The dual function  $h(\lambda)$  is plotted in Figure 8.3. Note that the maximum occurs for  $\lambda = 0$ . The constraint is satisfied with inequality at this point.  $h(0) = 0.1175$  implying that the minimum  $\|w\| = 0.3428$ . The minimizing  $x_e = -0.4254 + 0.0386i$  giving as the minimizing  $x$

$$x = \begin{bmatrix} -1.2935 + 0.1173i \\ -0.0037 - 0.1569i \\ -0.1880 - 0.2398i \end{bmatrix}.$$

Consequently the minimizing  $w$  is

$$w = \begin{bmatrix} -0.0037 - 0.1569i \\ -0.1880 - 0.2398i \end{bmatrix}.$$

In this case the constraint is not satisfied with equality. In fact

$$g(x) = -0.2362.$$

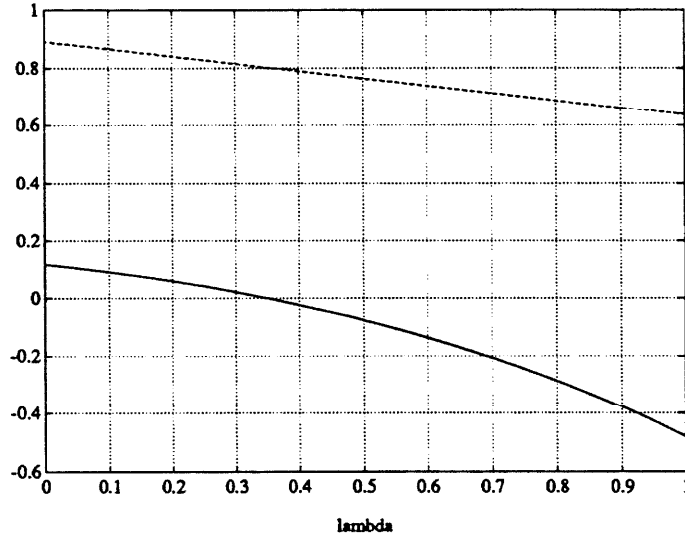


Figure 8.3: Case 2: Dual Function:  $h(\lambda)$  (solid line) and the minimum eigenvalue of the quadratic term:  $V^*(B + \lambda A)V$  (dashed line)

The Lagrange multiplier optimization has yielded a solution to the model validation problem. Again the geometric approach is compared.  $\tilde{N}$  is given by:

$$\tilde{N} = \begin{bmatrix} 0.5309 + 0.7089i & 0.0812 + 0.1638i & 0.8012 + 0.2470i \\ -0.7112 - 0.0645i & 0.1742 + 0.2299i & -0.1478 + 0.0385i \\ 0 & 0 & 0 \end{bmatrix}.$$

Note that a row of zeros has been added to make the second perturbation block square. The  $\psi_s(\tilde{N}, \mathcal{X})$  problem is posed with  $I_s = \{1\}$  and  $\bar{I}_s = \{2\}$ .

The  $W'(\alpha)$  regions are shown for  $\alpha = 5.5$  and  $\alpha = 8.51$  in Figure 8.4. Note that for  $\alpha = 5.5$ , the origin is on the boundary of  $W'(\alpha)$ . In fact, if the maximization were posed, as is done in the  $\mu$  or  $\mu_s$  cases, with  $0 \notin W'(\alpha)$  then, as is illustrated here, the solution would be conservative. In this example  $\psi_s(\tilde{N}, \mathcal{X})^2 = 8.51$  implying that

$$\min \|w\| = \frac{1}{\psi_s(\tilde{N}, \mathcal{X})} = \frac{1}{\sqrt{8.51}} = 0.3428.$$

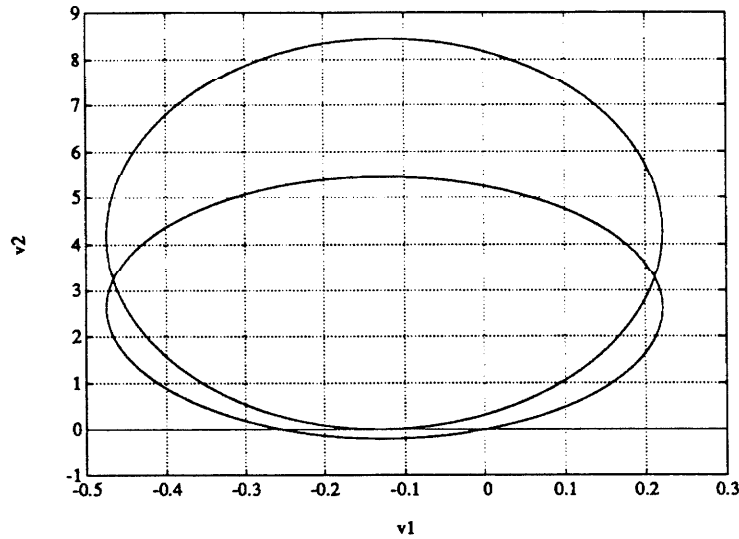


Figure 8.4: Case 2:  $W'(\alpha)$  for  $\alpha = 5.5$  &  $8.51$  and the supporting hyperplane defined by  $\langle \xi, \nu \rangle \geq 0$ ,  $\xi = [0, 1]^T$

Note that the halfspace containing  $W'(\alpha)$  is now defined by

$$\xi = \begin{bmatrix} 0 \\ 1 \end{bmatrix}$$

implying that the Lagrange multiplier associated with the saddlepoint is  $\lambda = 0$ . As expected, the values of  $\|w\|$  and  $\lambda$  agree with those obtained from the Lagrange multiplier optimization.

### 8.3 Case 3

Two examples will be considered. These are both based on the four block example derived by Doyle and used by Packard [10] to illustrate the gap between  $\mu$  and its upper bound. In the first the block structure is defined such that a single perturbation block boundary problem occurs. In the second a three block problem is defined for which no saddlepoint exists. This second example also illustrates a direct application of the model validation problem to the calculation of  $\mu$ .

Consider the system

$$P = \begin{bmatrix} & 1 \\ \tilde{P} & 1 \\ & 1 \\ & 1 \end{bmatrix}, \quad \text{where } \tilde{P} = U_b V_b^*.$$

$U_b, V_b \in \mathcal{C}^{4 \times 2}$  and are defined by

$$U_b = \begin{bmatrix} a & 0 \\ b & b \\ c & jc \\ d & f \end{bmatrix}, \quad V_b = \begin{bmatrix} 0 & a \\ b & -b \\ c & -jc \\ e^{j\phi_1} f & e^{j\phi_2} d \end{bmatrix}.$$

The constants are chosen such that  $U_b^* U_b = V_b^* V_b = I^{2 \times 2}$ . Select  $y = 1$  and  $u = 0$ . This choice of  $u$  eliminates the last column and makes the plant under consideration equivalent to that considered by Packard [10]. It will be seen in Section 8.3.2 that the choice of  $y = 1$  allows this formulation to address a  $\mu$  problem.

For this example, set  $\gamma = 3 + \sqrt{3}$  and  $\beta = \sqrt{3} - 1$ . Now define

$$a = \sqrt{\frac{2}{\gamma}}, \quad b = \frac{1}{\sqrt{\gamma}}, \quad c = \frac{1}{\sqrt{\gamma}}, \quad d = -\sqrt{\frac{\beta}{\gamma}}$$

$$f = (1 + j)\sqrt{\frac{1}{\gamma\beta}}, \quad \phi_1 = -\frac{\pi}{2}, \quad \phi_2 = \pi.$$

This gives

$$\tilde{P} =$$

$$\begin{bmatrix} & 0 & 0.2989 + 0.0000i & 0.2989 + 0.0000i & | & 0.3493 + 0.3493i \\ 0.2989 + 0.0000i & & & 0 & | & 0.2113 + 0.2113i \\ 0.0000 + 0.2989i & & 0.2113 - 0.2113i & & | & 0 \\ \hline 0.3493 + 0.3493i & -0.4278 - 0.2470i & -0.4278 + 0.2470i & & | & 0 \end{bmatrix}.$$

If the reader wishes to recreate this example, it is advisable to recalculate the values of  $\tilde{P}$  to greater precision than displayed here. The rounding error will obscure the characteristics illustrated by the example.

### 8.3.1 A Single Block Boundary Problem

The block structure is chosen as (3) making the model validation problem a single  $\Delta$  block problem ( $m = 1$ ).

Proceeding with the Lagrange optimization approach gives

$$x_0 = \begin{bmatrix} 0.4771 - 0.4771i \\ -0.5844 + 0.3374i \\ -0.5844 - 0.3374i \\ 0 \end{bmatrix}$$

and

$$V = \begin{bmatrix} -0.8165 + 0.0000i & 0 & 0 \\ -0.3943 - 0.1057i & -0.3536 + 0.6124i & 0 \\ -0.1057 - 0.3943i & 0.7071 + 0.0000i & 0 \\ 0 & 0 & 1.0000 \end{bmatrix}.$$

Note that the dimension of the search has been reduced from four to three. The functional and quadratic parts of the constraint are

$$B = \begin{bmatrix} 0 & 0 & 0 & 0 \\ 0 & 0 & 0 & 0 \\ 0 & 0 & 0 & 0 \\ 0 & 0 & 0 & 1 \end{bmatrix}$$

and

$$A_1 =$$

$$\begin{bmatrix} 0.8214 + 0.0000i & 0.0632 + 0.0632i & -0.0632 - 0.0632i & -0.2557 - 0.0000i \\ 0.0632 - 0.0632i & 0.8214 + 0.0000i & -0.0893 + 0.0000i & -0.0662 - 0.2470i \\ -0.0632 + 0.0632i & -0.0893 + 0.0000i & 0.8214 + 0.0000i & -0.2470 - 0.0662i \\ -0.2557 + 0.0000i & -0.0662 + 0.2470i & -0.2470 + 0.0662i & -0.7321 + 0.0000i \end{bmatrix}.$$

The quadratic term of the Lagrangian is

$$x_e^* \begin{bmatrix} 0 & 0 & 0 \\ 0 & 0 & 0 \\ 0 & 0 & 1 \end{bmatrix} x_e$$

$$+\lambda x_e^* \begin{bmatrix} 0.8660 + 0.0000i & 0.1294 + 0.0347i & 0.3132 - 0.0000i \\ 0.1294 - 0.0347i & 0.8660 + 0.0000i & -0.3025 + 0.0811i \\ 0.3132 + 0.0000i & -0.3025 - 0.0811i & -0.7321 + 0.0000i \end{bmatrix} x_e.$$

$C_e(\lambda)$  and  $d_e(\lambda)$  are given by

$$C_e(\lambda) = \begin{bmatrix} 0 \\ 0 \\ 0 \end{bmatrix}$$

and

$$d_e(\lambda) = \lambda.$$

If the dual function is maximized over  $\lambda \geq 0$ , the boundary of  $\Lambda_e$  is encountered at  $\lambda = 1$ . This is illustrated in Figure 8.5. The minimum eigenvalue of  $V^*(B + \lambda A)V$  is also plotted, and at  $\lambda = 1$  the eigenvalue is zero. Note that  $h(1) = 1$  and for  $\lambda > 1$   $h(\lambda) = -\infty$ .

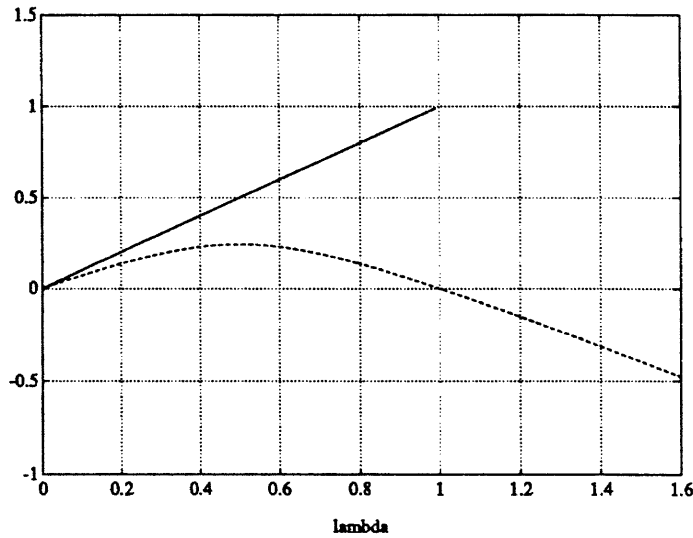


Figure 8.5: Case 3 with Block Structure (3): Dual Function:  $h(\lambda)$  (solid line) and the minimum eigenvalue of the quadratic term:  $V^*(B + \lambda A)V$  (dashed line)

The Lagrangian has no linear term. Therefore, the  $x$  achieving the minimum is  $x = 0$ . This reduces the dual function to  $h(\lambda) = \lambda$  as can be seen on the plot.



However, at  $\lambda = 1$  the search can be restricted to the kernel of  $V^*(B + A)V$  without affecting the value of the Lagrangian. Consider the constraint for the equality constrained case:

$$\begin{aligned} g_e(x_e) = & x_e^* V^* A V x_e \\ & + 2 \operatorname{Re} \left\{ x_e^* V^* A x_0 - x_e^* V^* \begin{bmatrix} P_{11}^* \\ P_{12}^* \end{bmatrix} P_{13} u \right\} \\ & - 2 \operatorname{Re} \left\{ x_0^* \begin{bmatrix} P_{11}^* \\ P_{12}^* \end{bmatrix} P_{13} u \right\} + x_0^* A x_0 - u^* P_{13}^* P_{13} u. \end{aligned}$$

In this example  $u = \begin{bmatrix} 0 \\ 0 \end{bmatrix}$  and

$$V^* A x_0 = \begin{bmatrix} 0 \\ 0 \\ 0 \end{bmatrix}$$

reducing the constraint to

$$g_e(x_e) = x_e^* V^* A V x_e + x_0^* A x_0. \quad (8.4)$$

For  $x_0$  given above  $x_0^* A x_0 = 1$ . Now consider the quadratic term of the Lagrangian at  $\lambda = 1$ . This has eigenvalues 0, 1, and 1. Selecting the eigenvector corresponding to the zero eigenvalue gives

$$x_{ek} = \begin{bmatrix} -0.3660 + 0.0000i \\ 0.3536 - 0.0947i \\ 0.8556 - 0.0000i \end{bmatrix}.$$

Lemma 5.12 predicts that  $x_{ek}^* V^* A V x_{ek} < 0$  and in fact it is

$$x_{ek}^* V^* A V x_{ek} = -0.7321.$$

Choosing  $x_e = 1.1688 x_{ek}$  makes Equation 8.4 equal to zero, satisfying the constraint exactly. This gives as an optimizing  $x$

$$\begin{aligned} x &= x_0 + V x_e \\ &= x_0 + 1.1688 V x_{ek} \\ &= \begin{bmatrix} 0.8264 - 0.4771i \\ -0.4940 + 0.6748i \\ -0.2470 - 0.2470i \\ 1.0000 - 0.0000i \end{bmatrix}. \end{aligned}$$

It is easily verified that this  $x$  meets the output equality constraint and corresponds to  $\|\Delta\| = 1$  and  $\|w\| = 1$ .

Now consider this example from the geometric point of view. Although the Lagrange multiplier approach required a search in the null space of the quadratic term of the Lagrangian, a saddlepoint was still found. This suggests that the geometric approach will also lead to a saddlepoint and, as expected, this is the case.

The choice of  $u = 0$  makes

$$\tilde{N} = U_b V_b^* = \begin{bmatrix} 0 & 0.2989 + 0.0000i & 0.2989 + 0.0000i & 0.3493 + 0.3493i \\ 0.2989 + 0.0000i & 0 & 0.2113 + 0.2113i & 0.4278 + 0.2470i \\ 0.0000 + 0.2989i & 0.2113 - 0.2113i & 0 & 0.2470 + 0.4278i \\ 0.3493 + 0.3493i & -0.4278 - 0.2470i & -0.4278 + 0.2470i & 0 \end{bmatrix}.$$

Again  $I_s = \{1\}$  and  $\bar{I}_s = \{2\}$ .

Figure 8.6 illustrates the set  $W'(\alpha)$  for  $\alpha = 1.0$ . Note that  $0 \in W'(1)$  and for  $\alpha > 1$ ,  $W'(\alpha) \cap \nu_- = \emptyset$ . The set  $W'(1.0)$  is contained in a halfspace described by

$$H(\xi) = \{ \nu \mid \langle \xi, \nu \rangle \geq 0 \}$$

where

$$\xi = \begin{bmatrix} 1 \\ 1 \end{bmatrix}.$$

This implies that the minimum  $\|w\| = 1$  and that a saddlepoint exists for  $\lambda = 1$ .

It is interesting to note that the complications of the Lagrange optimization are not reflected in the geometric approach. The nature of  $W'(\alpha)$  and its behavior as a function of  $\alpha$  differ little in qualitative terms from the example studied in Case 2.

The only significant difference is that  $W'(\alpha)$  and the supporting hyperplane now intersect at more than one point. Section 5.3 established the fact that when  $h_e(\lambda)$  is finite at the boundary  $\partial\Lambda_e$ , the Lagrangian  $L_e(x_e, \lambda)$  has a nontrivial kernel. In this case this is also evident from the geometric viewpoint. To see this note that when  $W'(\psi_s(\tilde{N}, \mathcal{X})^2)$  lies within a halfspace defined by  $\langle \xi, \nu \rangle \geq 0$ , the Lagrangian is given by

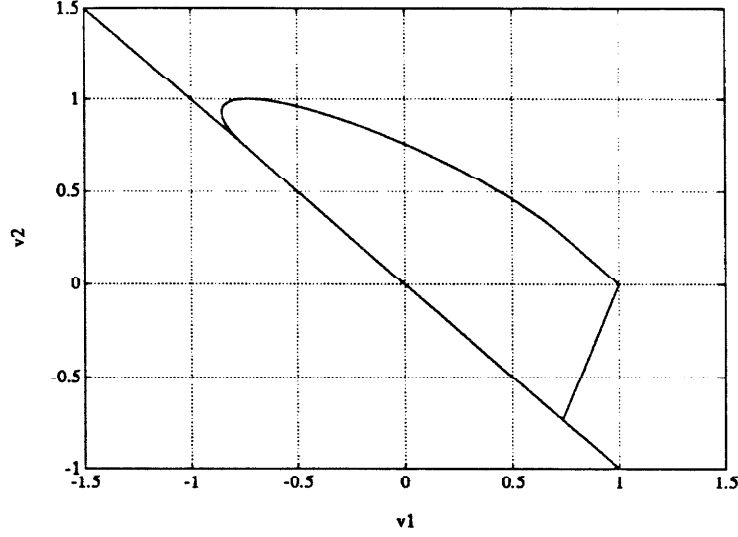


Figure 8.6: Case 3 for Block Structure (3):  $W'(\alpha)$  for  $\alpha = 1$  and the supporting hyperplane defined by  $\langle \xi, \nu \rangle \geq 0$ ,  $\xi = [1, 1]^T$

$$L_e(x_e, \lambda) = \frac{\langle \xi, \nu \rangle}{\xi_{m+1} \psi_s(\tilde{N}, \mathcal{X})^2} + \frac{1}{\psi_s(\tilde{N}, \mathcal{X})^2}.$$

From Figure 8.6 it is clear that the  $\nu$  for which  $\langle \xi, \nu \rangle = 0$  is not unique. Consequently, the  $x_e$  for which

$$L_e(x_e, \lambda) = \frac{1}{\psi_s(\tilde{N}, \mathcal{X})^2}$$

is also not unique, implying that for this value of  $\lambda$ , the Lagrangian has a nontrivial kernel.

### 8.3.2 An Application to $\mu$ - the 4 Block Counterexample

A block structure of (1,1,1) is assumed, and the question *is*  $\mu(\tilde{P}) < 1$ ? is addressed. This is exactly the four block counterexample where it is known that the upper bound cannot be used to answer this question.

For a  $\mu$  problem with a scalar output signal  $e$ , the model validation approach can be used directly by considering  $e$  to be known;  $y = e$ . If there exists  $x$  such that

$$\| [0 \ I] \tilde{P}x \| = 1, \quad \text{and} \quad \| [0 \ I] x \| < 1,$$

and for  $i = 1, \dots, m$ ,

$$\| [Q; 0] x \| = \| [Q; 0] \tilde{P} x \|,$$

then  $\mu > 1$ . In the scalar case it suffices to choose  $y = 1$ . Assume that the minimum  $\| [0 I] x \|$  is achieved by  $\bar{x}$  and

$$\tilde{P}\bar{x} = \theta, \quad |\theta| = 1.$$

Then  $\theta^*\bar{x}$  has the same norm and meets the constraints

$$\| [0 I] \theta^*\bar{x} \| = \| [0 I] \tilde{P}\theta^*\bar{x} \|$$

and

$$[0 I] \tilde{P}\theta^*\bar{x} = \theta^*\theta = 1.$$

The choice of  $u = 0$  will effectively reduce the full  $P$  interconnection structure to the required  $\tilde{P}$ . Clearly, if using the model validation approach, the minimum  $\|w\|$  meeting the constraints (including the output constraint that  $y = 1$ ) has norm greater than one, then  $\mu < 1$ .

For this example

$$\inf_{D \in \mathcal{D}} \sigma_{\max} \left( \begin{bmatrix} D & 0 \\ 0 & I \end{bmatrix} \tilde{P} \begin{bmatrix} D & 0 \\ 0 & I \end{bmatrix}^{-1} \right) = \sigma_{\max}(\tilde{P}) = 1.$$

However,  $\Lambda_e$  is not empty as

$$\sigma_{\max}(\tilde{P}_{11}) = 0.5176.$$

Although the upper bound for  $\mu$  is equal to one, Packard proves that  $\mu < 1$ . The best estimate for  $\mu$ , obtained by extensive searching, is 0.874.

Therefore, for all  $w$  meeting the uncertainty constraints,  $\|w\| > 1$  as  $\mu < 1$ . It will be shown that the minimum  $\|w\|$  cannot be found with the model validation techniques. If it could be found then it would be possible to calculate  $\mu$  for this problem by iterative application of the model validation approach. This is hardly surprising, given the demonstrated relationship between the Lagrange multipliers and the  $D$  used in the calculation of the upper bound of  $\mu$  in Section 5.1.1.

Lemma 8.1 will show why it is not possible to find the minimum  $\|w\|$ . For notational convenience consider an equivalent formulation of the quadratic term of the Lagrangian, using  $D$  defined by Equation 5.7.

$$x^*(B + \sum_{i=1}^m \lambda_i A_i)x = x^* \left( \begin{bmatrix} D^2 & 0 \\ 0 & I \end{bmatrix} - \tilde{P}^* \begin{bmatrix} D^2 & 0 \\ 0 & 0 \end{bmatrix} \tilde{P} \right) x \quad (8.5)$$

where

$$\tilde{P} = \begin{bmatrix} P_{11} & P_{12} \\ P_{21} & P_{22} \end{bmatrix}.$$

Note that in this case, with  $u = 0$ , this is actually the complete Lagrangian.

### Lemma 8.1

For scalar  $y = 1$ ,  $u = 0$ , and a model  $P$  such that

$$\inf_{D \in \mathcal{D}} \sigma_{\max} \left( \begin{bmatrix} D & 0 \\ 0 & I \end{bmatrix} \tilde{P} \begin{bmatrix} D & 0 \\ 0 & I \end{bmatrix}^{-1} \right) \geq 1,$$

$$\max_{\lambda} h_e(\lambda) \leq 1.$$

**Proof of Lemma 8.1:** Assume there exists  $\lambda$  such that  $h_e(\lambda) > 1$ . This implies, using the formulation introduced in Equation 8.5, that

$$h_e(\lambda) = \min_{x \in \mathcal{X}_e} x^* \left( \begin{bmatrix} D^2 & 0 \\ 0 & I \end{bmatrix} - \tilde{P}^* \begin{bmatrix} D^2 & 0 \\ 0 & 0 \end{bmatrix} \tilde{P} \right) x > 1.$$

Note that for  $x \in \mathcal{X}_e$ ,

$$x^* \tilde{P}^* \begin{bmatrix} 0 & 0 \\ 0 & I \end{bmatrix} \tilde{P} x = \|y\|^2 = 1.$$

Giving the result that for all  $x \in \mathcal{X}_e$ ,

$$x^* \left( \begin{bmatrix} D^2 & 0 \\ 0 & I \end{bmatrix} - \tilde{P}^* \begin{bmatrix} D^2 & 0 \\ 0 & I \end{bmatrix} \tilde{P} \right) x > 0. \quad (8.6)$$

$x$  can be partitioned as  $x_0 \oplus Vx_e$ . Note that  $x_0 \neq 0$ ; if it were, it would imply that  $e = 0$ . In the scalar case the span of  $\{x_0, V\}$  is the whole of the space in which  $x$  lies. In this case Equation 8.6 is true for all  $x$ . If there exists an  $x \notin \mathcal{X}_e$  such that

$$x^* \left( \begin{bmatrix} D^2 & 0 \\ 0 & I \end{bmatrix} - \tilde{P}^* \begin{bmatrix} D^2 & 0 \\ 0 & I \end{bmatrix} \tilde{P} \right) x \leq 0,$$

then  $x$  has a decomposition

$$x = \eta x_0 + Vy.$$

Now  $x/\eta \in \mathcal{X}_e$  and  $x/\eta$  will also violate Equation 8.6. Note that this argument can only be made for a scalar signal  $y$ . Choosing  $x_s$  as

$$x_s = \begin{bmatrix} D & 0 \\ 0 & I \end{bmatrix} x$$

gives, for all  $x_s$ ,

$$x_s^* \left( I - \begin{bmatrix} D & 0 \\ 0 & I \end{bmatrix}^{-1} \tilde{P}^* \begin{bmatrix} D^2 & 0 \\ 0 & I \end{bmatrix} \tilde{P} \begin{bmatrix} D & 0 \\ 0 & I \end{bmatrix}^{-1} \right) x_s > 0$$

which implies that

$$\sigma_{\max} \left( \begin{bmatrix} D & 0 \\ 0 & I \end{bmatrix} \tilde{P} \begin{bmatrix} D & 0 \\ 0 & I \end{bmatrix}^{-1} \right) < 1,$$

contradicting the assumptions of the Lemma. ▶

Now  $h_e(\lambda)$  is simply

$$h_e(\lambda) = \|[0 \ I]x\|^2 + \sum_{i=1}^m \lambda_i g_{ei}(x). \quad (8.7)$$

From Lemma 8.1, any  $x$  meeting the equality constraint will also satisfy

$$\|w\|^2 + \sum_{i=1}^m \lambda_i g_{ei}(x) \leq 1. \quad (8.8)$$

But it is known that in this example  $\|w\| > 1$ . Consequently,

$$\sum_{i=1}^m \lambda_i g_{ei}(x) < 0 \quad (8.9)$$

and the constraint can never be met exactly.

In fact, for this problem, attempting to answer the  $\mu$  question by the model validation method results in a boundary problem. For

$$\lambda = \begin{bmatrix} 1 \\ 1 \\ 1 \end{bmatrix}, \quad h_e(\lambda) = 1 \quad (8.10)$$

but the three constraints cannot be met exactly. It is possible to find  $x$  at the boundary such that all constraints, including the equality constraint, are met, but it is not possible to state that this  $x$  has the minimum  $\|w\|$ . Hence, it is not possible to answer the question *is  $\mu(\tilde{P}) < 1$ ?*

## Chapter 9

# An Experimental Example

An experimental chemical process control system is used as a model validation example. This system has many of the characteristics found in industrial process control problems. Although the complete system is described here, only a two-input two-output subsystem will be used as a model validation example. Additional identification and control work on the complete system is described by Smith *et al.* [3, 31].

The system will be described in some detail. A theoretical model is developed and used as a nominal nonlinear model. Several *ad hoc* techniques have been used to quantify the uncertainty, and these are discussed. A nonlinear model of the system, including an uncertainty description, is presented. The choice of a suitable linear model for design and analysis requires engineering judgement. As an example application of the model validation approach, two different linear models are compared in their ability to account for the observations of a particular experiment.

The techniques presented here are typical of those that a designer might apply in identifying a suitable robust control model: iterative application of first principles modeling, open loop experiments, and closed loop experiments. The goal of this chapter is to illustrate, by example, how model validation can be a useful tool in this procedure.

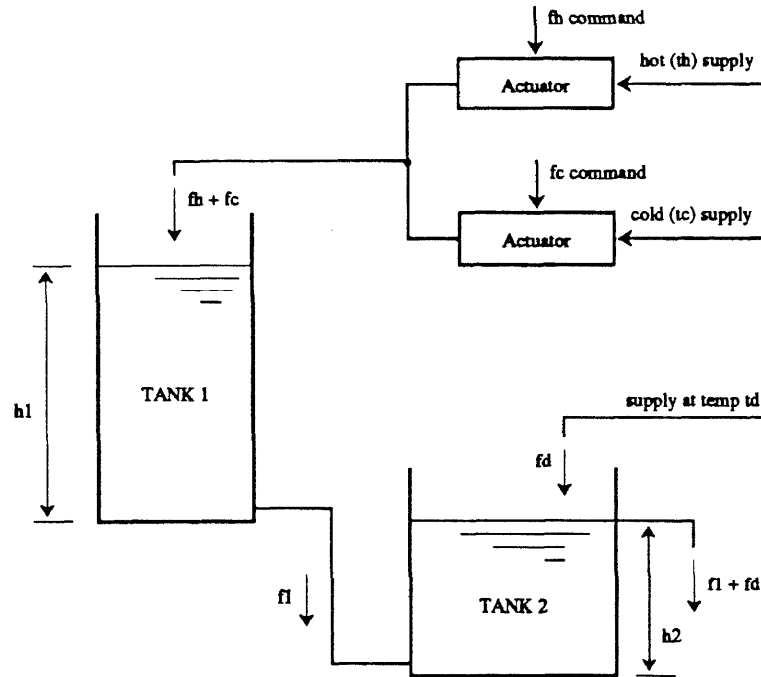


Figure 9.1: Schematic Diagram of the Two Tank System

## 9.1 The Two Tank Experiment

### 9.1.1 A Physical Description

The system, shown schematically in Figure 9.1, consists of two water tanks in cascade. The upper tank, referred to as tank 1, is fed by hot and cold water via computer controllable valves. The lower tank, referred to as tank 2, is fed by water from an exit at the bottom of tank 1. A constant level is maintained in tank 2 by means of an overflow. A fixed stream of cold water also feeds tank 2. It is the presence of this bias stream that allows the tanks to be maintained at different temperatures.

Tank 1 is  $5\frac{3}{8}$  inches in diameter and 30 inches in height. Tank 2 is  $7\frac{1}{2}$  inches in diameter. Four overflows are provided at  $5\frac{1}{4}$ ,  $7\frac{1}{4}$ ,  $9\frac{1}{4}$ , and  $11\frac{1}{4}$  inches. For the experiments described here, the overflow at  $7\frac{1}{4}$  inches was used. This configuration maintains the water level in tank 2 at  $4\frac{3}{4}$  inches below the base of tank 1.

The hot and cold water supplies are filtered through a 5 micron filter and regulated to 20 psig. Half inch piping is used for the main flow lines and the connection between tanks 1 and 2. Two half inch Kämmer valves (30 000 series) with electropneumatic



actuators are used to control the flows. These have a linear characteristic and a  $C_v$  of 1.0. Variable area flowmeters measuring from 0.2 to 2.0 gpm provide a means of calibrating the actuators. Approximately 72 inches of pipe connects the actuators to the flowmeters. The hot and cold flows are combined in a tee junction 10 inches from the flowmeters, and the mixed flow is piped a further 18 inches to tank 1. The pipe outlet is 31 inches above the base of tank 1. Approximately 36 inches of pipe connects the tanks, from the base of tank 1 to the base of tank 2. The tank 2 bias stream is fed from the cold supply via a needle valve and flowmeter. This arrangement allows manual adjustment of the bias stream flow from 0.015 to 0.3 gpm.

Isolated E type thermocouples are inserted into each of the tanks approximately  $\frac{1}{4}$  inch above the base. Omega MCJ thermocouple connectors provide the ice point reference. The temperature signals are amplified by Omega Omni-Amp amplifiers (gain: 1000). There is also provision to measure the temperature of the hot and cold flows prior to the valves and the mixed flow just before it enters tank 1.

A pressure sensor (0 to 5 psig) provides a measurement of the water level in tank 1. Both tanks are stirred with laboratory stirrers. Tank 1 has a shaft running the full length of the tank with three 2 inch propellers mounted on it. A single propeller stirs tank 2.

A Masscomp 5400 is used for the data acquisition and control. All signals from the experiment are filtered using fourth order butterworth filters, each with a cutoff frequency of 2.25 Hz. The Masscomp is equipped with analog/digital (AD12FA) and digital/analog (DA08F) boards, each with 12 bit resolution, and a floating point accelerator board. Software allows the designer to provide arbitrary control signals to the experiment and implement linear state space and nonlinear controllers. A sample time of 0.1 seconds has been used for the majority of the identification and control experiments.

### 9.1.2 The Scope of the Model Validation Problem

The model validation problem presented here is part of a sequence of problems that would naturally be considered in the process of identifying and designing controllers for the system. Wherever possible the system should be broken down into component parts for identification. Only a single experiment will be presented. Again this is representative of one of a series of similar experiments that a design engineer might perform.

The system to be examined will consist of only the top tank. The hot and cold flows ( $f_h$  and  $f_c$ ) will be considered as the inputs and the height ( $h_1$ ) and the temperature of the top tank ( $t_1$ ) will be the outputs.

The problem is most naturally considered with a bounded power assumption on the input and output signals. Output noise, on both  $h_1$  and  $t_1$ , will be the only unknown inputs to the interconnection structure.

A theoretical model will be developed and used as a nominal nonlinear model. Experiments have been performed in an attempt to quantify a bound on the uncertainty associated with this model. These procedures lead to a candidate interconnection structure which is then tested against an experimental datum with the model validation procedure. In the example presented here, two candidate interconnection structures are considered.

## 9.2 Modeling the System

### 9.2.1 Development of a Nominal Model

The top tank is considered from a first principles' point of view to give an initial estimate of a suitable nominal model. The choice of nominal model plus uncertainty description is not unique. Developing a nominal model from the theoretical equations is not necessarily the best technique; however, it does have an intuitive engineering appeal. Another possible approach is to attempt to identify the system by assuming that the only uncertainty is additive noise. The methods for doing this are well developed. Ljung [16] provides a comprehensive treatment of these methods.

In order to proceed it is necessary to make some typical, and unfortunately inaccurate, assumptions. These are as follows:

- No thermal losses in the system.
- Perfect mixing occurs in both tanks.
- The flow out of tank 1 is related only to the height of tank 1.
- There are no thermal or flow delays.

The system variables are given the following designations.

$f_{hc}$	command to hot flow actuator.
$f_h$	hot water flow into tank 1.
$f_{cc}$	command to cold flow actuator.
$f_c$	cold water flow into tank 1.
$f_1$	total flow out of tank 1.
$A_1$	cross-sectional area of tank 1.
$h_1$	tank 1 water level height.
$t_1$	temperature of tank 1.
$t_h$	hot water supply temperature.
$t_c$	cold water supply temperature.

Conservation of mass in tank 1 gives

$$\frac{d}{dt}(A_1 h_1) = f_h + f_c - f_1.$$

It is assumed that the flow out of tank 1 ( $f_1$ ) is a memoryless function of the height ( $h_1$ ). This is reasonable because of the incompressibility of the media. As the exit from tank 1 is a pipe with a large length to diameter ratio, the flow is proportional to the pressure drop across the pipe and thus to the height in the tank. With a constant correction term for the flow behavior at low tank levels, the height and flow can be related by an affine function.

$$h_1 = \alpha f_1 - \beta \quad \text{where } \alpha, \beta > 0 \quad \text{and} \quad f_1 \geq \beta/\alpha.$$

Therefore,

$$A_1 \alpha \frac{d}{dt} f_1 = f_h + f_c - f_1.$$

Defining  $f_1$  as a state variable leads to a linear state equation and an affine output equation for  $h_1$  (in the allowable range of  $f_1$ ).

$$\dot{f}_1 = \frac{-1}{A_1 \alpha} f_1 + \frac{1}{A_1 \alpha} f_h + \frac{1}{A_1 \alpha} f_c. \quad (9.1)$$

$$h_1 = \alpha f_1 - \beta. \quad (9.2)$$

Conservation of energy will lead to a model for the temperature of tank 1 ( $t_1$ ) as

$$\frac{d}{dt}(A_1 h_1 t_1) = f_h t_h + f_c t_c - f_1 t_1.$$

It is useful to define a variable

$$E_1 = h_1 t_1$$

which can loosely be thought of as the energy in tank 1. Now

$$\begin{aligned} f_1 t_1 &= \left( \frac{h_1 + \beta}{\alpha} \right) t_1 \\ &= \frac{1}{\alpha} \left( 1 + \frac{\beta}{h_1} \right) E_1. \end{aligned}$$

Defining  $E_1$  as a state variable gives a nonlinear state equation and a nonlinear output equation for  $t_1$ .

$$\dot{E}_1 = \frac{-1}{A_1 \alpha} \left( 1 + \frac{\beta}{h_1} \right) E_1 + \frac{t_h}{A_1} f_h + \frac{t_c}{A_1} f_c. \quad (9.3)$$

$$t_1 = \frac{1}{h_1} E_1. \quad (9.4)$$

Note that for a fixed  $h_1$ , the above equations are linear. This will be useful in the development of an uncertainty description.

The system of units has been normalized for the temperature, height, and input flows. The supply temperatures are therefore

$$t_h = 1.0 \quad \text{and} \quad t_c = 0.0.$$

Measurement of the physical system and scaling by the appropriate normalization factors gives the following:

$$A_1 = 91.4.$$

The above theoretical model is only a good approximation over a range of  $h_1$ :

$$0.15 \leq h_1 \leq 0.75.$$

The assumed relationship between  $f_1$  and  $h_1$  breaks down outside of the above range. Static measurements have been performed in order to estimate  $\alpha$  and  $\beta$ . Note that  $\alpha$  appears as a gain in the model equations and can also be estimated dynamically. These estimates yield

$$\alpha = 1.34 \quad \text{and} \quad \beta = 0.6.$$

Equations 9.1, 9.2, 9.3, and 9.4 provide a simple model for the top tank.

### 9.2.2 Development of a Description of the Uncertainty

This section will give only a very brief outline of some of the techniques used for quantifying the uncertainty in the model. There are no formal methodologies for doing this for robust control models; only *ad hoc* methods are discussed.

The techniques are arbitrarily divided into open and closed loop methods. In reality the distinction between modeling, identification, and control design is often blurred. The engineer generally works on the problem iteratively: identifying some aspect of a system, designing a controller, evaluating that controller, and using the information gained to refine the model of the system.

A fundamental feature of robust control models is their ability to model destabilizing uncertainty effects. It is difficult to distinguish such effects from noise or disturbances in an open loop experiment. Closed loop experiments can therefore be helpful in the development of a good robust control model.

Note that the model validation approach treated in this thesis applies equally to open or closed loop models of the system. Model validation is another tool which can be used to arrive at a suitable model.

#### Open Loop Experiments

Ljung [16] provides a very good treatment of open loop identification methods. These can be used to provide a nominal model and, as will be seen here, illustrate where the theoretical model fails to describe the system's behavior.

Note that when considered incrementally, the equations describing the behavior of  $h_1$  are linear and independent of the steady state values of  $h_1$  or  $t_1$ . Open loop experiments have been performed to estimate the transfer function between  $f_h + f_c$  and  $h_1$ .

Band limited noise, in several frequency bands, was used for the input signals. Data records were 8192 samples in length with sample rates of 1.0 Hz and 10.0 Hz. The transfer function estimates, presented below, have been obtained by the Welch method, using Hanning windows on sections of the data [32]. The data plotted in the figures comes from several window lengths, typically 1024 and 4096. Only the points with good coherency (typically greater than 0.95) are plotted.

The results of these experiments are shown in Figure 9.2. The transfer function predicted by Equations 9.1 and 9.2 are also plotted. The effects of the butterworth filter and the nominal actuator model (refer Section 9.3) are included in the theoretical transfer function. This filter accounts for the large amount of additional phase observed at frequencies beyond 0.1 Hz.

Note that the theoretical model agrees very well with the smoothed estimate of the transfer function over four frequency decades. From this, one might surmise that the theoretical model describes the system very well. This is quite possibly true, although the smoothing will tend to obscure any deviations from the average. In some loose average sense, the theoretical model does describe the system well. An engineer would feel comfortable in assigning relatively little uncertainty to the theoretical model of the  $h_1$  behavior. Contrast this with the situation that arises in the  $t_1$  case.

For  $h_1$  fixed, the  $E_1$  state variable equation (9.3) and the  $t_1$  output equation (9.4) are linear. Experiments have been performed at  $h_1 = 0.15, 0.25, 0.47,$  and  $0.75$ . The input waveforms were generated such that  $f_{hc} = -f_{cc}$  which maintains a constant  $h_1$ . Figure 9.3 shows a smoothed estimate of the empirical transfer function between  $f_{hc} - f_{cc}(= 2f_{hc})$  and  $t_1$  calculated from the experimental data and estimated from the model (Equations 9.3 and 9.4 and the Butterworth filter). For the data shown,  $h_1 = 0.15$  and  $h_1 = 0.75$ . The other cases lie between the two curves shown.

There are obvious discrepancies at much lower frequencies than in the  $h_1$  case. Note in particular the extra phase, particularly in the  $h_1 = 0.75$  case. This is not altogether unexpected as the tank is tall and thin and poorly stirred, in contrast to the assumptions made in the development of the theoretical model. At the higher levels some loss in gain is also evident. Clearly the theoretical model is better at the lower heights. The uncertainty model must be able to capture these discrepancies.

### Closed Loop Experiments

Two types of closed loop experiment have been performed. The first is the implementation of a relay controller designed to drive the system into stable limit cycles. The second type involves the implementation of a series of linear controllers and analysis using  $\mu$ .

Åström [33] uses relay controllers to drive a closed loop system to stable limit cycles.

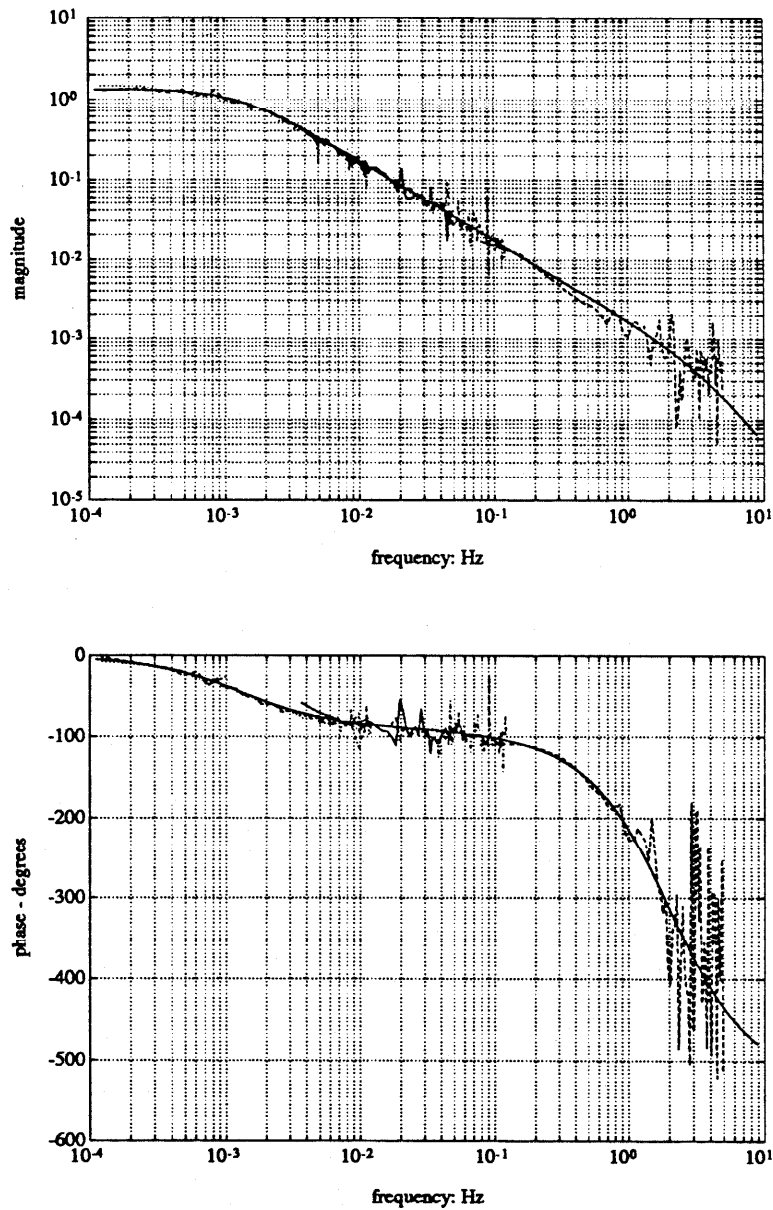


Figure 9.2: Transfer Function Between  $f_{hc} + f_{ce}$  and  $h_1$ . Experimental data and theoretical model (solid line)

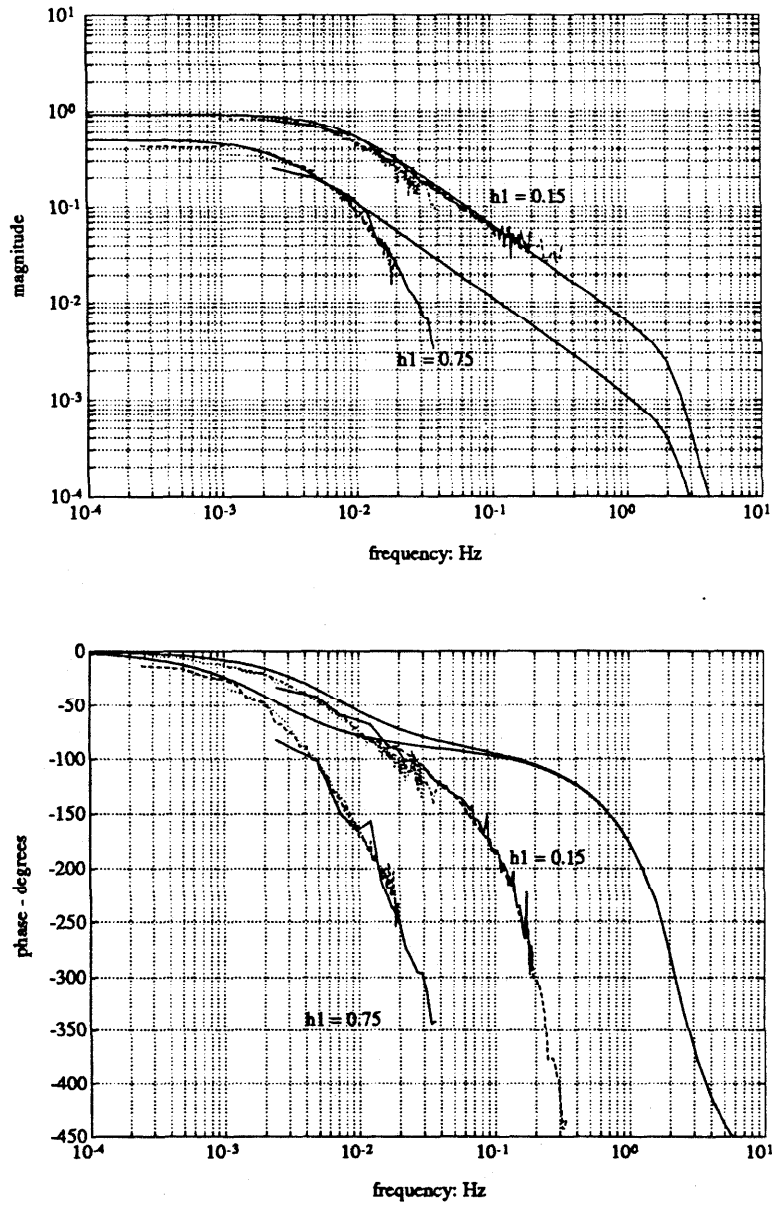


Figure 9.3: Transfer Function Between  $f_{hc} - f_{cc}$  and  $t_1$ . Experimental data and models (solid lines).  $h_1 = 0.15$  and  $h_1 = 0.75$



This technique works for a large class of systems including the two tank system. In the experiments performed here, a decoupled controller (into height and temperature loops) was used with a relay in the temperature control loop. This allowed stable control of the tank height ( $h_1$ ) and produced limit cycles in  $t_1$ . These experiments were performed at fixed heights ( $h_1 = 0.15, 0.25, 0.47, \text{ and } 0.75$ ).

With a simple relay the closed loop system will limit cycle at the frequency where the response has a phase of 180 degrees. The gain at this frequency can also be estimated from the input-output data. This experiment will identify the system at a single point. Using this information, a new controller is designed to introduce some lead into the system. This new closed loop system limit cycles at a higher frequency giving an additional point at which the plant can be identified. In practice this technique can be repeated until the nonlinear and/or inconsistent effects dominate and the closed loop system no longer limit cycles consistently. This also provides information on the frequency at which uncertainty should dominate in the model.

The uncertainty description can also be improved by using  $\mu$  analysis. Comparison of the stability of a closed loop system predicted by  $\mu$  analysis with the observed stability gives information on the applicability of a particular model set.

The proposed technique is then as follows:

- Design a series of nominally stable controllers.
- Predict, by  $\mu$  analysis, the robust stability of each controller.
- Experimentally determine the stability of each controller on the physical system.
- Comparison of the stability predictions and experiments can determine that the system is not described by an element of the model.
- Refine the uncertainty description and iterate on this procedure.

Several points must be noted here. The number of controllers required, and their characteristics, is not obvious. This technique can only make a definitive statement when a theoretically stable controller is found to be unstable on the true system. In such a case the set of plants described by the uncertainty model does not include the behavior of the physical system. The converse situation does not give as conclusive a result. If a system

(constructed with a particular controller) is theoretically not robustly stable, then there exists at least one plant in the described set which will be destabilized by that controller.

### 9.3 A Numerical Model of the System

The identification experiments described in the previous section have been used to estimate a model of the system. A general nonlinear model with uncertainty is presented. This model is intended to be valid over the range  $0.15 \leq h_1 \leq 0.75$ . In order to test this model, and develop a model validation example, an operating point is selected and a linear model developed about that point. The subsequent linear model is then transformed into an equivalent digital system.

#### 9.3.1 A Full Range Nonlinear Model with Uncertainty

Figure 9.4 is a block diagram of the nonlinear tank 1 model derived by the procedures of the previous section. The uncertainty is included as a multiplicative perturbation at the output of each of the nominal  $h_1$  and  $t_1$  models.

In the frequency range of interest, the actuators can be modeled as a single pole system with rate and magnitude saturations. The rate saturation has been estimated from observing the effect of triangle waves of different frequencies and magnitudes. The following model has been estimated for the actuators.

$$f_h = \left[ \frac{1}{(1 + 0.05s)} \right] f_{hc} \quad (9.5)$$

with            magnitude limit:    1.0  
                   rate limit:                3.5

Note that the rate limit determines the actuator performance rather than the pole location. For a linear model some of the effects of rate limiting can be included in an uncertainty model. For the experiments described here, the saturations have little effect and are ignored. Hence

$$P_{act} = \frac{1}{1 + 0.05s}$$

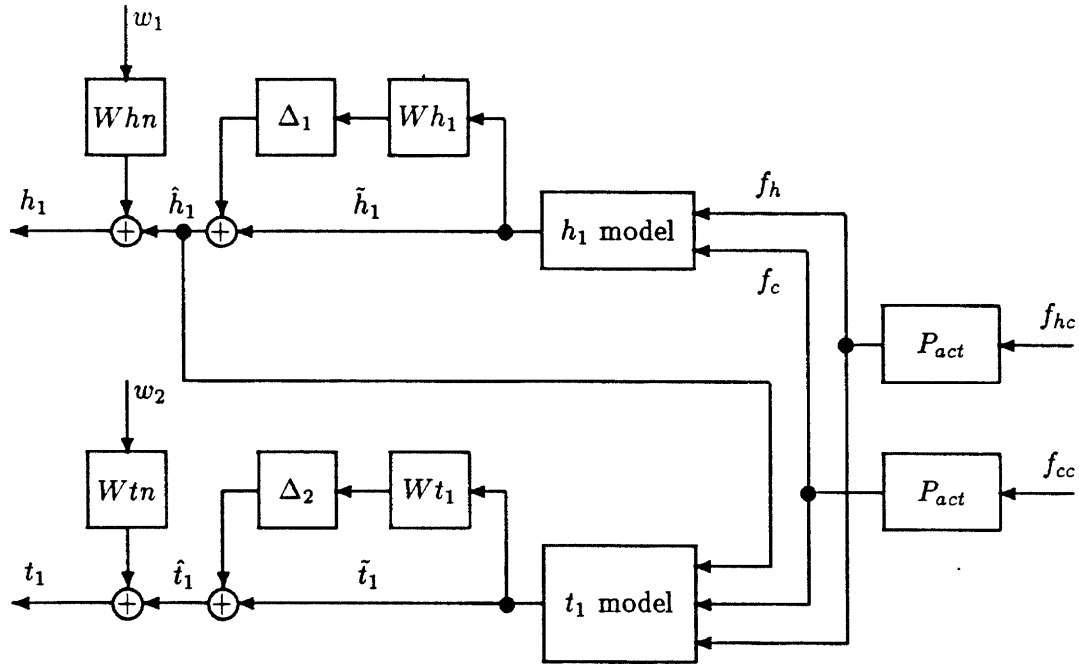


Figure 9.4: A Numerical Nonlinear Model of Tank 1

The block labeled  $h_1$  model is described by the following equations.

$$f_1 = \left[ \frac{1}{1 + 122.5s} \right] (f_h + f_c) \quad (9.6)$$

$$\tilde{h}_1 = 1.34f_1 - 0.6 \quad (9.7)$$

$\tilde{h}_1$  is simply the nominal height in tank 1. The block  $t_1$  model is given by

$$\dot{E}_1 = \frac{-1}{122.5} \left( 1 + \frac{0.6}{\hat{h}_1} \right) E_1 + \frac{1}{91.4} f_h \quad (9.8)$$

$$\tilde{t}_1 = \frac{1}{\hat{h}_1} E_1 \quad (9.9)$$

where  $\tilde{t}_1$  denotes the nominal temperature of tank 1. Note that the nonlinear model for  $t_1$  includes an input  $\hat{h}_1$ . As can be seen from Figure 9.4, this is the height with the inclusion of uncertainty. The question of whether to use  $\tilde{h}_1$  or  $\hat{h}_1$  for this input is open to debate. In this case the weight  $W_{h_1}$  will be so small that it makes little difference which signal is used. The equation given here is a more conservative description.

The weights for the perturbations have been estimated as

$$W_{h1} = \frac{0.5s}{0.25s + 1}$$

and

$$W_{t1} = 0.1 + \frac{35h_1s}{0.2s + 1}$$

As expected from the earlier experiments, the uncertainty weight associated with  $t_1$  increases with  $h_1$ .

The model does not include any sensor dynamics. In the frequency range of interest, unity gain is a good enough model of both the thermocouple and the pressure sensor. Any multiplicative uncertainty can be absorbed into the existing output uncertainty weights:  $W_{h1}$  and  $W_{t1}$ . Weighted additive noise is included on each measured output. It is assumed that this noise is bounded in power. Measurements on a quiescent system give the following estimates.

$$W_{hn} = 0.01$$

$$W_{tn} = 0.03$$

The model validation procedure will directly test these values.

This gives a candidate nonlinear model for the top tank. In the next section an operating point will be selected and a linear model developed for consideration as a model validation example.

### 9.3.2 A Linear Model

The operating point is selected as  $h_1 = 0.47$  and  $t_1 = 0.5$ . This requires actuator positions close to the midpoint and consequently avoids saturation issues in both  $h_1$  and the input flows.

The first of two linear models is now developed. This is not a standard linearization of the nonlinear model as the cross coupling between height and temperature will be ignored. If such a model, with uncertainty, could adequately describe the system, then the resulting controller design problem would be simplified. It will be seen that the

uncertainty associated with the temperature is large; it is this that tempts one to attempt using a simplified nominal model.

In the derivation of the temperature model, it will be assumed that the height is fixed. This results in a simplified linear model for the top tank. In practice one hopes that the model equations are good for small variations about the nominal height. In this example large deviations will also be considered. In a robust control framework, it is hoped that the discrepancies in the behavior due to the effects of changing  $h_1$  will be captured in the uncertainty description.

This emphasizes a fundamental point in using robust control models to describe any system. The criterion of importance is that the linear model plus uncertainty be able to describe the actual effects observed in the system.

These issues arise in the choice of  $W_{t1}$ . The previous section gave an equation for  $W_{t1}$  which was a function of  $h_1$ . The means used to estimate a suitable  $W_{t1}$  were really only applicable to small deviations about the nominal  $h_1$ . Some faith is required to apply this weight to a description of the full nonlinear behavior. It is also not clear which value should be used for  $h_1$  in the derivation of  $W_{t1}$ ;  $h_1 = 0.47$  (the nominal  $h_1$ ) or  $h_1$  equal to the maximum likely to occur in practice. Note that the maximum value of  $h_1$  gives the most conservative estimate of the weight. For this problem the value  $h_1 = 0.47$  will be used. The suitability of the resulting model can then be tested against experimental data.

Linearizing the  $h_1$  and  $t_1$  model equations at  $h_1 = 0.47$  gives

$$\tilde{h}_1 = \left[ \frac{1.34}{1 + 122.5s} \right] (f_h + f_c) = h_{lin}(f_h + f_c)$$

$$\tilde{t}_1 = \left[ \frac{1.25}{1 + 53.8s} \right] f_h = t_{lin}f_h.$$

The weights on the output perturbations are selected as

$$W_{h1} = \frac{0.5s}{1 + 0.25s}$$

$$W_{t1} = \frac{0.1 + 16.5s}{1 + 0.2s},$$

and the weights for the additive output noise are

$$W_{hn} = 0.01$$

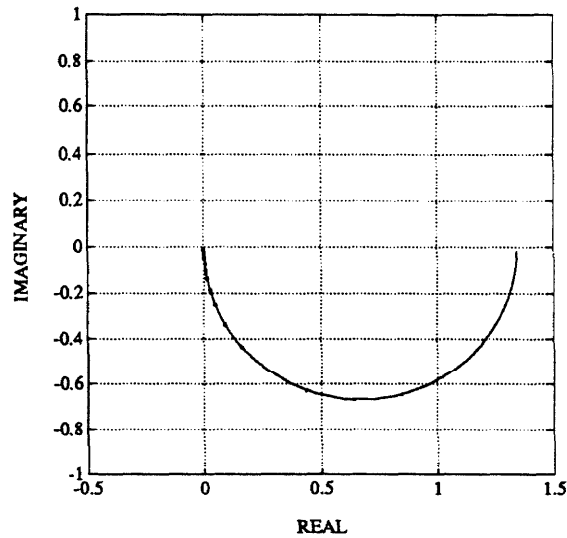


Figure 9.5: Nyquist Plot of the Transfer Function:  $f_h + f_c$  to  $h_1$ . Circles indicate the equivalent additive uncertainty bound

$$W_{tn} = 0.03.$$

Figure 9.5 shows a Nyquist plot of the transfer function  $f_h + f_c$  to  $h_1$ . The Nyquist plot of the transfer function from  $f_h$  to  $t_1$  is illustrated in Figure 9.6. The perturbation uncertainty is illustrated by circles about the nominal transfer function at each frequency. Note that this diagram illustrates the perturbation uncertainty in an additive form although the above mathematical description is in multiplicative form. For SISO models the additive weight is simply the product of the plant and the multiplicative weight.

The uncertainty on the  $f_h + f_c$  to  $h_1$  transfer function is very small. It is almost indistinguishable on the plot. The system is very close to linear with regard to the height model. It will be seen that the height output uncertainty weight  $W_{h1}$  is in fact adequate. It appears that the temperature uncertainty weight is greater than zero as the frequency approaches infinity. This is not actually the case; if more high frequencies were included on the plot, the weight would collapse into the origin. While the temperature uncertainty weight appears to be generous, it will be seen that the model does not adequately describe the temperature response.

Define the inputs and outputs associated with  $\Delta_i$  as  $z_i$  and  $v_i$  respectively. The

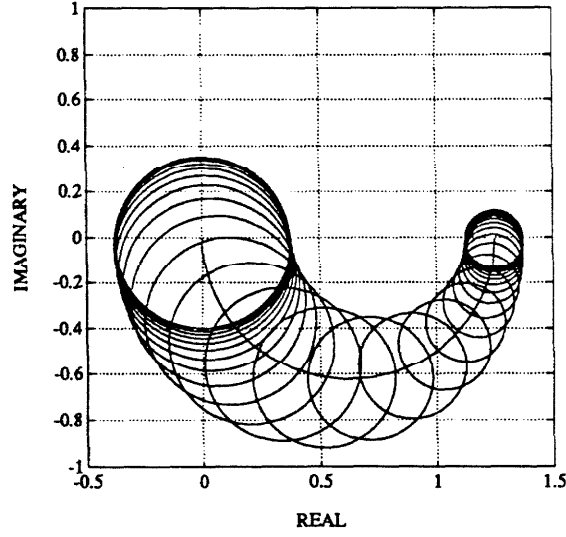


Figure 9.6: Nyquist Plot of the Transfer Function:  $f_h$  to  $t_1$ . Circles indicate the equivalent additive uncertainty bound

interconnection structure  $P$  is therefore

$$\begin{bmatrix} z_1 \\ z_2 \\ h_1 \\ t_1 \end{bmatrix} = P \begin{bmatrix} v_1 \\ v_2 \\ w_1 \\ w_2 \\ f_{hc} \\ f_{cc} \end{bmatrix}$$

$$= \left[ \begin{array}{cc|cc|cc} 0 & 0 & 0 & 0 & W_{h1}h_{lin}P_{act} & W_{h1}h_{lin}P_{act} \\ 0 & 0 & 0 & 0 & W_{t1}t_{lin}P_{act} & 0 \\ \hline 1 & 0 & W_{hn} & 0 & h_{lin}P_{act} & h_{lin}P_{act} \\ 0 & 1 & 0 & W_{tn} & t_{lin}P_{act} & 0 \end{array} \right] \begin{bmatrix} v_1 \\ v_2 \\ w_1 \\ w_2 \\ f_{hc} \\ f_{cc} \end{bmatrix}$$

where  $P$  is shown divided up into the usual partitions,  $P_{ij}$ .

The perturbation block has two elements;

$$\Delta = \begin{bmatrix} \delta_1 & 0 \\ 0 & \delta_2 \end{bmatrix}$$

giving a block structure of (1,1). In the  $\psi_s$  problem this will give

$$I_s = \{1, 2\} \quad \text{and} \quad \bar{I}_s = \{3\}.$$

Certain features are immediately obvious. Firstly,  $P_{11} = 0$  and  $P_{12} = 0$ . This means that the quadratic term of the Lagrangian is positive definite for all  $\lambda_i > 0$ . The boundary case ( $\lambda \in \partial\Lambda$ ) cannot occur.

In order to consider the problem numerically, the state space representation is introduced. The matrix transfer function  $P(s)$  can be represented as

$$P(s) = C(sI - A)^{-1}B + D = \left[ \begin{array}{c|c} A & B \\ \hline C & D \end{array} \right].$$

The numerical values of the above  $A$ ,  $B$ ,  $C$ , and  $D$  matrices are given in Appendix A (Equations A.1, A.2, A.3, and A.4).

### 9.3.3 The Discrete Version of the Interconnection Structure

Section 3.3.1 outlined a means of formulating a digital version of the model validation problem. In order to apply this approach to this example, an equivalent digital interconnection structure is developed.

Consider  $P(s)$  to be preceded by a zero order hold and followed by a sampler of period  $T$ . Figure 9.7 illustrates the required digital system.

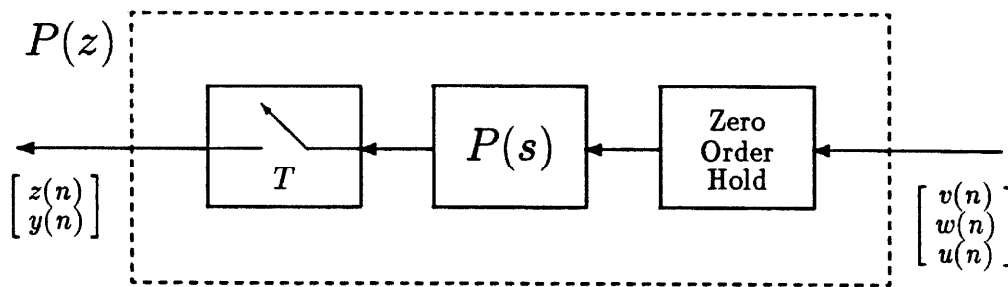


Figure 9.7: The Equivalent Digital System:  $P(z)$

Kwakernaak and Sivan [19] discuss this problem for time varying  $A$ ,  $B$ ,  $C$ , and  $D$  matrices and varying periods for the zero order hold and the sampler. In the example



presented here it is assumed that the sampler and the zero order hold operate synchronously without delay and with a fixed period,  $T$ . In this case the discrete system is given by

$$P(z) = C_d(zI - A_d)^{-1}B_d + D_d$$

where

$$A_d = e^{AT}, \quad B_d = \int_0^T e^{A\tau} B d\tau, \quad C_d = C, \quad \text{and} \quad D_d = D.$$

For the example considered here,  $T = 0.1$ . Appendix A gives the discrete time state space matrices  $A_d$  and  $B_d$  (Equations A.5 and A.6). The model is now in a form suitable for application of the model validation techniques.

## 9.4 A Model Validation Problem

### 9.4.1 The Experimental Datum

Consider an experiment which closely matches the assumptions on the digital model validation problem. The noise is assumed to be of bounded power and the inputs and outputs of the system are periodic.

A periodic input signal was applied to the flow actuators. Figure 9.8 shows a window of data taken from this experiment. Several periods elapsed before this data was taken in order to remove the initial transient.

The sampling period was 0.1 seconds and 4096 sample points were recorded during the experiment. The period of the input signal was 204.8 seconds, and the record therefore contains two periods. Several points about the datum should be noted. These pertain to using the DFT for spectral analysis but are also applicable to this problem; the initial and final points in the record are at the same value, and the record contains an integer number of periods. Discontinuities or partial periods will distort the frequency domain representation of the signals. Using a Fast Frequency Transform (FFT) algorithm to calculate the DFT can introduce these problems if the number of samples in the record is not a power of two. Some algorithms, those in Matlab [32] for example, pad the record with zeros in order to increase its length to a power of two.

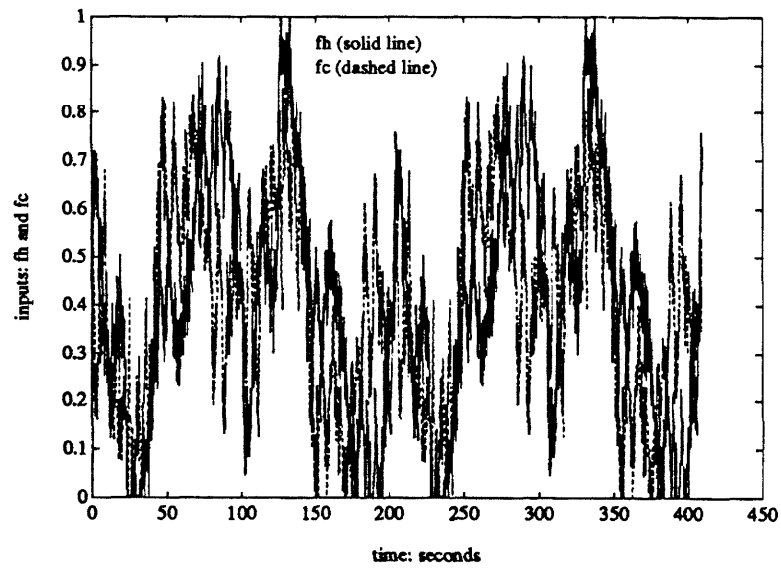
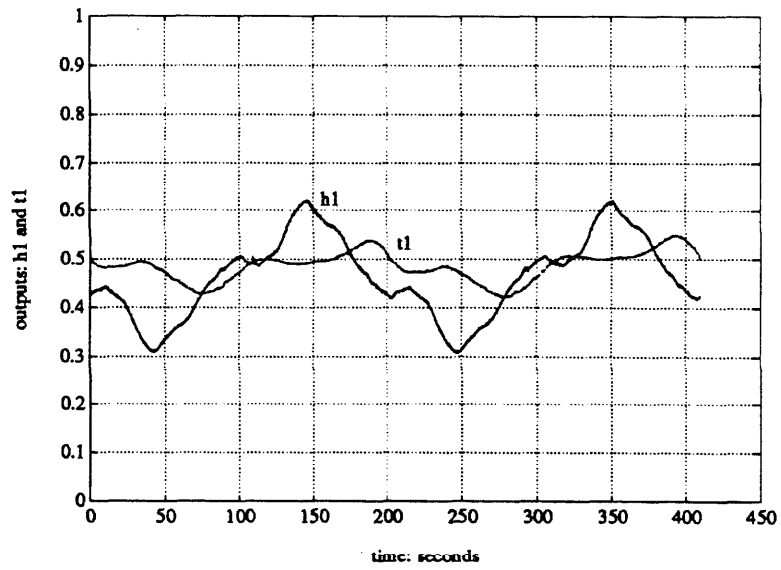


Figure 9.8: Model Validation Experiment: Input/Output Datum

Both the input and output signals have a bias. As the linear model represents deviations from the operating point, the mean value of each signal was subtracted off before performing the DFT.

The following DFT pair was used.

$$Y(k) = \sum_{n=0}^{L-1} y(n)e^{-j\frac{2\pi}{L}kn}$$

$$y(n) = \frac{1}{L} \sum_{k=0}^{L-1} Y(k)e^{j\frac{2\pi}{L}kn}.$$

Figure 9.9 shows the magnitude of the DFT of  $u(n)$  and  $y(n)$ . Only the positive frequency values are plotted.

This datum arises from a periodic input experiment. It is not necessary to choose a periodic input. A suitable experiment could begin with the system in a quiescent state with zero input; an input could then be applied and eventually returned to zero, allowing the system to return to the quiescent state. Analysis in the digital domain will, however, impose the assumption of periodicity. This poses no problem for the input  $u$ ; the experiment postulated above begins and ends with  $u$  at zero and could easily be considered as one period of a periodic experiment.

The norm-bounded unknown input  $w$  cannot be dealt with as easily. While one might be comfortable with the assumption that the spectral characteristics are similar between periods, the equality constraint imposed by the inputs  $u$  and outputs  $y$  forces the use of the assumption that  $w$  is also periodic. This is an unavoidable consequence of the fact that the experiment consists of a finite data record.

However, the analysis of the system will proceed with this assumption. Although this may introduce some conservativeness, this example will show that useful engineering judgements can be based on the results.

#### 9.4.2 Solving the Constant Matrix Problems

Each discrete frequency point gives a constant matrix problem. Only the points from  $k = 0$  to 2048 are considered. At each point  $P(z)$  is evaluated:

$$P(k) = P(z) \Big|_{z=e^{j\frac{2\pi}{1024}k}}.$$

The input-output relationship at each frequency is simply the matrix relationship:

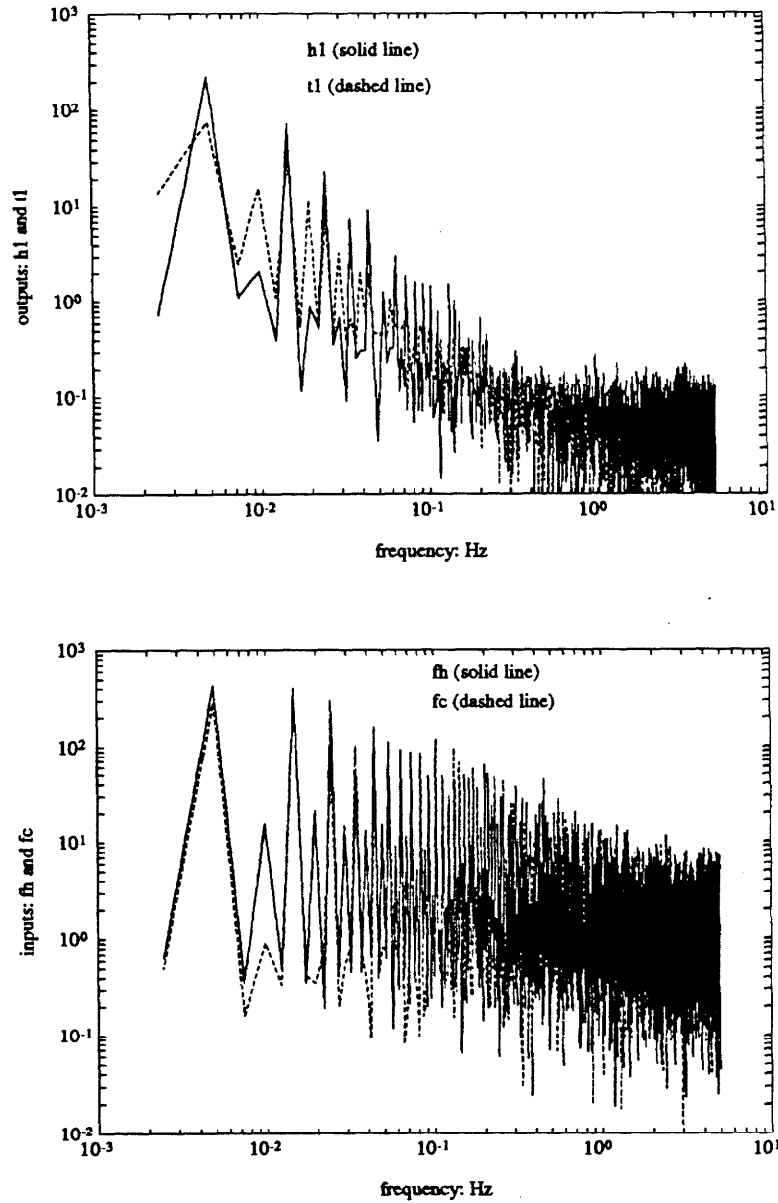


Figure 9.9: Magnitude of the Discrete Fourier Transform of  $y(n)$  (upper plot) and  $u(n)$  (lower plot)

$$\begin{bmatrix} Z(k) \\ Y(k) \end{bmatrix} = P(k) \begin{bmatrix} V(k) \\ W(k) \\ U(k) \end{bmatrix}.$$

The goal is to minimize the function

$$\|w(t)\|_{\mathcal{P}} \approx \frac{1}{L} \left\{ |W(0)|^2 + 2 \sum_{k=1}^{L/2-1} |W(k)|^2 + |W(L/2)|^2 \right\}^{1/2}$$

which is achieved by minimizing  $|W(k)|^2$  at each  $k$ . Choosing the Euclidean norm spatially gives, for a vector valued  $W(k)$ ,

$$|W(k)|^2 = W(k)^* W(k).$$

The minimum  $\|w\|$  optimization problem then becomes, for each  $k$ ,

$$\begin{aligned} \min_{X(k)} f(X(k)) \quad \text{subject to} \quad & g_i(X(k)) \leq 0, \quad i = 1, \dots, m \\ & \text{and} \quad g_e(X(k)) = 0, \end{aligned}$$

where

$$f(X(k)) = X(k)^* \begin{bmatrix} 0 & 0 \\ 0 & I \end{bmatrix} X(k),$$

$$\begin{aligned} g_i(X(k)) &= X(k)^* \begin{bmatrix} T_i & 0 \\ 0 & 0 \end{bmatrix} X(k) \\ &\quad - \begin{bmatrix} X(k)^* & U(k)^* \end{bmatrix} P(k)^* \begin{bmatrix} T_i & 0 \\ 0 & 0 \end{bmatrix} P(k) \begin{bmatrix} X(k) \\ U(k) \end{bmatrix} \end{aligned}$$

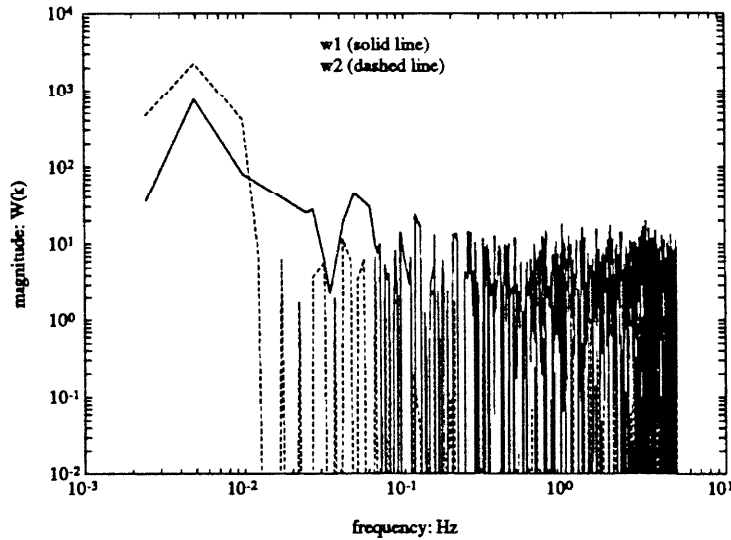
and

$$g_e(X(k)) = Y(k) - P_{23}(k)U(k) - [P_{21}(k) \ P_{22}(k)] X(k).$$

This is exactly the constant matrix problem discussed in Chapters 5, 7, and 8.

The block structure is (1,1), and to set up the  $\psi_s$  problem, consider  $I_s = \{1, 2\}$  and  $\bar{I}_s = \{3\}$ .

The author has written a software program to attempt to solve this problem based on the optimization package NPSOL available from the Systems Optimization Laboratory of Stanford University [34]. The user interface is via Matlab [32]. The program attempts to find a solution to the optimization problem via a Sequential Quadratic Programming (SQP) method.

Figure 9.10: Magnitude of  $W(k)$ 

In this example there are only two uncertainty blocks. The dimension of  $X(k)$  is four and the dimension of  $Y(k)$  is two. Consequently,  $\dim(V) \geq 2$ , and if the feasible region has an interior, a saddlepoint is guaranteed to exist (Lemma 7.13). At every frequency point the program found the Kuhn-Tucker saddlepoint.

The results of this optimization are presented in the next section.

### 9.4.3 A Discussion of the Results

The optimization approach discussed in the previous section yields  $X(k)$  for  $k = 0, \dots, 2048$ . Figure 9.10 shows  $|W(k)|$  for  $k = 1, \dots, 2048$ .

$$\|w(t)\|_P \approx \frac{1}{L} \left\{ |W(0)|^2 + 2 \sum_{k=1}^{L/2-1} |W(k)|^2 + |W(L/2)|^2 \right\}^{1/2} = 1.3184.$$

As this is larger than one, there is no element in the model set (which includes the assumption that  $\|w\|_P \leq 1$ ) which can account for the experimental datum. Examination of Figure 9.10 indicates that there are several values of  $k$  for which  $W(k)$  dominates the problem. This is hardly surprising as the  $U(k)$  and  $Y(k)$  are also large at these points.

The noise on the temperature output ( $w_2$ ) is considerably larger than that on the height output ( $w_1$ ). This suggests that the model for temperature may require modification.

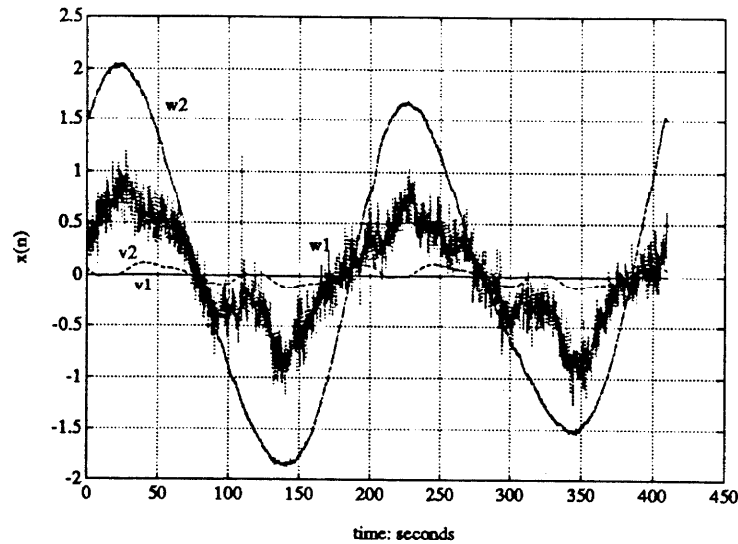


Figure 9.11: Time Domain Results:  $x(n)$

It is tempting at this point to examine the time domain version of  $W(k)$  by performing an inverse transform. This can be done by calculating the value of  $X(k)$  for the remaining values of  $k$ . For  $k = 2049, \dots, 4095$   $X(k)$  is the complex conjugate of  $X(4096 - k)$ .

Figure 9.11 shows the time domain version of  $x(n)$  ( $v(n)$  and  $w(n)$ ). The noise contribution  $w(n)$  appears to be larger than that of the perturbation  $v(n)$ . It should be borne in mind, however, that the noise signals are weighted in order to make the `NORM` comparison with one. The scaling is 0.01 for  $w_1$  and 0.03 for  $w_2$ .

The noise on the temperature output ( $w_2$ ) is almost a sinusoid of the same period as the input signal. Recall that the nominal model for the temperature response is minimum phase even though it is known from the previous input-output experiments that considerable delay is expected (refer to Section 9.2.2 and Figure 9.3). The intent was to select the perturbation weight  $W_{t1}$  large enough to account for the nonminimum phase behavior. It can be seen by examining  $v_2$  and  $z_2$  (although  $z_2$  has not been plotted here) that the perturbation block does account for some of the residual ( $y - P_{23}u$ ). It seems from this experiment that the output noise signal  $w_2$  also accounts for a significant amount. One must be careful in making such judgements based on examination of  $X(k)$  or  $x(n)$ . These signals are only an example of a single signal, compatible with the system model, and describing the input-output behavior.

This experiment indicates that the model presented in Section 9.3.2 cannot account for the observed behavior ( $\|w\|_P \geq 1.3184$ ). There are several immediate possibilities for modifying the model so that this datum may be accounted for. One is to simply scale the  $w$  input. Applying an additional scaling factor of 0.75 is sufficient. The alternative is to modify the weights on the perturbation blocks. The discussion in the previous paragraph suggests that modifying  $W_{t_1}$  in order to increase its value at least at the dominant frequency of the response may lower the norm of the  $w$  required to account for the datum.

Examining the time history  $w(n)$  shows that  $w_2$ , when considered at the output  $t_1$ , has a peak magnitude of  $\pm 0.06$ . This is of the order of the deviation in  $t_1$  itself, suggesting that something more fundamental is wrong with the model. An examination of the nominal behavior shows that, in fact, the nominal model does a very poor job of approximating the observed datum. The model validation analysis given here indicates that the perturbation uncertainty is inadequate to account for the discrepancy. The next section will formulate a better model and repeat the model validation analysis.

## 9.5 Analysis of a More Sophisticated Model

The previous section indicated that the nominal model was inadequate and that the perturbation uncertainty description could not correct the deficiencies. The fundamental reason for this is that the previous model had treated the system much like two single-input single-output (SISO) systems rather than a multivariable system.

There is a strong coupling between the height and the temperature which is not captured in the previous model. Section 9.3.2 discussed the compromise of treating  $h_1$  to be fixed in the temperature model (Equations 9.8 and 9.9). It was hoped that the effects of changing  $h_1$  could be captured by perturbation uncertainty. The model validation analysis suggests that they cannot.

A more sophisticated nominal model, including the cross coupling, will now be developed.



### 9.5.1 A Nominal Linear Model

Consider a notation for incremental variable

$$E_1 = \partial E_1 + \bar{E}_1$$

where  $\bar{E}_1$  is the steady state value of  $E_1$ , and  $\partial E_1$  is the incremental variable. The nonlinear output equation for the temperature (Equation 9.9) can be rearranged to give

$$\begin{aligned} \bar{E}_1 + \partial E_1 &= (\bar{t}_1 + \partial t_1)(\bar{h}_1 + \partial h_1) \\ &= \partial t_1 \partial h_1 + \bar{t}_1 \partial h_1 + \bar{h}_1 \partial t_1 + \bar{t}_1 \bar{h}_1. \end{aligned}$$

Using the fact that

$$\bar{E}_1 = \bar{h}_1 \bar{t}_1$$

and dropping the second order term gives the following incremental variable output equation:

$$\partial t_1 = \frac{1}{\bar{h}_1} [1 - \bar{t}_1] \begin{bmatrix} \partial E_1 \\ \partial h_1 \end{bmatrix}.$$

This gives a more representative output equation. Now consider the state equation for  $E_1$  (Equation 9.8). Using incremental variables, this is now

$$A_1 \frac{d(\partial E_1 + \bar{E}_1)}{dt} = - \left( \frac{\partial h_1 + \bar{h}_1 + \beta}{\alpha} \right) (\partial t_1 + \bar{t}_1) + (\partial f_h + \bar{f}_h) t_h + (\partial f_c + \bar{f}_c) t_c.$$

Note that

$$\frac{d\bar{E}_1}{dt} = 0$$

and the steady state relationship is

$$-\bar{h}_1 \bar{t}_1 + \bar{f}_h t_h + \bar{f}_c t_c = 0.$$

Again the higher order terms are dropped giving as a state equation for  $\partial E_1$ ,

$$\partial E_1 = \left[ \frac{1}{1 + \alpha A_1 s} \right] (\alpha \partial f_h t_h + \alpha \partial f_c t_c - \beta \partial t_1).$$

The height model equations (Equations 9.6 and 9.7) are unchanged by introducing incremental variables. The  $\partial$  notation will now be dropped. Substituting in the values for  $\alpha$ ,

$A_1$ ,  $t_h$ , and  $t_c$  gives the new model. Note that the selected operating point is  $\bar{h}_1 = 0.47$  and  $\bar{t}_1 = 0.5$ .

$$\begin{aligned} h_1 &= \left[ \frac{1.34}{1 + 122.5s} \right] (f_h + f_c) \\ E_1 &= \left[ \frac{1}{1 + 122.5s} \right] (1.34f_h - 0.6t_1) \\ t_1 &= \frac{1}{0.47}(E_1 - 0.5h_1). \end{aligned}$$

Note the existence of a significant coupling between  $h_1$  and  $t_1$ . For  $h_1 = 0$  (meaning that the height is fixed), the temperature model equations reduce to those of the previous model. The perturbation uncertainty and noise models have not been changed.

Appendix A contains a state space representation of this new model (Equations A.7, A.8, A.9, and A.10).

### 9.5.2 The Model Validation Analysis

The experiment considered in Section 9.4 will again be used as the datum. The previously outlined procedure was used to construct an equivalent digital problem.

The optimization problem was again formulated and solved at each discrete frequency point. Figure 9.12 gives the results of this optimization in both the frequency and time domains. The scales used are the same as those in Figures 9.10 and 9.11.

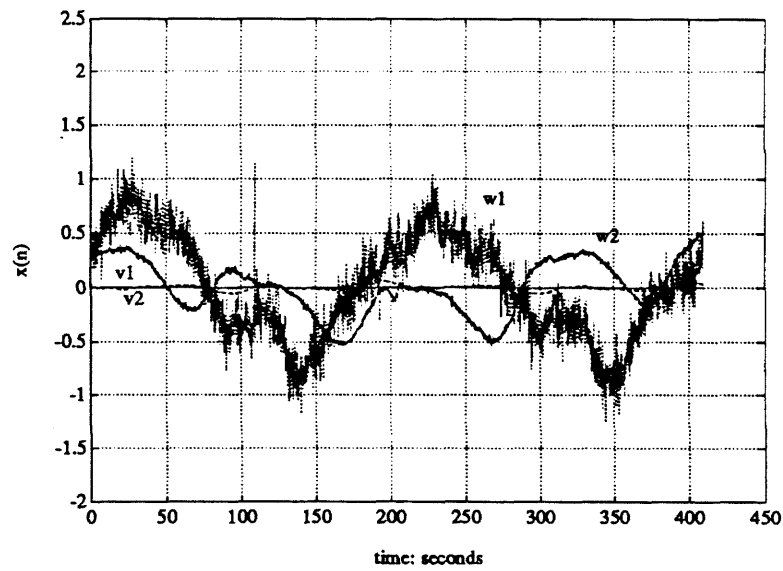
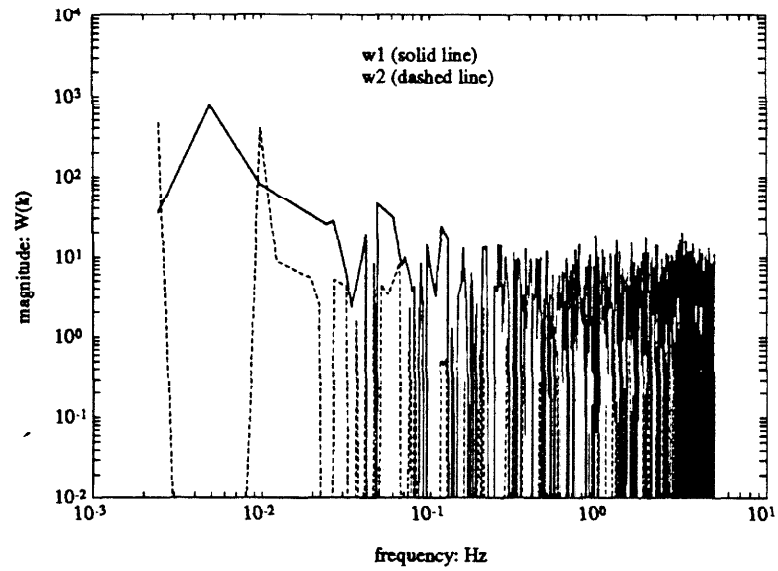
The revised model has removed most of the noise component from  $w_2$  at 0.0049 Hz. Consequently, the time domain noise signal,  $x(n)$ , has a much lower peak to peak amplitude. The norm test gives

$$\|w(t)\|_P \approx \frac{1}{L} \left\{ |W(0)|^2 + 2 \sum_{k=1}^{L/2-1} |W(k)|^2 + |W(L/2)|^2 \right\}^{1/2} = 0.5294.$$

This datum can be accounted for by the model with  $\|w\|_P < 1$ .

## 9.6 A Discussion of the Example

The nonlinear tank problem has been considered in some detail. In any identification/design problem the true system cannot be described by a nominal model. Robust control models now give a means of including perturbation uncertainty, but it is still a

Figure 9.12: Model Validation Results:  $W(k)$  and  $x(n)$

matter of judgement whether or not the model with uncertainty is adequate to describe the system. The model validation procedure gives a means of addressing this question on an experiment by experiment basis.

The tank example illustrates typical steps in arriving at a suitable robust control model. As with any other complex physical problem, other issues are invariably involved: SISO versus MIMO considerations, saturation, nonlinear versus linear models, . . . . These have not been discussed in detail here, but it has been demonstrated, by example, how one can address these issues by considering the more fundamental question, *does the model account for the datum?*

## Chapter 10

# Conclusions and Future Directions

Most engineers would be able to give some meaning to the term model validation. However, this is the first attempt, as far as this author knows, at rigorously defining the term and studying the resulting problems for robust control models.

The model validation question studied here provides a means of investigating the ability of a robust control model to describe a physical system. As such, it can be considered as the converse of the identification problem, the generation of a model from experimental data. Identification methods rely on assumptions at some level. Even if good identification tools were available for robust control models, the model validation techniques discussed here would still be essential for gaining confidence in the model and the validity of its underlying assumptions.

The results presented in this thesis have many similarities to those pertaining to  $\mu$ . The introduction of the general interconnection structure in Chapter 7 shows why this is the case: both problems can be considered as coming from a more general underlying problem. The imposition of certain constraints, those arising from known inputs and outputs, for example, changes the nature of the general problem. However, the convexity properties and the relationship between Lagrange multipliers and an upper bound remain relatively unchanged. Model validation can be considered as a more general form of robust control analysis, one in which known components are also included.

The current  $\mu$  analysis methods have been extended considerably to include systems and assumptions beyond those examined here for the model validation problem. The approach taken in this thesis strongly suggests that many of the same extensions can be developed for the model validation theory.

Future research work should then include the following:

Extensions to the block structure. Currently, only complex full subblocks are treated. Repeated scalars, and more generally repeated blocks, need to be added to the range of structures that can be considered. The fact that the set  $\mathcal{D}$  can be defined for these block structures and an upper bound to  $\mu$  calculated suggests that there exists an equivalent Lagrange problem. For repeated blocks the convexity property (for three or fewer blocks) breaks down. A study of the equivalent model validation problem from the geometric framework should shed further light on why this is so.

Real valued  $\Delta$  blocks. The  $\mu$  theory with regard to real valued perturbations is still being developed. However, such perturbations can be a natural way to model some systems, and the model validation theory should be able to address such models. Doyle [35] has also pointed out that extending the model validation theory to real perturbations would allow a direct means of doing robust parameter identification.

Time varying  $\Delta$  blocks. Some nonlinear systems can be modeled by a linear interconnection structure with time varying perturbations. A more thorough consideration of the consequences of the digital framework will be required before time varying perturbations can be considered in the model validation framework. With a finite amount of data, it might be possible, albeit extremely unattractive, to generate a realization of the known inputs and known outputs. The time varying case greatly complicates the model validation theory as it is no longer possible to break a problem up into finite frequency by frequency constant matrix problems.

Time domain approaches. Transforming the system to the frequency domain introduces periodicity assumptions on the unknown inputs. If the problem is left in the time domain, such assumptions are no longer necessary. However, the choice

of initial condition for the system introduces further degrees of freedom in the optimization. It may be necessary to place assumptions on the initial conditions in order to formulate a meaningful problem. Note also that the usual frequency varying perturbation bound now has no real meaning and it is far from clear what should be used in its place. Finally, the problem does not break down into a series of constant matrix problems. This approach should be considered as a long term research problem.

The above suggestions for extensions apply to the model validation theory. Chapter 7 has introduced a more general analysis problem for robust control models. Further work needs to be done in studying in detail each subproblem and its physical meaning.

It is the function of the control theorist to provide tools which allow the engineer to understand the physical system and the tradeoffs involved in controlling it.  $H_\infty$  theory provides a means of generating controllers, and  $\mu$  provides a means of studying the robust performance and robust stability properties of the system models. The model validation theory now provides a means of studying the relationship between robust control models and reality and, as such, is another tool that the engineer can add to her repertoire.

## Appendices

### A State Space Realizations for the Experimental Example

State space realizations of the systems described in Chapter 9 are presented here. Continuous time representations are of the form

$$P(s) = C(sI - A)^{-1}B + D = \left[ \begin{array}{c|c} A & B \\ \hline C & D \end{array} \right],$$

and discrete time state space representations are of the form

$$P(z) = C_d(zI - A_d)^{-1}B_d + D_d = \left[ \begin{array}{c|c} A_d & B_d \\ \hline C_d & D_d \end{array} \right].$$

#### Continuous Time Interconnection Structure (Section 9.3.2)

The state space representation of the interconnection structure presented in Section 9.3.2 is

$$A = \left[ \begin{array}{cccccc} -20.000 & 0 & 0 & 0 & 0 & 0 \\ 0 & -20.000 & 0 & 0 & 0 & 0 \\ 20.000 & 20.000 & -0.0080 & 0 & 0 & 0 \\ 0 & 0 & 0.0110 & -4.0000 & 0 & 0 \\ 20.000 & 0 & 0 & 0 & -0.0186 & 0 \\ 0 & 0 & 0 & 0 & 0.0232 & -5.0000 \end{array} \right], \quad (\text{A.1})$$



$$B = \begin{bmatrix} 0 & 0 & 0 & 0 & 1.0000 & 0 \\ 0 & 0 & 0 & 0 & 0 & 1.0000 \\ 0 & 0 & 0 & 0 & 0 & 0 \\ 0 & 0 & 0 & 0 & 0 & 0 \\ 0 & 0 & 0 & 0 & 0 & 0 \\ 0 & 0 & 0 & 0 & 0 & 0 \end{bmatrix}, \quad (\text{A.2})$$

$$C = \begin{bmatrix} 0 & 0 & 0.0219 & -8.0000 & 0 & 0 \\ 0 & 0 & 0 & 0 & 1.9200 & -412.00 \\ 0 & 0 & 0.0110 & 0 & 0 & 0 \\ 0 & 0 & 0 & 0 & 0.0232 & 0 \end{bmatrix}, \quad (\text{A.3})$$

and

$$D = \begin{bmatrix} 0 & 0 & 0 & 0 & 0 & 0 \\ 0 & 0 & 0 & 0 & 0 & 0 \\ 1.0000 & 0 & 0.0100 & 0 & 0 & 0 \\ 0 & 1.0000 & 0 & 0.0300 & 0 & 0 \end{bmatrix}. \quad (\text{A.4})$$

**Discrete Time Interconnection Structure (Section 9.3.3)**

The state space representation of the interconnection structure presented in Section 9.3.3 is given below. In this example  $T = 0.1$  and  $A_d$ , and  $B_d$  are given by

$$A_d = \begin{bmatrix} 0.1353 & 0 & 0 & 0 & 0 & 0 \\ 0 & 0.1353 & 0 & 0 & 0 & 0 \\ 0.8642 & 0.8642 & 0.9992 & 0 & 0 & 0 \\ 0.0005 & 0.0005 & 0.0009 & 0.6703 & 0 & 0 \\ 0.8636 & 0 & 0 & 0 & 0.9981 & 0 \\ 0.0011 & 0 & 0 & 0 & 0.0018 & 0.6065 \end{bmatrix} \quad (\text{A.5})$$

and

$$B_d = \begin{bmatrix} 0 & 0 & 0 & 0 & 0.0432 & 0 \\ 0 & 0 & 0 & 0 & 0 & 0.0432 \\ 0 & 0 & 0 & 0 & 0.0567 & 0.0567 \\ 0 & 0 & 0 & 0 & 0.0000 & 0.0000 \\ 0 & 0 & 0 & 0 & 0.0567 & 0 \\ 0 & 0 & 0 & 0 & 0.0000 & 0 \end{bmatrix}. \quad (\text{A.6})$$

The matrices  $C_d$  and  $D_d$  are equal to their continuous time counterparts, Equations A.3 and A.4 respectively.

### Continuous Time Interconnection Structure (Section 9.5.1)

The continuous time state space representation of the interconnection structure presented in Section 9.5.1 is given by

$$A = \begin{bmatrix} -20.0000 & 0 & 0 & 0 & 0 & 0 \\ 0 & -20.0000 & 0 & 0 & 0 & 0 \\ 20.0000 & 20.0000 & -0.0080 & 0 & 0 & 0 \\ 0 & 0 & 0.0110 & -4.0000 & 0.0000 & 0 \\ 26.8000 & 0 & 0.0070 & 0.0000 & -0.0186 & 0 \\ 0 & 0 & -0.0117 & 0.0000 & 0.0174 & -5.0000 \end{bmatrix}, \quad (\text{A.7})$$

$$B = \begin{bmatrix} 0 & 0 & 0 & 0 & 1.0000 & 0 \\ 0 & 0 & 0 & 0 & 0 & 1.0000 \\ 0 & 0 & 0 & 0 & 0 & 0 \\ 0 & 0 & 0 & 0 & 0 & 0 \\ 0 & 0 & 0 & 0 & 0 & 0 \\ 0 & 0 & 0 & 0 & 0 & 0 \end{bmatrix}, \quad (\text{A.8})$$

$$C = \begin{bmatrix} 0 & 0 & 0.0219 & -8.0000 & 0.0000 & 0 \\ 0 & 0 & -0.9619 & 0.0000 & 1.4329 & -412.0000 \\ 0 & 0 & 0.0110 & 0 & 0 & 0 \\ 0 & 0 & -0.0117 & 0.0000 & 0.0174 & 0 \end{bmatrix}, \quad (\text{A.9})$$

and

$$D = \begin{bmatrix} 0 & 0 & 0 & 0 & 0 & 0 \\ 0 & 0 & 0 & 0 & 0 & 0 \\ 1.0000 & 0 & 0.0100 & 0 & 0 & 0 \\ 0 & 1.0000 & 0 & 0.0300 & 0 & 0 \end{bmatrix}. \quad (\text{A.10})$$

## Bibliography

- [1] J. Doyle and A. K. Packard, "Uncertain multivariable systems from a state space perspective," in *Proc. Amer. Control Conf.*, vol. 3, pp. 2147–2152, 1987.
- [2] D. Laughlin, D. Rivera, and M. Morari, "Smith predictor design for robust performance," *Int. J. of Control*, vol. 46, pp. 477–504, 1987.
- [3] R. S. Smith, J. Doyle, M. Morari, and A. Skjellum, "A case study using  $\mu$ : Laboratory process control problem," in *Proc. Int. Fed. Auto. Control*, vol. 8, pp. 403–415, 1987.
- [4] J. Doyle, "Structured uncertainty in control system design," in *Proc. IEEE Control Decision Conf.*, pp. 260–265, 1985.
- [5] G. Zames, "On the input-output stability of nonlinear time-varying feedback systems, parts I and II," *IEEE Trans. Auto. Control*, vol. AC-11, pp. 228–238 and 465–476, 1966.
- [6] J. Doyle and G. Stein, "Multivariable feedback design: Concepts for a classical/modern synthesis," *IEEE Trans. Auto. Control*, vol. AC-26, pp. 4–16, Feb. 1981.
- [7] J. Doyle, "Analysis of feedback systems with structured uncertainties," *IEE Proceedings, Part D*, vol. 133, pp. 45–56, Mar. 1982.
- [8] M. K. H. Fan and A. L. Tits, "Characterization and efficient computation of the structured singular value," *IEEE Trans. Auto. Control*, vol. AC-31, pp. 734–743, 1986.

- [9] M. K. H. Fan and A. L. Tits, " $m$ -form numerical range and the computation of the structured singular value," *IEEE Trans. Auto. Control*, vol. AC-33, pp. 284–289, 1988.
- [10] A. K. Packard, *What's new with  $\mu$* . Ph.D. thesis, University of California, Berkeley, 1988.
- [11] M. Safanov and J. Doyle, "Minimizing conservativeness of robust singular values," in *Multivariable Control* (S. Tzafestas, ed.), New York: Reidel, 1984.
- [12] B. A. Francis, *A Course in  $H_\infty$  Control Theory*, vol. 88 of *Lecture Notes in Control and Information Sciences*, Berlin: Springer-Verlag, 1987.
- [13] J. Doyle, K. Glover, P. Khargonekar, and B. Francis, "State-space solutions to standard  $H_2$  and  $H_\infty$  control problems," *IEEE Trans. Auto. Control*, vol. AC-34, pp. 831–847, 1989.
- [14] J. C. Doyle, "Lecture notes on advances in multivariable control." ONR/Honeywell Workshop, Minneapolis, MN, 1984.
- [15] J. C. Doyle, "Guaranteed margins for LQG regulators," *IEEE Trans. Auto. Control*, vol. AC-23, pp. 756–757, 1978.
- [16] L. Ljung, *System Identification, Theory for the User*, Information and System Sciences Series, New Jersey: Prentice-Hall, 1987.
- [17] G. H. Golub and C. F. Van Loan, *Matrix Computations*, Baltimore: John Hopkins, 1983.
- [18] A. V. Oppenheim and R. W. Schaffer, *Digital Signal Processing*, New Jersey: Prentice-Hall, 1975.
- [19] H. Kwakernaak and R. Sivan, *Linear Optimal Control Systems*, New York: Wiley-Interscience, 1972.
- [20] D. A. Wismer and R. Chattergy, *Introduction to Nonlinear Optimization, A Problem Solving Approach*, System Science and Engineering Series, New York: North Holland, 1978.

- [21] O. L. Mangasarian, *Nonlinear Programming*, Systems Science Series, McGraw-Hill, 1969.
- [22] R. T. Rockafellar, *Convex Analysis*, New Jersey: Princeton University Press, 1970.
- [23] D. G. Luenberger, *Optimization by Vector Space Methods*, New York: Wiley, 1969.
- [24] H. Kuhn and A. Tucker, "Nonlinear programming," in *Proc. of the Second Berkeley Symposium on Mathematical Statistics and Probability* (J. Neyman, ed.), pp. 481–492, University of California Press, 1951.
- [25] M. K. H. Fan and A. L. Tits, "Geometric aspects in the computation of the structured singular value," in *Proc. Amer. Control Conf.*, pp. 437–441, 1986.
- [26] M. K. H. Fan and A. L. Tits, "On the generalized numerical range," *Linear and Multilinear Algebra*, vol. 21, pp. 313–320, 1987.
- [27] A. S. Householder, *The Theory of Matrices in Numerical Analysis*, New York: Blaisdel, 1964.
- [28] F. Hausdorff, "Der Wertvorrat einer Bilinearform," *Math. Z.*, vol. 3, pp. 314–316, 1919.
- [29] O. Toeplitz, "Das algebraische Analogon zu einem Satze von Fejér," *Math. Z.*, vol. 2, pp. 187–197, 1918.
- [30] E. Gilbert, "An iterative method for computing the minimum of a quadratic form on a set," *SIAM Journal on Control*, vol. 4, pp. 61–80, 1966.
- [31] R. S. Smith and J. Doyle, "The two tank experiment: A benchmark control problem," in *Proc. Amer. Control Conf.*, vol. 3, pp. 403–415, 1988.
- [32] The MathWorks, Inc., Sherborn MA, *Pro-Matlab User's Guide*, 1986.
- [33] K. Åström, "Towards intelligent control." Plenary Lecture, American Control Conference, Atlanta, Georgia, 1988.
- [34] P. E. Gill, W. Murray, M. A. Saunders, and M. H. Wright, "User's guide for NPSOL (version 4.0): A Fortran package for nonlinear programming," Tech. Rep. Technical

Report: SOL 86-2, Systems Optimization Laboratory, Dept. of Operations Research, Stanford University, 1986.

[35] J. C. Doyle, 1989, private communication.